Characterization of the bed, critical boundary shear stress, roughness, and bedload transport in the Connecticut River Estuary

Author: Kendall Valentine

Persistent link: http://hdl.handle.net/2345/bc-ir:104550

This work is posted on eScholarship@BC,
Boston College University Libraries.

Boston College Electronic Thesis or Dissertation, 2015

Copyright is held by the author, with all rights reserved, unless otherwise noted.

Boston College

The Graduate School of Arts and Sciences

Department of Earth and Environmental Sciences

CHARACTERIZATION OF THE BED, CRITICAL BOUNDARY SHEAR STRESS, ROUGHNESS, AND BEDLOAD TRANPSORT IN THE CONNECTICUT RIVER ESTUARY

a thesis

by

KENDALL MARIE VALENTINE

submitted in partial fulfillment of the requirements

for the degree of

Master of Science

August 2015

© copyright by KENDALL MARIE VALENTINE
2015

Abstract

This study characterizes the bed of the Connecticut River estuary in terms of grain size and bed morphology (bedforms), and relates these physical properties to river discharge, tidal currents, and sediment transport. Over four field excursions (November 2012, May 2013, November 2013, and May 2014), 383 sediment cores were collected, in addition to bathymetry surveys, current velocity, suspended sediment concentration, temperature, and salinity measurements. A three-dimensional circulation and sediment transport model calculated boundary shear stress over the same time periods that the field experiments were carried out, using observed tides and river discharge to drive the model. The bed of the estuary is composed mostly of sand, with small amounts of fine sediments (< 30%). The sand fraction of the distribution is transported primarily as bedload, while the fine fraction is transported in the water column. Deposition of fine sediments is limited by the landward extent of the salt intrusion. Large bedforms (1-2 m) are consistently oriented seaward. The critical shear stress for the median grain size is exceeded each tidal cycle. This means that active transport is occurring. Bedload transport is dominantly seaward during high discharge conditions. During low discharge periods, net bedload transport is landward in the lower estuary and seaward in the upper estuary. Bathymetry surveys from previous studies, pre-Hurricane Sandy surveys, and post-Hurricane Sandy echosounder surveys show consistent bedform fields over a span of 25 years. This suggests that the major processes driving bed morphology in the Connecticut River estuary, including river discharge, tides, and sediment supply, have not changed in the past 25 years. The smaller bedforms (<1 m) observed in the field are able to be formed by maximum spring tidal currents and the larger bedforms (1-2 m) are able to be formed by annual flood events. Extreme events would likely form plane beds or antidunes, which were not observed in the field. Therefore, the bedforms observed in the field reflect typical conditions rather than extreme events.

Table of Contents

Table of Figures:

List of Tables:

Acknowledgements

First, I would like to thank my advisor, Dr. Gail Kineke, for her guidance, all of the lessons she has taught me, and her constant pursuit for excellence.

I would also like to thank my thesis committee: Dr. Noah Snyder, Dr. John Ebel, and Dr. Dave Ralston. Coursework from both Noah and John helped shape my thesis, and the feedback all three provided added significantly to my thesis and my understanding. I would especially like to thank Dave for his guidance and patience helping me through this project.

I would like to thank Dr. W. Rocky Geyer for his insight throughout this project. I thank Dr. Tim Milligan and Dr. Brent Law for the advice and laughs in the field.

I also thank Dr. Ken Galli. His constant optimism and willingness to help in any situation gave me hope through the hours and hours of grain size, working in the lab, and writing.

I especially want to thank Ellen Kristiansen for being a wonderful lab partner. Through nights of filtering, debugging Matlab code, and several (hundred) games of solitaire, she was always there with me. I would also like to thank Austin Hopkins, Bianca Bello, Dave Beutel, and Katie Lavallee for their support on my thesis, amongst other things.

I thank my parents and sister, Jessica, for always trying to listen to me about this project (and everything else) and their support for the last 24 years.

Lastly, I would like to thank my soon-to-be husband, Adrian Cole, for the countless times he read drafts of my thesis, discussed data, and consoled me when difficult times arose. I believe he too learned quite a lot about the Connecticut River estuary and sediment transport over the last two years, and for that I am forever grateful.

This project was partially funded by NSF Grant (1232928).

Variables

C_D	Drag coefficient
C_1	Proportionality constant (0.19)
D	Particle diameter
D_{10}	10^{th} percentile particle diameter
D_{50}	Median particle diameter
D_{90}	90^{th} percentile particle diameter
f	Frequency
g	Gravitational constant (9.8 m/s^2)
i	Flow direction, 1 is along-channel, 2 is across-channel, 3 is vertical
k	Wave number
k'_b	Total hydraulic roughness
k_{bg}	Grain roughness
k_{br}	Form drag roughness
k_{bm}	Moveable bed roughness
L	Characteristic length scale
P	Rouse parameter
q_b	Bedload transport rate
Re	Reynolds number
Re_*	Particle Reynolds number
TKE	Turbulent kinetic energy
u	Velocity
u_z	Velocity of the flow at height z above the bed
u_*	Shear velocity
u'	Deviation from the mean velocity in the along-channel direction
v'	Deviation from the mean velocity in the across-channel direction
w'	Deviation from the mean velocity in the vertical direction
w_s	Settling velocity
z	Height above the bed
z_0	Roughness length
α_i	Kolmogorov constant, α_1=0.51, α_2=α_3=(4/3)α_1=0.69
β	Shields parameter
ε	Energy dissipation
η	Wave/ripple height
κ	von Kármán's constant (0.41)
λ	Wave/ripple wavelength
ν	Kinematic viscosity
ρ	Density of the fluid
ρ_s	Density of the solid
τ_b	Boundary shear stress
τ_c	Critical boundary shear stress
τ'_c	Critical boundary shear stress due to skin friction
τ_m	Modeled boundary shear stress
τ_o	Observed boundary shear stress
Ψ'_{max}	Shields parameter using τ'_c
ϕ	Wentworth phi size
$\phi_{ii}(k)$	Spectral density of velocity in direction ii at wavenumber k

1. Introduction

Estuaries, the meeting place of fresh and salt water, are valuable ecosystems (Barbier et al. 2011). The health of these coastal environments has environmental, biological, and economical implications. Estuaries are dynamic environments that are subject to sea level rise, tides, storms, and anthropogenic effects. Understanding the movement of sediment within estuaries provides insight into contaminant transport, navigation and dredging practices, and the overall health of the system.

Sediment transport depends on the flow and nature of the bed, or boundary, which includes grain size, roughness, and cohesiveness. If sediment transport is to occur, the stress imposed on the bed by the flow must exceed a critical value to initiate particle movement. The interaction of the flow with the bed is affected by the configuration and composition of the bed itself. Variations in grain size can change the roughness of the bed on a small scale (100 μm – 2 mm), while bedforms, like sand waves, can alter the roughness on a larger scale (1-2 meters).

The Connecticut River delivers ~70% of the total sediment load to Long Island Sound (Gordon, 1980). The majority of the sediment transported in the Connecticut River is medium sand that is moved as bedload (Horne and Patton, 1989). Previous work suggests that the Connecticut River is able to constantly move sand out of the estuary (Horne and Patton, 1989). Prior studies suggest that fine sediments delivered to the estuary are quickly exported to Long Island Sound (Patton and Horne, 1992). Recent research by Woodruff et al. (2013) found enhanced accumulation of fine sediments in coves in the estuary, indicating that our understanding of sediment transport is lacking.

Contaminants often sorb onto fine sediments (Mehta et al., 1989); therefore, knowing the dispersal pathways and accumulation sites of fine sediments in the Connecticut River estuary may have important implications for contaminant transport and the health of the ecosystem.

The purpose of this study is to characterize the bed in terms of grain size and bedforms, evaluate sediment transport, and explore the role of bed roughness from both grain size and bedforms in sediment transport throughout the Connecticut River estuary. Detailed flow measurements at different locations in the estuary during different seasons allow direct calculations of bottom stress over a range of conditions. Comprehensive bathymetry surveys and 383 cores capture the bottom conditions throughout the estuary during multiple sampling periods. These data, in combination with the Quadratic Stress Law, a practical and simple relationship between nearbed flow velocity and the shear stress on the bed, allow quantification of the bottom roughness and estimates of bedload transport.

2. Background

This section focuses on important information on the study site and the relevant scientific background needed before delving into the specifics of the study. Following the background description, the specific objectives of the project are outlined, as well as how this project fits into the scope of a larger study.

2.1 Site Description

The Connecticut River, located on the eastern seaboard of the United States, originates in the southern reaches of Canada and empties into Long Island Sound (Figure 1). The Connecticut has an average discharge of 450 m^3/s (Meade, 1966; Merriman and Thorpe, 1976 in Patrick, 1996). The spring melt is most commonly associated with the highest discharge (~2500 m^3/s) and delivers high sediment loads, on the order of 10^6 tons per year, to the estuary and Long Island Sound (Horne and Patton, 1989). Storm events in the fall occasionally result in discharges higher than those during the spring melt. The tidal range varies between 0.6 m and 1.4 m (Horne and Patton, 1989). Due to the range in discharge and tides, the estuary has been classified as both a salt-wedge estuary (Meade, 1966; Garvine, 1975) and a partially-mixed estuary (Garvine, 1974). The bed is primarily composed of sand, with a gradual fining towards the mouth (Horne and Patton, 1989). Regions upstream of tidal influence have sandy beds with a layer of silt (Boyd, 1976). Parts of the estuary exhibit sand waves, reaching amplitudes of up to 1 m (Horne and Patton, 1989).

2.2 Flow, Shear Velocity and Boundary Shear Stress

A typical mean velocity profile of a steady current over a boundary is composed of an outer layer, a log layer, and a laminar sublayer (Figure 2; Dyer, 1986). At the bed, the flow velocity must be zero (the "no-slip" condition), which causes the flow velocity to decrease as the boundary is approached. In a thin layer closest to the bed, the flow is dominated by viscous forces and is referred to as the laminar sublayer. Above this is the logarithmic region of the velocity profile and the flow is fully turbulent. The log layer is the deviation from a linear velocity profile due to turbulence (Dyer, 1986). A free stream velocity is reached where the flow is no longer affected by the presence of the boundary. In smooth turbulent flow, the roughness of the bottom is smaller than the height of the laminar sublayer. In rough turbulent flow, the roughness of the bottom pokes through the laminar sublayer. A flow is defined as turbulent or laminar using the dimensionless Reynolds number:

$$Re = \frac{uL}{\nu} \qquad (1)$$

where u is the velocity of the flow, L is the characteristic length scale, and ν is the kinematic viscosity of the fluid. If *Re* > 2000, the flow is turbulent; if *Re* is small the flow is laminar (Middleton and Southard, 1984).

The log layer is described by the von Kármán-Prandtl equation (Dyer, 1986),

$$\frac{u_z}{u_*} = \frac{1}{\kappa} ln \frac{z}{z_0} \qquad (2)$$

where u_*, the shear velocity, is a convenient proxy for the boundary shear stress, τ_b, and is defined as $u_* = \sqrt{\frac{\tau_b}{\rho}}$; ρ is the density of the fluid, u_z is the velocity of the flow at height above the bed, z, κ is von Kármán's constant (0.41), and z_0 is the roughness length, defined as the height above the bed where the velocity profile would go to zero.

The von Kármán-Prandtl equation, or the "Law of the Wall," is based on the relationship that the velocity gradient (*du/dz*) above the bed relies only on the distance above the bed (*z*) and the shear velocity (u_*) and can be expressed as:

$$\frac{du}{dz} = \frac{u_*}{\kappa z} \qquad (3)$$

Integrating this equation to determine the velocity at any height of the bed yields

$$u_z = \frac{u_*}{\kappa}\ln(z) + C \qquad (4)$$

where *C* is a constant of integration. In rough turbulent flow (*Re*>2000), flow is influenced by the length of the roughness elements. Assuming the boundary condition that the velocity goes to zero near the bed, somewhere between *z*=0 and the height of the roughness elements, or at z_0, equation 4 becomes

$$u_z = \frac{u_*}{\kappa}\ln\left(\frac{z}{z_0}\right) \qquad (5)$$

This equation can be rearranged into equation 2, a familiar form of the "Law of the Wall".

2.3 Sediment Size and Threshold of Motion

A common way to describe sediment is by particle size using the Wentworth phi scale, where $\phi = -log_2 D$, and *D* is the particle diameter (mm) (Folk, 1966). *Coarse* sediment refers to sizes larger than 63 um (ϕ < 4) and *fine* sediment, *silts* and *clays* collectively referred to as muds, are smaller than 63 um (ϕ > 4). Sediment begins to move when the boundary shear stress, τ_b, exceeds a critical value, τ_c. Shields (1936) determined τ_c for a range of sediment sizes and types and expressed it in terms of an empirical relationship between two dimensionless numbers, the particle Reynolds number, $Re_{*,} \frac{u_* D}{\nu}$, and the Shields parameter $\beta = \frac{\tau_c}{(\rho_s - \rho) g D}$, where ρ_s is the density of the solid (Shields, 1936 in Middleton and Southard, 1984). Using the Shields parameter, the bed grain size can be used to determine the flow necessary to move the sediment based on prior experiments (Figure 3). Shields' experimental results yield an "envelope" of values that may initiate particle motion (Middleton and Southard, 1984). Shields' (1936) experiments were run in flumes with non-cohesive sediments under particle Reynolds numbers between 2 and 600; additional studies have extended the relationship to particle Reynolds numbers outside of the original range (e.g. Vanoni, 1964; Mantz, 1977; Buffington, 1999; Dancey et al., 2002; Dey, 2003). For all of these formulations, if $\tau_b > \tau_c$, the sediment is mobile. The criterion for threshold of motion is not valid for cohesive sediments (muds).

Sediment can be transported through two main modes: bedload and suspended load (Middleton and Southard, 1984). Bedload is the fraction that moves close to the bed via rolling, saltating, and sliding. Bedload is supported by the bed, not by the flow. Suspended load is the sediment that is transported in the water column by turbulent eddies. The mode of sediment transport can be described by the Rouse Parameter, *P* (Middleton and Southard, 1984; Milligan et al. 2001). This dimensionless number represents the a ratio between settling and mixing,

$$P = \frac{w_s}{\kappa u_*} \tag{6}$$

where w_s is the settling velocity. If *P* is greater than ~2.5, the sediment will be transported as bedload. If *P* is between 0.8 and 1.2, sediment will be transported as suspended load. Between 1.2 and 2.5, sediment is being moved by both bedload and suspended load. For $P < 0.8$, the sediment is considered washload (Middleton and Southard, 1984).

2.4 Bed Roughness and the Drag Coefficient

The drag coefficient is an empirical constant that encapsulates the interaction between the bottom roughness and the overlying flow. The drag coefficient is derived from the von Kármán-Prandtl equation (Equation 2; Komar, 1976). Rearranging equation 2 and substituting $\tau_b = \rho u_*^2$ yields

$$\tau_b = \rho u_z^2 \left[\frac{\kappa}{ln\frac{z}{z_0}}\right]^2 \tag{7}$$

For a given height above the bed and bed roughness, z, z_0, and κ are collected into a single constant, C_D, or the drag coefficient, resulting in

$$\tau_b = \rho C_D \overline{u_z}^2 \tag{8}$$

(Soulsby, 1997). The drag coefficient for a given flow and bed condition varies depending on the height above the bed; thus for field applications velocity is commonly measured at 100 cm above the bottom and C_D is referred to as C_{100}. This simplified form (Equation 8) is known as the Quadratic Stress Law (QSL) and allows calculation of boundary shear stress with a single mean near-bed velocity measurement.

Previous studies have determined a range of drag coefficients for different bed and sediment characteristics (Sternberg, 1972). While Sternberg (1968, 1972) found differences in C_D by up to a factor of two, he suggested that a mean value of 3.0×10^{-3} could be broadly applicable in many cases without bedforms larger than 5 cm or high sediment transport rates. Following Sternberg's investigation of roughness and sediment composition, others focused on quantifying z_0 and C_D for different bed types. Calculated roughness lengths vary up to two orders of magnitude for different sediment and bed compositions, while the drag coefficient vary by a factor of three (Table 1; Soulsby, 1983).

2.5 Bedforms

Bedforms are features, such as waves or ripples, which are formed by the movement of sediment by fluid flow. These features can be symmetric to indicate bidirectional flow, or they can be unidirectional. Unidirectional bedforms have one side steeper than the other, which indicates the direction of flow. For non-planar beds (those with bedforms), the total shear stress is composed of two components: skin friction and form drag. Skin friction is the component of shear stress acting on the sediment particles. Form drag is present when there is obstruction to the flow, like bedforms, that cause pressure differences, altering the stress felt by the flow (Wright, 1995). As form drag increases the amount of skin friction, or shear stress felt by the bed, decreases.

Likewise, the bed roughness, z_0, is affected by obstructions to the flow. Roughness is defined as

$$z_0 = \frac{k'_b}{30} = \frac{k_{bg}}{30} + \frac{k_{br}}{30} + \frac{k_{bm}}{30} \qquad (9)$$

where k'_b is the total hydraulic roughness, k_{bg} is the grain roughness ($\approx D$), k_{br} is the form drag roughness, and k_{bm} is the moveable bed roughness (Wright, 1995). A simple formulation of k_{br} is

$$k_{br} = 4\eta \qquad (10)$$

where η is the height of the ripples or sand waves (Madsen and Wikramanayake, 1991). The role of moveable bed roughness, or bedload roughness, is defined as (Grant and Madsen, 1982; Wright, 1995)

$$k_{bm} = 30D\psi'_{max} \qquad (11)$$

where

$$\psi'_{max} = \frac{\tau'_c}{gD\rho(\rho_s/\rho - 1)} \qquad (12)$$

and τ'_c is the skin friction component of critical shear stress. The bedload roughness is largest when form drag is zero ($\tau'_c = \tau_c$), and decreases with increasing form drag. Calculations in the present study reflect the maximum potential roughness due to bedload and assume $\tau'_c = \tau_c$.

2.6 Objectives

This study is part of a larger project, Frontogenesis and Fine-Sediment Trapping in a Highly Stratified Estuary, funded by the National Science Foundation (NSF Proposal 1232928). The project as a whole is focusing on frontogenesis (formation of fronts) within the water column and the potential for trapping of fine sediments in the Connecticut River estuary. In addition to hydrography and flow, these objectives require knowledge of the bathymetry, sediment type and morphology of the estuary in order to understand the conditions necessary for frontogenesis. This project aims to quantify the bed in terms of grain size and bedforms, and relate these properties of the bed to river discharge, tidal currents, and sediment transport.

3. Methods

3.1 Field Program

In order to address the objectives, four field experiments were conducted in the Connecticut River estuary: November 2012 (N12), May 2013 (M13), November 2013 (N13), and May 2014 (M14) on the *R/V Discovery* (Ryan Marine Inc.) and the *R/V Lowell Weicker* (University of Connecticut). The study area extends from the mouth of the Connecticut River at Long Island Sound to 12 km upstream (Figure 4). Sampling was focused in "frontal zones" which were chosen based on previous studies (Geyer *et al*., 2010). These studies identified localized areas of intensified density gradients within the estuary, primarily immediately downstream of river constrictions. These areas can form secondary Estuarine Turbidity Maxima (ETMs) and have the potential to trap fine sediments (Friedrichs, 2009). Other parts of the NSF project are examining the physical processes responsible for frontogenesis and impact on suspended-sediment transport.

3.2.1 Flow Conditions

The mean discharge of the Connecticut River over the duration of all experiments was comparable to published average discharge rates (~450 m^3/s; U.S. Geological Survey, 2015, Thompsonville; Figure 5A). For the N12 and M13 field experiments, the flow was near average with no precipitation events immediately preceding data collection. The lowest discharge condition was observed during the N13 experiment; the highest discharge occurred during the M14 experiment, where the flow during sampling was about double the yearly average for the Connecticut River. The cumulative discharge leading up to the sampling period was highest during M14 and lowest during

N13 (Figure 5B). Tidal amplitudes were similar between field experiments; on average the tidal range was ~0.9 m in M13 and M14 and ~1.2 m in N13 based on data from a tide gauge at Old Lyme, CT (U.S. Geological Survey, 2015, Old Lyme).

3.2.2 Bed Characterization

Bottom sediment samples were taken using a HAPS corer (KC Denmark; Figure 6). Samples were taken at stations in across-channel transects throughout the study area, with particular focus on the frontal zones (Figure 4). Each transect consisted of five stations across the channel. Additional cores were taken in each progressive field season; the cores from the prior seasons were repeated and additional cores were added to improve the spatial resolution.

Cores were photographed, described, measured, extruded and subsampled. In N12 and M13, approximately the top 1 cm of sediment was sampled. In N13 and M14, sediment from the top 0.5 cm and 0.5 – 2 cm were sampled and put into bags. Samples were stored under cold dark conditions in the field. Once the samples were returned to the lab, they were frozen.

During the M14 field sampling, if the overlying water column in the core barrel contained a substantial amount of suspended sediment, the water was also sampled using a siphon. The sample was filtered through a pre-weighted 0.45-micron filter, dried and reweighed to calculate the suspended sediment concentration (mg/L).

Acoustic bathymetric surveys were done using a Knudsen Engineering dual frequency echosounder (1610 series) during the M13, N13, and M14 experiments. Data were collected using a 50 kHz and 200 kHz signal at a sampling frequency of 5 Hz. Specific transects were identified and surveyed during the experiment; the echosounder was also used during all other measurements to obtain water depth at each station or core location. Side-scan and multi-beam sonar surveys were collected in the study area by the U.S. Geological Survey in August 2012 in advance of the N12 sampling (Ackerman, *in preparation*).

3.2.3 Water Column Measurements

A tripod (after Sternberg et al., 1991) outfitted with a conductivity, temperature, and depth sensor (RBR-CTD), acoustic Doppler velocimeter (ADV; Nortek), optical backscatter sensor (OBS), and pumps to take *in-situ* water and suspended sediment samples (Figure 7), was deployed during each of the field experiments at anchor stations throughout the study area (Figure 4). The ADV sampled at 16 Hz, providing high-resolution velocity data. In M14, an acoustic backscatterance sensor (ABS) was also attached to the tripod. The tripod was deployed and sampled from the surface to the seabed, remaining on the bottom for a period of about 10 minutes to obtain near-bottom measurements of velocity and suspended sediment concentration. The *in-situ* pump samples were filtered in the field and reweighed in the lab for calibration of the OBS. A profiling CTD with OBS was also deployed every five minutes while at anchor. A CTD cast was taken immediately before each core. Continuous current profiles were taken with a hull-mounted acoustic Doppler current profiler (ADCP; RD Instruments).

3.3 Laboratory Work

3.3.1 Grain-Size Analysis

Samples from cores were analyzed for grain size following standard procedure (Folk and Ward, 1957). Subsamples of the sediment cores were weighed, dried, and reweighed to calculate the water content of the sample. Samples were then processed with 30 % hydrogen peroxide to remove organic matter. To prevent flocculation, a 0.2% Calgon solution was added to the processed sediment. The sediment was wet sieved through a 63-micron sieve and both the coarse and fine fractions were dried. The coarse fraction (>63 microns) was dry sieved in 0.5ϕ increments ranging from -1 to 4ϕ using a Ro-Tap and the fine fraction was sized using a 5120 SediGraph III (Micromeritics Instrument Corporation). Samples were run in the SediGraph with a baseline solution of 0.2% sodium metaphosphate and were sonicated prior to analysis.

3.3.2 Loss on Ignition

Loss on ignition was performed on each sample following standard procedure (Dean, 1972). Samples were dried and left in a preheated furnace at 550 °C for one hour to combust organic matter. Post-weights were recorded and the mass loss during this period was calculated.

3.4 Three-Dimensional Circulation and Sediment Transport Model

A three-dimensional circulation and sediment transport model for the Connecticut River estuary is currently in development (Ralston, *pers. comm.*). The model is similar to the models developed for the Merrimack River estuary (Ralston et al., 2010) and the Hudson River (Ralston et al. 2012). The numerical model of the Connecticut River estuary uses a Finite Volume Coastal Ocean Model (FVCOM) with a sediment transport component derived from the Community Sediment Transport Modeling System (CSTMS) with an unstructured grid of triangles as individual cells and sigma levels for depth (Figure 8). Grid sizes are smaller in areas of interest (10 m resolution) and larger in more distant regions. The driving mechanisms for the model are river discharge, tides, offshore salinity in Long Island Sound, wind, sediment-discharge relationships for the Connecticut, and bed sediment composition. The model uses a variable roughness proportional to the water depth to incorporate bedform roughness. Model outputs of interest include time series of boundary shear stresses, current velocities, suspended-sediment concentrations, and net deposition and erosion throughout the estuary. The results reported in this study are from a low-resolution model run with output every 30 minutes.

3.5 Analyses

3.5.1 Grain Size

Statistical measures of grain size were calculated using the Folk and Ward graphical method (Figure 9) with the GRADISTAT software package (Blott and Pye, 2001). The primary statistical grain-size parameters used in this analysis are D_{10}, D_{50}, and D_{90}. The D_{50}, or median grain size, is a measure of central tendency in the size distribution. The grain size diameter at which 90 percent of the grains are equal or smaller than is defined as the D_{90}, and likewise the diameter at which 10 percent of the grains are equal to or smaller is defined as the D_{10}. For descriptive purposes, the sediment was classified based on the Wentworth grain size chart (Wentworth, 1922). The sediment samples were divided into two fractions: *coarse* and *fine*. The *fine* sediments are defined as those less than 63 microns; the percentage of *fines* is used as a descriptor of the sediment at each sample location. Sorting was also quantified using the Folk and Ward graphical method; sorting refers to the spread or standard deviation of the grain size distribution.

3.5.2 Critical Shear Stress

Critical shear stresses for the D_{10}, D_{50}, and D_{90} at each core location were determined using an empirical formulation of the Shields curve (Soulsby and Whitehouse, 1997). These calculated critical shear stresses, τ_c, were compared to the observed shear stress in the field, τ_o, and the shear stress predicted by the model, τ_m.

3.5.3 Boundary Shear Stress

Velocity data from the ADV were used to calculate shear stress according to three common methods (e.g. Kim et al. 2000): Reynolds stresses, Turbulent Kinetic Energy (TKE), and Inertial Dissipation (ID). The direct estimates of τ_o then can be used to calculate z_0 and C_D, which provide insight on the bottom characteristics. Each of these methods has advantages and drawbacks. The Reynolds Stress method uses measurements of velocity fluctuations and has the potential to be most accurate, but slight changes in the positioning of the sensor can distort and corrupt these measurements. The TKE method has consistent results, but relies on an empirical constant to determine the shear stress. This constant is not always consistent with the literature. Using the ID method, the sensor location is sensitive; to have adequate separation between the production and dissipation of energy in the spectrum, the sensor must not be too close to the bed (Kim et al., 2000).

These methods assume a steady and horizontally uniform flow, and that the measurements are taken within the log layer. The velocity measurements were rotated into the direction of maximum variance before the analysis was done. In this way, both the mean of *v* and *w* were approximately zero. In ideal situations, this rotation would not be necessary because the tripod should self-orient into the direction of the flow, but this was not always true due to changes in the flow during the measurements as well as poor placement of the tripod in reference to sand waves.

3.5.4.1 ADV Data Processing and Data Quality

Every 10-minute time series of velocity for each time the tripod was on the bottom was evaluated for data quality. The criteria for excluding and/or altering the averaging period were as follows (Figure 10):

1. Unstable tripod from pressure data on the ADV
2. Unstable pitch and tilt, as recorded on the ADV
3. Mean velocity <10 cm/s
4. Accelerating or decelerating flow (more than a 25% change in the mean velocity over the averaging period)
5. Vertical velocity > 0.1 cm/s
6. Unstable heading, as recorded by the ADV
7. Incorrect orientation of the tripod compared to the flow, as determined from the sign (+/-) of velocity data from the ADV

For data that met the excluding criteria, the length of the dataset was shortened and then the data were reevaluated. Data that did not meet these conditions after shortening the time series were excluded from analysis. See appendix for details on data quality analysis.

3.5.4.2 Reynolds Stresses

Shear stress determined from Reynolds stresses using the covariance method requires high frequency velocity measurements at one height above the bed within the log layer and is formulated as follows (Dewey and Crawford, 1988; Kim et al., 2000; Thompson et al., 2003):

$$\tau_b = -\rho\overline{u'w'} \tag{13}$$

where *u'* and *w'* are the deviations from the mean velocity in the along-channel and vertical directions (Figure 11A). This method relates vertical transfer of momentum to the shear stress exerted on the bed, or shear production (Middleton and Southard, 1984; Thompson et al., 2003).

Reynolds shear stresses are derived from the Reynolds-averaged Navier-Stokes equations (Pope, 2000). In a turbulent flow, if a water particle moves upward, resulting in a positive *w* effect, it moves into a faster flow and thus slows down surrounding water particles, resulting in a negative effect. Likewise, if a turbulent motion moves a particle downward resulting in a negative *w* effect, it moves into a slower flow and thus speeds up the surrounding particle resulting in a positive u effect. Therefore, *u'w'* is always negative and the minus sign in Equation 13 results in a positive stress on the bed.

3.5.4.3 Turbulent Kinetic Energy

The TKE method relates velocity fluctuations to the bed stress (Soulsby, 1983; Stapleton and Huntley, 1995; Thompson et al., 2003),

$$TKE = \frac{1}{2}\rho(\overline{u'^2} + \overline{v'^2} + \overline{w^2}) \tag{14}$$

where *u'*, *v'*, and *w'* are the deviations from the mean velocities in the x, y, and z directions, respectively. Using the calculated TKE, the boundary shear stress can be calculated using an empirical relationship formulated through models (Soulsby and Dyer, 1981; Galperin et al., 1988) or by examining flows under a variety of conditions (Soulsby, 1983; Stapleton and Huntley, 1995 in Thompson et al., 2003),

$$\tau_b = C_1 TKE \tag{15}$$

Modeling studies found that C_1 = 0.20, while experimental values yielded a value of 0.19 for all environments, which is now commonly used (Kim et al., 2000; Mariotti et al., 2014). However, some studies have found variations in C_1 (Kim et al., 2000). The calculation for TKE typically uses a spectral splitting method in the presence of wave bands (Soulsby, 1983 in Stapleton and Huntley, 1995), but can also be done without the aid of spectral analysis when a wave band is not present.

To implement this method, the spectra of the three velocity components were calculated. The area under these spectra is used as the velocity fluctuations and the turbulent kinetic energy density was calculated (Figure 11B).

3.5.4.4 Inertial Dissipation

The ID method follows the same assumptions, and also assumes a balance between shear production and energy dissipation (Tennekes and Lumley, 1972 in Kim et al., 2000). By substituting the Reynolds stress and the logarithmic profile equations into the balance between shear production and energy dissipation, one can relate the shear velocity to the energy dissipation,

$$u_* = (\varepsilon \kappa z)^{1/3} \tag{16}$$

where ε is the energy dissipation. The inertial subrange exists in the spectrum between the low frequencies that produce energy and the high frequencies that dissipate energy, which takes the form

$$\phi_{ii}(k) = \alpha_i \varepsilon^{2/3} k^{-5/3} \tag{17}$$

where $\phi_{ii}(k)$ is the spectral density of the velocity in one direction at wave number k and α is the Kolmogorov constant. These equations can then be combined and Taylor's "frozen turbulence" hypothesis can be applied to convert the frequency spectra into wave-number spectra, which yields the final equation to calculate the shear stress using the ID method (Kim et al. 2000).

$$u_* = \left(\frac{2\pi\kappa z}{\bar{u}}\right)^{1/3} \left(\frac{\phi_{ww}(f) f^{5/3}}{\alpha_3}\right)^{1/2} \tag{18}$$

It is most common to use only the vertical velocity spectra because these fluctuations are more likely due to turbulence rather than waves or other sources (Stapleton and Huntley, 1995; Kim et al., 2000). In the spectrum, the inertial subrange is determined to be when $f^{5/3}\phi_{ww}(f)$ is constant. Using this frequency range, the shear velocity, and therefore shear stress, were calculated (Figure 11C).

3.5.5 Drag Coefficient and Roughness

The Quadratic Stress Law (Equation 8) was employed to solve for the drag coefficient using the velocity and different boundary shear stress calculation methods for each anchor station site (Soulsby, 1997; Thompson et al., 2003)

$$C_D = \frac{\tau_b}{\rho u_z^2} \tag{19}$$

Using the von Kármán-Prandtl equation (Equation 2) and the calculated values of shear stress from velocity at a known height above the bed, the roughness parameter, z_0, was also determined. For comparison, the boundary shear stress was calculated using the Quadratic Stress Law using the magnitude of the velocity and a generalized drag coefficient (3×10^{-3}; Sternberg 1972).

3.5.6 Bedload Transport Rates

In the case where $P > 2.5$ and the boundary shear stress exceeds the critical shear stress, the sediment is assumed to be transported as bedload. To quantify bedload transport, q_b, we used the Yalin bedload formulation (Yalin, 1972)

$$q_b = 0.635r\sqrt{\frac{\tau_b}{(\rho_s-\rho)gD}}\left[1-\frac{1}{ar}\ln(1+ar)\right]\sqrt{\left(\left(\rho_s/\rho\right)-1\right)gD^3} \qquad (20)$$

where

$$r = \frac{\tau_b-\tau_c}{\tau_c} \qquad (21)$$

$$a = 2.45\left(\frac{\tau_c}{(\rho_s-\rho)gD}\right)^{0.5}\left(\frac{\rho}{\rho_s}\right)^{0.4} \qquad (22)$$

and q_b is the bedload transport rate, reported in g/cm/s. The transport was integrated over a tidal cycle to evaluate net magnitude and direction of transport.

3.5.7 Bedforms and Knudsen Echosounder Data Processing

Distinct bedform fields (BFFs) were identified using the USGS bathymetry survey (USGS, *unpublished data*). Transects from the bathymetry data and from the echosounder data for the different BFFs were identified and analyzed. The shapes of the bedforms were used to determine orientation (Middleton and Southard, 1984).

Bedforms were quantified using a Fourier transform, which determined the component waveforms and corresponding amplitudes. Data from the echosounder surveys were interpolated for equal sample spacing and processed using a moving-average filter. The filtered data were windowed using a Hanning window and each overlapping section of the surveys was transformed using the Fourier transform, which identified the dominant waveforms that made up the sand waves. Transects from the echosounder were cross-correlated with transects from each BFF defined on the USGS survey to determine similarity.

4. Results

4.1 Bed Sediment Distribution and Characteristics

Grain size analysis results from 383 samples are presented in detail in Appendix A and are summarized in Figures 12-21. Grain size analysis confirmed, as previously shown by Horne and Patton (1989), that most of the bottom of the Connecticut River is sandy with small amounts of fine sediment (Figure 12, 13). Bottom sediment generally fined towards the mouth of the estuary (Figure 14, 15). The median grain size was finer in the center of the channel (across-channel stations 2-4) near the mouth compared to upriver (Figure 15). Peaks of finer grain size and percent fines within the northern parts of the study area (example: 8 km from the mouth, Figure 14) broke a monotonic fining trend.

Within the channel in M13 and M14, fine sediments were restricted to the southern part of the estuary (up to 8 km and 4 km of the mouth, respectively), while in N12 and N13, fine sediments were found within the channel throughout the study area (Figure 14A). However, fine sediments were confined to the sides of the channel in the northern parts (Figure 14B).

The majority of cores were composed of medium to fine sand. The average D_{50} for all cores was 1.7ϕ for the coarse fraction. Eighty-eight of 383 cores exhibited a "mud drape." These cores were characteristically sandy, but had a thin veneer (0.5 – 3 mm) of finer grained material on the top of the core (e.g. Figure 6D). The mud drape was observed throughout the estuary for all field seasons. Of the 383 cores, 16 were composed of 75 -100 % fine sediments. These muddy cores were found near the mouth of the estuary or on the western sides of the channel ~8 km north of the mouth (Figure

12).

The grain size and the percent fines were more variable towards the mouth of the estuary compared to upriver sites (Figure 14, 15). Fine sediments were found on the sides of the channels, but significant amounts of deposited fine sediments were not found in the main channel (Figure 16). The western side of the estuary had significantly more fines compared to the center of the channel ($p<0.001$), but the eastern side was not significantly different in terms of percent fine material compared to the center of the channel. In the lower estuary, the fines were not restricted to the sides of the channel (Figure 17D). However, in the northern parts of the study area, fines were either nonexistent (Figure 17A) or were only present on the sides of the channel (Figure 17B, 17C). Approximately 5 km north of the mouth where the channel is oriented north-south, the fine sediments were present on both sides of the channel (Figure 17C). Where the channel turns, approximately 8 km north of the mouth, the fines were restricted to the western side of the channel (Figure 17B).

In areas with only sand present, the mode was well defined (Figure 18A). In areas with both sand and mud present, the distribution was bimodal, with peaks in both the coarse fraction and in the finer fraction (Figure 18B). The sediment was the least sorted near the mouth and became more sorted in the upstream parts of the estuary (Figure 19). Over the field seasons N12, M13, and N13 the sediments on average were poorly sorted (Figure 20). Sediments from N13 were the most poorly sorted of all field experiments. In M14, the sediments were moderately well to moderately sorted.

Sediment characteristics in M14 were significantly different than the sediment characteristics in N13. The D_{50} was significantly different ($p = 0.023$), the D_{50} of the coarse fraction was significantly different (p=0.026), and the percentage of fine sediments in the estuary was significantly different (p=0.005). Median grain size and percent fines in the estuary between the first three consecutive field seasons were not significantly different. The D_{50} in M13 was the lowest, while the D_{50} in M14 was the highest. Both fall seasons (N12 and N13) had similar grain size characteristics.

The fine fraction of sediments on the bed had a D_{50} of 5-10 microns (Figure 21). If the fine fraction is acting as single grains, the calculated settling velocity of these particles was 0.0144 – 0.0577 mm/s.

4.2 Loss on Ignition

LOI varied from 0.29 to 14.94 % within the Connecticut River estuary, with a mean of 1.97 ± 2.08 % over all field seasons and no significant differences between the field seasons (Table 2, Appendix A.3). The organic matter was not evenly distributed throughout the estuary and tended to be near the sides of the channel (Figure 22). Organic matter was proportional to the percent of fine sediments (Figure 23). Low values of LOI, and the associated small amounts of fine sediments, indicate that biological factors are likely not significant in sediment transport in the estuary; there was no evidence of cohesive biofilms that might affect erosion within the channel.

4.3 Calculated Critical Shear Stresses

The critical shear stresses were calculated for the D_{50}, D_{10}, and D_{90} of each surface sediment sample (Figures 24-26, Appendix A.4). The necessary stress to mobilize the median grain size ranged from 0.02 to 1.7 N/m^2, which relates to a shear velocity of 0.0044 to 0.041 m/s. N13 and M14 datasets have comparable and intensive sampling schemes and can be directly compared. The critical shear stress required to mobilize the D_{50} and D_{90} was relatively homogeneous and consistent between all field seasons (Figure 24, 26). The critical shear stress required to mobilize the D_{10} was higher throughout the estuary in M14 compared to N13, particularly ~8 km from the mouth (Figure 25). The D_{10} was larger in M14 compared to N13, leading to greater critical shear stresses.

Observed shear stress at anchor stations, τ_o, exceeded the critical shear stress for the D_{50} during maximum flow (Figures 27-32), suggesting that the 50% of the sandy bed was mobile at some point during the measurement periods. The Rouse parameter was greater than 2.5 for all measurement periods when τ_o exceeds the critical shear stress, indicating that the sediment was being transported as bedload. No full tidal cycle records were captured using the tripod, and therefore bedload transport was reported as cumulative bedload over the time the measurements were taken instead of averaged over the tidal cycle (Figures 27-32). Generally, the shear stress from the QSL agreed with or overestimated bedload transport during the anchor stations compared to the Reynolds, TKE, and ID methods, with some exceptions (Figure 27, 29). The QSL did not take into account additional roughness created by the bedforms; a constant drag coefficient of 3×10^{-3} is applicable for planar beds (Sternberg 1972). The additional roughness from the bedforms created form drag, which decreased the effective shear stress on the bed leading to the smaller shear stresses, as calculated by the Reynolds, TKE, and ID methods. The QSL method did not include the larger roughness elements and therefore overestimated skin friction, shear stress, and bedload sediment transport.

4.4 Modeled Mobilization and Transport

Comparing model output for 1-month simulations of N13 and M14 to the critical shear stress revealed that the bottom sediment was mobilized frequently, during both the ebb and flood (Figure 33-35). The percent of the time that the median grain size on the bed was mobilized was greater in M14, under high discharge conditions (~1250 m^3/s), compared to low discharge conditions (N13; 400 m^3/s) (Figure 33). The tidal amplitudes in the model were roughly 1.4 m on average in both model runs (two month-long simulations). In the northern part of the study area, the bed was most frequently mobilized during the ebb for both N13 and M14. Towards the southern part of the study area, the bed was more frequently mobilized during the flood compared to the northern part of the estuary.

In N13, the bed was mobilized equally during the flood compared to the ebb, but in different patterns (Figure 34). Under flood conditions, the amount of the time the bed was mobilized was homogenous throughout the estuary; on average the bed was mobilized 40% of the time during the flood. Conversely, during the ebb the bed was mobilized in a gradient from north to south. In the northern reaches of the estuary, the bed was mobilized more frequently compared to the areas near the mouth.

The mobilization of the bed was more asymmetric throughout the tidal cycle in M14 (Figure 35). During the ebb, a majority of the core locations were mobilized about 60-80% of the time. The northern locations were mobilized about 80% of the time; the only locations that were mobilized less than 50% were in the southern reaches of the estuary. In contrast, during the flood, mobilization was more homogenous throughout the estuary. The area approximately 4-5 km from the mouth was mobilized most frequently (about 50% of the time), while the rest of the study site was mobilized less frequently, with an average frequency of 30%.

The Rouse parameter, *P*, exceeded 2.5 the majority of the time for median grain size particles for both N13 and M14 model simulations (Figure 36). This indicates that the sediment was being transported as bedload, as opposed to suspended load. The D_{50} of the coarse fraction of the sediment was being moved in the water column only 2.7 % of the time during the November 2013 model run and 2.4 % of the time during May 2014.

Tidally averaged bedload transport rates for the median grain size under low discharge conditions (N13) and high discharge conditions (M14) indicate that most areas consistently had ebb-dominated transport patterns (Figure 37). In M14, the sediment was moving towards the Sound for the majority of sample locations. Under low discharge conditions (N13), the lower estuary had areas with net northward transport while the upper estuary had net southward transport. The magnitude of net bedload transport was smaller in N13 compared to M14. Bedload calculations assumed transportable material is available; sandy bed material is not commonly a limiting factor in bedload transport (Horne and Patton, 1989).

The D_{10} often was within the mud fraction for the mud drape, and therefore was a way to represent the mobilization of the mud drape. Additionally, the floc sizes (100 – 200 microns, Milligan pers. comm.) in the water column were comparable to the D_{10}. Assuming the flocs in the water column made up the mud drape, which was supported by visual evidence of flocs in the mud drape, the D_{10} of the disaggregated bottom sediment was representative of the mud drape sediment. In N13, the D_{10} was mobilized heterogeneously, with no apparent pattern, throughout the estuary, while in M14 the upper estuary was mobilized ~70% of the time and the lower estuary was mobilized 30-40% of the time (Figure 38). The mobilization of the D_{10}, or mud drape, was similar between the ebb and flood during N13 (Figure 39). The lower estuary (~2 km from the mouth) and the area ~8 km from the mouth were mobilized frequently (>50% of the time), while the middle estuary (~6 km from the mouth) was mobilized ~30% of the time. In M14, there was asymmetry between the mobilization during the flood and ebb (Figure 40). During the flood, the sediment (D_{10}) was mobilized on average 40% of the time, with peaks of mobilization ~5 km from the mouth and adjacent to the mouth. During the ebb, the upper estuary was mobilized 80-100% of the time; the lower estuary is mobilized less frequently. The net bedload transport per tidal cycle of the D_{10} in N13 was near zero, with dominant seaward transport ~12 km from the mouth and net landward transport ~5 km from the mouth (Figure 41A). Adjacent to the mouth, bedload was near zero. Landward transport was dominant at locations up to ~10 km from the mouth. During M14, the net bedload of the D_{10} was seaward in the upper estuary; in the lower estuary (0-4 km from the mouth), the net transport was near zero, with some landward transport (Figure 41B). Net bedload transport calculations of the D_{10} assumed that sediment was available for transport at each location; transport could have been limited by sediment supply. The Rouse parameter for the D_{10} indicated that the sediment was often transported as suspended load or a mixture of suspended and bed load.

4.5 Shear Stresses, Drag Coefficients, and Roughness

Calculated boundary shear stress values from the Reynolds and TKE methods were similar (1:1 ratio), while the ID method underestimated shear stress (Figure 42). Furthermore, the Reynolds stresses and the shear stresses derived from the TKE method were similar to the shear stresses calculation using the QSL with a constant drag coefficient of 3×10^{-3}. The drag coefficients and roughness lengths for each measurement period indicated variations in roughness throughout the estuary (Figure 43).

Percent fines and the drag coefficient over all methods were significantly related as an exponential function (Figure 44, R^2=0.13, $p<0.05$). The greater the percent of fines in the sediment, the lower the drag coefficient. However, once a certain threshold of fine sediment was reached, changes in the drag coefficient were small and insignificant. No relationship was evident between the D_{50} and the drag coefficient (Figure 45).

Calculated z_0 values from the ADV data were smaller than those calculated using hydraulic roughness (Table 3) in areas with bedforms; in areas with no bedforms, z_0 was on the same order of magnitude using the Reynolds, TKE, and ID methods compared to the roughness length calculated using Equation 9. The form drag component of the hydraulic roughness was the largest component; it was 1-2 orders of magnitude larger than the contributions due to the grain diameter and bedload.

4.6 Comparison of model and field data

Modeled shear stress and field observations of shear stress were comparable (Figures 27-32). The amplitudes of the shear stresses were similar (Figures 27-29), and the timing of the shear stresses was aligned for the most part (Figure 28-31) with only slight phase changes (Figures 27, 32). Shear stresses were compared from field observations at anchor stations to shear stresses at the nearest core locations from that field experiment. This small discrepancy in location could account for slight phase shifts and amplitude differences. Likewise, bedload transport rates were also comparable between model and field data (using the QSL). Shear stress measurements without using a constant drag coefficient of 3.0×10^{-3} (Reynolds, TKE, and ID methods) also agreed relatively well with the modeled shear stresses. However, the shear stresses and transport rates using these methods were lower compared to those calculated using the model or the QSL (Figures 30-32).

While bedload transport rates between the model and field data were comparable, the cumulative bedload transport rates over the measurement period differed by up to a factor of 2 (Figure 30). These differences in cumulative transport could lead to erroneous net bedload transport rates using the modeled shear stress. The field measurements did not capture a full tidal cycle, so I am unable to determine whether the tidally averaged bedload was affected by the differences between the model and the observations. Further comparison between modeled and observed shear stress are discussed in section 5.4.

4.7 Bedform Fields

Eight distinct bedform fields (BFF 1-8) with different morphologies (i.e. characteristic wavelengths and amplitudes) were identified on the USGS survey within the estuary (Figure 46). The largest sand waves were in the northern part of the study area; the amplitude of the sand waves decreased moving towards Long Island Sound. The majority of the waves were ebb-oriented; only the southern part of the southern-most bedform field displayed flood-dominated bedforms (Figure 46).

The characteristic wavelengths of the BFFs are described in Table 4. BFF1 was characterized by ebb-oriented sand waves with amplitudes of 2 m (Figure 47A). In BFF2 and BFF3, the sand waves had amplitudes of 0.5 m (Figure 47B,C). BFF4, which was located where the channel constricts, had amplitudes of 2 meters (Figure 47D). BFF5 was characterized by 1 meter sand waves (Figure 47E). Sand waves in BFF6 had amplitudes of 0.5 m (Figure 47F). The bedforms within BFF7 had amplitudes of 1 – 1.5 m (Figure 47G). While the sand waves in BFF8 in the northern portion were ebb-dominated, as denoted by shape, they were not as unidirectional as the other bedforms in the northern BFFs. They had a 0.5 m amplitude (Figure 47H). The middle transect in BFF8 also had the same amplitude as the northern transect in BFF8, but the bedforms had a more ebb-dominated shape (Figure 47I). The southern-most transect in BFF8 hosted flood-dominated bedforms with similar amplitudes as the other transects in BFF8 (Figure 47J). The reported amplitudes were approximations; the bedforms are modified during the tidal cycle (Horne and Patton, 1989) and therefore more measurements are required to determine the amplitudes more precisely. Wavelengths and bedform orientation from transects identified from the echosounder surveys agreed with transects from the USGS survey (e.g. Figure 48; Table 4).

5. Discussion

5.1 Discharge-Driven Bed Morphology and Bedload Sediment Transport

The bottom sediment characteristics and net bedload sediment transport direction suggest that river discharge governs the bed morphology of the estuary, and tidal influences are secondary. In M14, instantaneous discharge, as well as cumulative discharge leading up to sampling, was the highest of all sampling periods (~1250 m^3/s; Figure 5) and is referred to as the "high-discharge condition". N13 had the both the lowest instantaneous discharge of all sampling periods, the lowest cumulative discharge leading up to sampling of all sampling periods (~400 m^3/s; Figure 5), and was lower than the annual long-term average (~450 m^3/s) discharge and will be considered the "low-discharge condition".

5.1.1 High-Discharge Conditions – May 2014

Under high discharge conditions during M14, grain size decreased towards the mouth of estuary (Figure 15). The gradual fining of the grain size of the coarse fraction of the sediment towards the river mouth is consistent with hydrodynamic control (McLaren, 1981). Well-sorted sediments are also a marker of a system dictated by unidirectional flow; in M14, the sediments were more sorted compared to other field seasons (Figure 20). This indicates that under high-discharge conditions (M14), the river was the primary force affecting the grain size distributions and tidal and residual currents are secondary. The decrease in sorting near the mouth under high-discharge conditions suggests that tidal influences do affect the grain size distributions in the lower estuary. The high river discharge, leading to the expulsion of the salt intrusion from the estuary, did not allow the storage of fine sediments on the bed within the channel; the only locations with storage of fines are the sides of the channel (Figure 17) or the coves (Woodruff et al., 2013). The estimated boundary shear stresses from the *river alone* using the river discharge and cross-sectional area of the channel (Anderson and Anderson, 2010) for ~8 km and ~6 km from the mouth were 1.77 N/m^2 and 1.82 N/m^2 during high-discharge (M14), respectively. This is compared to boundary shear stresses of 0.66 N/m^2 and 0.67 N/m^2 during low-discharge (N13) at the same locations, once again ignoring tides. During high-discharge, the calculated shear stress values for the *river alone* were more than double the shear stress from the river alone during low-discharge and exceed the observed shear stresses (τ_o). [This is compared to an extreme event like the five-year flood Hurricane Irene with a peak discharge of 3625 m^3/s, which relates to calculated stresses from the *river alone* of 9.5 and 9.8 N/m^2 at the same locations.] This is in comparison with measured shear stresses, representative of the role of the tides, of ~1 N/m^2 in both N13 (6 and 8 km from the mouth) and M14 (6 km from the mouth). During M14, the shear stress from discharge plays a larger role, while in N13, the tides play a larger role compared to discharge near the mouth. The high-discharge period (M14) exhibited the largest average D_{50}, further supporting the correlation between discharge and the sediment distributions.

Net bedload calculations for the median grain size suggested net southward transport during high-discharge conditions throughout the majority of the estuary (Figure 37B). Near the mouth in the lower estuary was a region of net landward bedload transport. These patterns of bedload transport were reflected in the bedform orientation. Bedforms throughout the majority of the estuary, historically (Horne and Patton, 1989) and from the present study, were ebb-oriented, or suggested southward sediment transport. The only observed flood-oriented bedforms were very near the mouth and were surrounded by ebb-oriented and bidirectional bedforms (BFF8, Figure 46, 47). The bedform orientations agree with net bedload transport under high-discharge conditions, indicating that these bedforms are representative of high-discharge conditions.

Under the high-discharge conditions, the tides only influenced the bed morphology of the estuary near the mouth. The sediment distributions had higher variance near the mouth and were more poorly sorted. Furthermore, the flood-oriented bedforms near the mouth and net bedload calculations indicated that sediment was driven landward, likely by the tidal currents.

5.1.2 Low-Discharge Conditions – November 2013

During low discharge periods (N13) grain size and sorting changes reflected a more balanced discharge-tidal regime. The sediments were more poorly sorted (Figure 20) and the median grain size was significantly different than the D_{50} during high discharge.

Net bedload transport calculations for the D_{50} indicated seaward movement of bedload sediment in the upper estuary and landward movement in the lower estuary, up to 8 km north of the mouth (Figure 37A). The direction of net bedload transport under low-flow conditions did not correspond to bedform direction in the middle of the estuary; only the northern-most bedforms correspond to the seaward bedload transport and the southern-most bedforms correspond to the landward bedload transport. In the middle of the estuary, the direction of net bedload transport varied. This indicates that tides are playing a larger role in bedload transport ~8-10 km from the mouth compared to bedload transport in the same location under high-discharge conditions.

Ultimately, the grain size and sorting are able to respond to discharge changes and tidal currents, but the larger scale bedforms (> 0.5 m) reflect the high-discharge condition and are only altered on smaller scales due to tidal transport.

5.2 Two Distinct Sediment Populations

Bottom sediment samples showed two sediment size classes in the Connecticut River estuary: sand and mud. The sand (mean D_{50} = 300 μm) and mud (mean D_{50} = 5-10 μm) made up a bimodal sediment distribution (Figure 18B) throughout most of the estuary (Appendix A.2). In the upper estuary, the sediment tended toward a unimodal distribution with only the sand fraction present, while in the lower estuary (0 to 3 km) both fractions were present in all samples.

The sand fraction made up the majority of the bed of the estuary. The sand fraction moved primarily as bedload; the Rouse parameter for the D_{50} exceeded 2.5,the threshold between bedload and suspended load, and was less than 12, an approximate threshold for grain movement, ~25% of the time in N13 and ~30% of the time in M14. The threshold of a P value of 12 for the threshold of grain movement was determined experimentally by comparing the P value to the calculated critical shear stress for each core location. This indicates that the sediment was moving as bedload 25% of the time in N13 and 30% of the time in M14. On average, the sand was not being transported the majority of the time (Figure 36); this varied by location and phase of the tide (Figure 33-35). Furthermore, the sand waves were oriented southward, which is indicative of net seaward bedload transport.

The mud fraction was primarily found on the margins of the estuary (Figure 12, 17). Fine sediments were consistently found throughout all field seasons on the western sides of the channel ~8 km from the mouth. Fine sediments were also commonly found as a ‘mud drape’ (Figure 6D). Although the locations of these two types of mud areas (muddy cores or cores with a mud drape) were different, the grain size distributions of the muds were similar throughout the estuary (Figure 21), suggesting that the mud fraction distribution was homogenous throughout the estuary, even though the absolute amount of mud in the estuary varied. The fine sediment in the water column had a similar distribution to that of the mud found on the bed, both in the mud drape and on the margins (Figure 49, Milligan pers. comm.), suggesting that it is the same material throughout the estuary, both on the bed and in the water column.

The Rouse parameter suggested that the muds were moving through the estuary primarily as suspended load; however, these calculations are from disaggregated particles. The value of P suggested that these particles would almost *never* settle, but we know that this was not the case, as we saw mud accumulation on the sides of the channel and in the coves (Woodruff et al. 2013), as well as the mud drape. The sides of the channel and the coves are likely stress refuges that have low enough shear velocities to allow particles to settle; however the mud drape occurred in areas that experience high stresses. The presence of the mud drape suggests enhanced particle settling; the settling velocity of the disaggregated particles was small and cannot account for a layer of mud on the bed. For the Rouse Parameter to suggest that these particles are being transported as suspended load, the necessary shear velocity is 0.000029 – 0.00012 m/s (or a boundary shear stress of $8.8 \times 10^{-7} - 1.4 \times 10^{-5}$ N/m^2). This relates to a current velocity of 0.00054 - 0.0022 m/s at one meter above the bed. During the measurement periods and in the model, velocities consistently exceeded this value. Without enhanced settling, the mud drape could not exist. Potential mechanisms for enhanced settling include flocculation, stratification, and sediment trapping at fronts. Direct measurements of suspended particles showed floc sizes in the range of 100-200 microns, indicating that flocs were present and are at least one of the mechanisms for enhanced settling (Kineke et al. 2014).

High accumulation rates of fine sediments in the coves (Woodruff et al. 2013) can be explained by northward movement of fines during low-discharge conditions; muds initially delivered to Long Island Sound are transported northwards into the estuary with the migration of the salt intrusion. The landward extent of the salt intrusion, which is dictated by river discharge, correlates with the location of fine sediments within the channel of the estuary (Figure 50, Wehof pers. comm.). Under high discharge conditions, the salt wedge is expelled from the estuary and most fine sediments are in suspension and discharged to Long Island Sound. Fine sediments were only found in lower 4 km from the mouth in the channel in M14, under the highest discharge conditions and the southern-most position of the salt intrusion. In M13, under moderate-flow conditions (~500 m^3/s; Figure 5), the salt intrusion did not extend beyond 10 km from the mouth; fine sediments were present in the channel up to 10 km north of the mouth. Under the low-discharge conditions, the salt intrusion extended throughout the entire study area and fine sediments were observed in the channel throughout the estuary. The landward transport of fine sediments accompanies the migration of the salt, introducing them to the channel in the upper reaches of the estuary and eventually onto the margins or into the coves. Similarly, using the D_{10} as a proxy for the mud drape, the calculated net bedload transport of the D_{10} had landward transport up to ~10-11 km from the mouth in N13 and ~4 km from the mouth in M14 (Figure 41). This corresponds to the same distances landward that fine sediments were observed in the channel, suggesting that the fine fraction of sediments are transported landward.

5.3 Roughness

Although the roughness length and drag coefficient were highly variable, the results showed specific trends that affect sediment transport patterns. The drag coefficient was correlated to percent fines (Figure 44). The amount of mud in the location affected the drag coefficient more than small changes in the grain size (C_{100} is not related to D_{50}).

Calculations of the drag coefficient from current velocity measurements showed variations that can be attributed to the surrounding bedform fields. In BFF8 near the mouth of the estuary there was a trend in the drag coefficient in all three methods with changing current velocity (Figure 31). I hypothesize that the "cyclical" variations were due to roughness from the bedforms near the study area. Net bedload calculations at this location were both seaward and landward; this indicates that the bedforms were often reworked and modified during by tidal currents. Furthermore, the sand waves were more bidirectional in this area, with evidence of both flood and ebb currents. Migrating sand waves (or migrating ripples on top of the sand waves) and changes in the shape of the bedforms through the tidal cycle can change the drag coefficient. Likewise, in BFF4 there were changes in C_{100} during the flood tide that follow the same trend (Figure 27). Bathymetry surveys showed smaller ripples on top of the sand waves in this region; the large stoss surface of the sand waves are conducive to forming smaller sand waves that change through a tidal cycle.

The location of the tripod relative to the bedforms affected the roughness calculation. One station was located between two bedform fields and due to the change in tides, the measurements were taken in two locations ~120 m from each other (May 14, 2014; Figure 30). For the first half of the time series, the flow was flooding; during the second half of the time series, the flow was ebbing. From 10:00 to 13:00, the measurements are downstream of BFF8. In the later part of the time series, the flow had passed along a narrow area without bedforms, immediately to the northeast of BFF7. These different pathways affected what roughness is being measured (Figure 51). Early in the time series, C_{100} was variable; later in the time series the drag coefficient was constant (Figure 30C). The variable roughness from the bedforms could also suggest tidal modification of the bedforms, while the constant drag coefficient from the planar bed demonstrates that flat beds have constant roughness.

A variable value for the roughness or drag coefficient should be used when calculating sediment transport in places with bidirectional flow and bedforms. Using a constant value, or taking the mean of measured roughness length or drag coefficient over time, does not capture the variable bottom that interacts with the flow. The "scatter" in the drag coefficient data within each method (scatter between methods is from the use of the different methods) represented real variations in the drag coefficient, roughness, and changes to the relative effects of form drag and skin friction over time.

The discrepancy in the roughness length between those calculated using k'_b (Equation 9) and those using the ADV data directly was partially accounted for by the position of bedforms and effective shear stress due to skin friction. In areas with bedforms, k_{bm}, the bedload roughness, was overestimated. When bedforms are present, the stress felt by the bed is less than the total shear stress; the bedforms dissipate some of the turbulent energy. Therefore the effective energy that transports bedload is decreased, causing bedload transport to be over-predicted compared to actual rates.

5.4 Observations and the Model

Many of the differences between observed shear stresses and those determined using the model can be attributed to stratification and bedforms. At the anchor station between BFF7 and BFF8 on May 14th, 2014, the shear stress between 14:30 and 17:00 was much larger in the model compared to the measured stresses (Figure 30). At the time of peak shear stress calculated by the model (τ_m; ~4 N/m^2), the tide was ebbing and a thin layer of saline water close to the bed was present (Kristiansen, pers. comm.). This thin layer of stratification was not in the model output used in these calculations. Stratification suppresses turbulence, which would explain the lower values of τ_o during this time period.

The largest phase shifts observed between τ_m and τ_o occur in areas of large bedforms. On November 5th, 2013 in BFF4, the modeled shear stress was much higher in the beginning of the time series compared to the measured shear stress (Figure 27). This anchor station was near the largest bedforms and takes place during the flood and the transition to slack water. A similar phase shift occurred within BFF8 (Figure 32). In this case, the anchor station was located on the transition between BFF8a and BFF8b, where the shape of the bedform crests changed (Figure 46). The irregular shape was likely more affected by tidal modification of the bedforms, which could have led to the difference between τ_o and τ_m. Other anchor stations (Figure 28, 29) had no phase shift and were in areas with small or no bedforms.

5.5 Long Term Bathymetric Patterns

The BFFs of the Connecticut River estuary were persistent over a minimum of 25 years, under normal conditions as well as following storm conditions, based on previous work (Horne and Patton, 1989), the USGS bathymetric data (Figure 46, 47) and the echosounder data from this study (Figure 48, Table 4). While the individual sand waves were modified by the tides and migrate accordingly, the overall morphology of each BFF remained a constant. Horne and Patton (1989) identified major bedform fields and compared 1980s bathymetry with navigational charts dating to the early 1900s. They found that the bed morphology in the Connecticut River estuary did not appreciably change during that time period. With an increased number of surveys, this study was able to distinctly identify five of the bedform fields described by Horne and Patton (1989) as five of the BFFs identified from the USGS survey (Table 4).

Furthermore, the survey done by the USGS was completed just prior to Hurricane Sandy. Hurricane Sandy, which made landfall on October 29, 2012, was a large event that impacted the coastline of the Connecticut River estuary. The wavelengths of the BFFs identified from this survey were similar to those from the echosounder surveys taken following the hurricane (Table 4). The similarities between the bed morphologies over 25 years between the study by Horne and Patton (1989) and the side-scan sonar survey, in addition to consistent bedform wavelengths before and after a major storm, suggest that the major processes driving bed morphology in the Connecticut River estuary, including river discharge, tides, and sediment supply, have not changed.

Near the mouth (2 km from the mouth), the D_{50} is on average 200-250 microns. The mean flow velocities necessary for large sand waves for this grain size are 0.60-

0.90 m/s; for ripple formation for this grain size, the mean flow velocities would need to be 0.15-0.60 m/s (Blatt et al., 1980). In M14, velocity measurements 1 mab achieved 0.40-0.50 m/s. In N13, velocity measurements 1 mab reached 0.50-0.60 m/s during maximum flood. Approximately 8 km from the mouth, the D_{50} is 350-375 microns. This relates to mean flow velocities of 0.50-1.00 m/s for dunes and 0.20-0.50 m/s for ripples (Blatt et al., 1980). In N13 at maximum flood, velocities reached 0.40 m/s 1 mab. During an extreme event (ex: Hurricane Irene), the estimated flow velocities exceeded 1.75 m/s 1 mab, which lies in the range of upper plane bed or antidunes (Blatt et al. 1980), which were not observed in the field. The maximum flow velocities during the average tidal cycle in N13 and M14 at 1 mab are comparable to the necessary depth-averaged velocities to form ripples and nearing the dune/sand wave regime.

5.6 Comparison to the Hudson River Estuary

Similarities between the underlying geology and structure of the Hudson River estuary and the Connecticut River estuary provide for a direct comparison between these two systems. Both estuaries are classified as drowned river valley estuaries and have a general north-south geometry. The salinity structures of both estuaries are considered partially-mixed (Garvine, 1974; Geyer et al. 2001). The maximum landward extent of the salt intrusion in Hudson River estuary is much longer (80 km) compared to that of the Connecticut River estuary (15 km).

The Hudson River supplies an estimated 0.2 – 1 million tons of sediment to New York Harbor annually (Bokuniewicz, 2006). The bed of the estuary is composed of primarily fine material; however the channel in the lower estuary is made of medium and fine sands (Ralston et al. 2012). The Hudson River estuary is known to have large sand waves on the bed, oriented primarily seaward (Bokuniewicz, 2006). There is evidence for some landward oriented bedforms in bifurcated channels. Sand waves have been observed in New York Harbor oriented landward (Bokuniewicz, 2006). Modeled suspended-sediment transport in the estuary suggests strong landward movement of sediment within the channels and seaward transport of sediment on the shoals (Ralston et al., 2012).

The Connecticut River is estimated to deliver on the order of millions of tons of sediment to Long Island sound per year, suggesting that the Connecticut delivers more sediment. The Hudson River estuary contains more fine sediments; however the distribution of sand in the channel and fines in the margins is consistent between both estuaries. The sand waves present in the channels in both estuaries have similar morphologies; they are landward near the mouth and seaward in the upper estuary. The present study suggests seaward bedload transport in the mid-to-upper estuary and landward bedload transport near the mouth. Furthermore, this study suggests landward advection of fine suspended sediments during low-discharge conditions within the channel, similar to the landward transport of fine sediments described in the Hudson. In the Connecticut River estuary, further work is needed to determine the fine suspended sediment transport direction on the margins of the channel. Although there are differences in the length of the estuary and the amount of fine sediments, the transport patterns within the two estuaries are very similar.

5.7 Future Work

Sediment sampling was limited by water depth and boat capabilities; we were unable to survey areas in depths less than ~2 m and therefore only know the sediment distribution within the channel. Determining the sediment distribution on the margins could help identify areas of fine sediment trapping; fine sediments were not found preserved on the bed in the channel and therefore no fine sediment trapping mechanism leading to localized accumulation is supported by the bed grain size data. Another avenue of future exploration is to look at the specific behavior and configuration of the sediment. Different packing of the bed with the same sediment composition can lead to different critical shear stresses. Additionally, the behavior of the mud in the estuary is an area of interest. If the mud drape is not cohesive and the muds on the sides of the channel are found to be cohesive, this could alter transport patterns and could be a part of a potential trapping mechanism. Lastly, future work should examine the role of bedforms in dissipating energy and shear stress.

6. Summary

Through intensive, high-resolution surveys of the Connecticut River estuary over four field experiments spanning two years and utilizing a three-dimensional circulation and sediment transport model, we are able to conclude that the annual high discharge conditions are likely responsible for seaward-oriented sand waves that are only slightly modified by tidal currents under low discharge periods. The grain size of the bed of the estuary changes between high and low discharge periods, reflecting the recent flow regime (Figure 13). During high discharge conditions, net bedload transport is primarily seaward throughout the estuary (Figure 37B). Under low discharge conditions, net bedload transport is landward in the lower estuary and seaward in the upper estuary (Figure 37A). The net amount of sediment transported per tidal cycle is greater under high discharge conditions (Figure 37).

The estuary bed is characterized by two distinct sediment populations: the sandy fraction and a fine fraction (Figure 12, 13). The fine fraction is preserved on the margins or near the mouth of the estuary; the mud is not observed in the channel bed beyond the extent of the salt intrusion (Figure 14). The salt intrusion likely plays an important role in transporting sediment recently discharged into Long Island Sound or deposited near the mouth of the estuary. The balance of discharge and tidal mixing sets the distance of the tidal intrusion in the estuary; the tidal resuspension of fines at medium to low discharge allows landward transport and eventual deposition in margins and coves within the estuary (Figure 50).

Roughness in the estuary is variable and is dominated by bedforms (Figure 43). Tidal modification of the bedforms, in addition to the change in direction of the flow can alter the roughness lengths. Additionally, relative location of measurements to bedforms can result in different estimates of roughness within or between bedform fields. Bedload calculations are sensitive to roughness changes, and therefore should be incorporated into transport models.

Bathymetry surveys from prior studies in the 1980s (Horne and Patton, 1989), a detailed pre-Hurricane Sandy USGS side-scan and multibeam sonar survey (Figure 46, 47), and post-Hurricane Sandy echosounder surveys (Figure 48, Table 4) show consistent bedform fields over a span of 25 years. This suggests that the major processes driving bed morphology in the Connecticut River estuary, including river discharge, tides, major storms and sediment supply, have not changed significantly in the past 25 years. The smaller bedforms (<1 m) observed in the field are able to be formed by maximum spring tidal currents and the larger bedforms (1-2 m) are able to be formed by annual flood events. Extreme events would likely form plane beds or antidunes, which were not observed in the field. Therefore, the bedforms observed in the field reflect typical conditions rather than extreme events.

7. References

Ackerman, S.D., Foster, D.S., Moore, E.M., Irwin, B.J., Blackwood, D.S., In preparation, 2015, High-resolution geophysical and sampling data collected at the mouth of Connecticut River, Old Saybrook to Essex, 2012, USGS Field Activity 2012-024-FA: U.S. Geological Survey data release.

Anderson, R.S., and S.P. Anderson, 2010, *Geomorphology,* Cambridge University Press, Cambridge.

Barbier, E.B., Hacker, S.D., Kennedy, C., Koch, E.W., Stier, A.C., and B.R. Silliman, 2011, The value of estuarine and coastal ecosystem services, *Ecological Monographs* 81: 169-193.

Blatt, H., Middleton, G., and R. Murray, 1980, *Origin of Sedimentary Rocks*, Prentice-Hall Inc, Englewood Cliffs.

Blott, S.J., and K. Pye, 2001, GRADISTAT: a grain size distribution and statistics package for the analysis of unconsolidated sediments, *Earth surface processes and Landforms* 26(11): 1237-1248.

Bokuniewicz, H., 2006, "Sedimentary Processes in the Hudson River Estuary", *The Hudson River Estuary*. Ed. Jeffrey S. Levinton and John R. Waldman. 1st ed. Cambridge: Cambridge University Press,. pp. 39-50.

Bowden, K.F., and L.A. Fairbairn, 1956, Measurements of turbulent fluctuations and Reynolds stresses in a tidal current, *Pro. Royal Soc., London*, 237(1210): 422-438.

Boyd, W.A., 1976, Hydrography, in The Connecticut River Ecological Study, p. 25-34.

Buffington, J.M., 1999, The legend of A.F. Shields, *Journal of Hydr. Engineering*, ASCE, 125(4): 376-387.

Channon, R.D., and D. Hamilton, 1971, Sea bottom velocity profiles on the continental shelf southwest of England, *Nature*, 231: 383-385.

Charnock, H., 1959, Tidal friction from currents near the sea bed, *Geophys. J.R. Astron. Soc.*, 2:215-221.

Dancey, C.L., Diplas, P., Papanicolaou, A., and M. Bala, 2002, Probability of individual grain movement and threshold condition, *Journal of Hydr. Engineering,* ASCE, 128(12): 1069-1075.

Dean, W.E., 1972, Determinations of carbonate and organic matter in calcareous sediments and sedimentary rocks by loss-on-ignition: comparison with other methods, *Journal of Sediment. Petrol.,* 44: 242-248.

Dewey, R.K., and W.R. Crawford, 1988, Bottom stress estimates from vertical dissipation rate profiles on the continental shelf, *Journal of Physical Oceanography*, 18: 1167-1177.

Dey, S., 2003, Threshold of sediment motion on combined transverse and longitudinal sloping beds, *Journal Hydr. Research*, 41(4): 405-415.

Dyer, K.R., 1970, Current velocity profiles in a tidal channel, *Geophys. J.R. Astron. Soc.*, 22:153-161.

Dyer, K.R., 1972, Bed shear stresses and the sedimentation of sandy gravels, *Marine Geology*, 13: M31-M36.

Dyer, K.R., 1980, Velocity profiles over a rippled bed and the threshold of movement of sand, *Estuarine Coastal Marine Science*, 10:181-199.

Dyer, K.R., 1986, *Coastal and Estuarine Sediment Dynamics*, John Wiley and Sons, Chichester: pp. 342.

Friedrichs, C.T., 2009, York River physical oceanography and sediment transport, *Journal of Coastal Research*: 17-22.

Folk, R.L., 1966, A review of grain-size parameters, *Sedimentology*, 6: 73:93.

Folk, R.L., and W.C. Ward, 1957, Brazos River bar: a study in the significance of grain size parameters, *Journal of Sedimentary Research* 27.1, 3-26.

Galperin, B., Kantha, L.H., Hassid, S., and A. Rosati, 1988, A quasi-equilibrium turbulent energy model for geophysical flows, *Journal of Atmospheric Science*, 45: 55-62.

Garvine, R.W., 1974, Physical Features of the Connecticut River Outflow During High Discharge, *Journal of Geophysical Research* 79(6), 831-846.

Garvine R.W., 1975, The distribution of salinity and temperature in the Connecticut River Estuary, *Journal of Geophysical Research* 80(9): 1176-1183.

Geyer, W. R., Lavery, A. C., Scully, M. E., and Trowbridge, J. H., 2010, Mixing by shear instability at high Reynolds number, *Geophysical Research Letters*, v. 37, L22607, p. 1-5.

Geyer, W.R., Woodruff, J.D., and P. Traykovski, 2001, Sediment transport and trapping in the Hudson River estuary, *Estuaries* 24(5), 670-679.

Gordon, R.B., 1980, The sedimentary system of Long Island Sound, in Saltzman, B., ed., *Estuarine physics and chemistry: Studies in Long Island Sound: Advances in Geophysics*, 22:1-35.

Grant, W.D., and O.S. Madsen, 1982, Movable bed roughness in oscillatory flow, *Journal of Geophysical Research*, 87: 469.

Heathershaw, A.D., 1981, Comparisons of measured and predicted sediment transport rates in tidal currents, *Marine Geology*, 42: 75-104.

Heathershaw, A.D., and F.D.C. Hammond, 1979, Swansea Bay (Sker) Project Topic Report, 6. Offshore sediment movement and its relation to observed tidal current and wave data, *Inst. Oceanogr. Sci. Rep.*, 93: 119 pp.

Horne, G.S., and P.C. Patton, 1989, Bedload-sediment transport through the Connecticut River estuary, *Geological Society of America Bulletin* 101: 805-819.

Kim, S.-C., Friedrichs, C.T., Maa, J.P.-Y., and L.D. Wright, 2000, Estimating bottom stress in tidal boundary layer from Acoustic Doppler Velocimeter data, *Journal of Hydraulic Engineering*, 126(6): 399-406.

Kineke, G.C., Kristiansen, E.R., Ralston, D.K., and W.R. Geyer, 2014, Fine sediment transport in the Connecticut River estuary, Ocean Sciences poster presentation.

Komar, P.D., 1976, Boundary layer flow under steady unidirectional currents, *Marine Sediment Transport and Environmental Management*: 91-106.

Lesser, R.M., 1951, Some observations of the velocity profile near the sea floor, *Tran. Am. Geophys. Union*, 32: 207-211.

Madsen, O.S., and P.N Wikramanayake, 1991, *Simple Model for Turbulent Wave-Current Bottom Boundary layer Flow,* DRP-91-1, Ralph M. Parsons Laboratory, Massachusetts Institute of Technology, Cambridge, 150.

Mantz, P.A., 1977, Incipient transport of fine grains and flakes by fluids – extended shield diagram, *Journal of the Hydraulics division* 103: ASCE 12992.

Mariotti, G., Valentine, K., and S. Fagherazzi, 2014, Time-dependent behavior of cohesive sediments subjected to erosion and deposition cycles, *Ocean*

Dynamics.

McCave, I.N., 1973, Some boundary-layer characteristics of tidal currents bearing sand in suspension, *Mem. Soc. R. Sci. Liege*, 6e Ser., pp. 187-206.

McLaren, P., 1981, An interpretation of trends in grain size measures, *Journal of Sed. Petrology* 51: 611-624.

Meade, R.H., 1966, Salinity variations in the Connecticut River, *Water Resource Research* 2(3): 567-579.

Mehta, A.J., Hayter, E.J., Parker, W.R., Krone, R.B., and A.M. Teeter, 1989, Cohesive Sediment Transport. I: Process Description, *Journal Of Hydraulic Engineering*, 115: 1076-1093.

Merriman, D. and L.M. Thorpe, 1976, *The Connecticut River Ecological Study: The Impact of a Nuclear Power Plant*, American Fisheries Society, Washington, D.C., pp. 251.

Middleton, G.V., and J.B. Southard, 1984, *Mechanics of sediment movement,* SEPM.

Milligan, T.G., Kineke, G.C., Blake, A.C., Alexander, C.R., and P.S. Hill, 2001, Flocculation and Sedimentation in the ACE Basin, South Carolina, *Estuaries* 24(5): 734-744.

National Science Foundation Proposal 1232928, 2012, Frontogenesis and Fine-Sediment Trapping in a Highly Stratified Estuary.

Patrick, R., 1996, *Rivers of the United States, Volume III: The Eastern and Southeastern States*, "Main Stem – Connecticut River," John Wiley & Sons, Inc., New York, New York: p. 114 - 117.

Patton, P.C., and G.S. Horne, 1992, Response of the Connecticut River estuary to late

Holocene sea level rise, *Geomorphology*, 5: 391-417.

Pope, S.B., 2000, *Turbulent Flows*, Cambridge University Press, pp. 771.

Ralston, D.K., Geyer, W.R., and J.A. Lerczak, 2010, Structure, variability, and salt flux in a strongly forced salt wedge estuary, *Journal of Geophysical Research*, 115: doi:10.1029/2009JC005806.

Ralston, D.K., Geyer, W.R., and J.C. Warner, 2012, Bathymetric controls on sediment transport in the Hudson River estuary: Lateral asymmetry and frontal trapping, *Journal of Geophysical Research,* 117: doi:10.1029/2012JC008124.

Shields, A., 1936, Anwendung der Ahnlichkeits Mechanik und der Turbulenzforschung auf die Geshieve Bewegung, Preussische Versuchanstalt fur Wasserbau und Schiffbau, Berlin.

Soulsby, R., 1997, *Dynamics of marine sands: a manual for practical applications*. Thomas Telford.

Soulsby, R.L, 1983, Chapter 5 The bottom boundary layer of shelf seas, *Physical Oceanography of Coastal and Shelf Seas*, 35: 189-266.

Soulsby, R.L., and K.R. Dyer, 1981, The form of the near-bed velocity profile in a tidally accelerating flow, *Journal of Geophysical Research* 86: 8067-8074.

Soulsby, R. L., and R. J. S. Whitehouse, 1997, Threshold of sediment motion in coastal environments, 145.

Stapleton, K.R., and D.A. Huntley, 1995, Seabed stress determination using the inertial dissipation method and the turbulent kinetic energy method, *Earth Surface Processes and Landforms*, 20: 807-815.

Sternberg, R.W., 1968, Friction factors in tidal channels with differing bed roughness, *Marine Geology*, 6: 243-260.

Sternberg, R.W., 1972, “Predicting initial motion and bedload transport of sediment particles in the shallow marine environment”, Swift, Duane,and Pilkey, ed., *Shelf Sediment Transport*, Dowden, Hutchinson and Ross, Inc., Stroudsburg, 61- 82.

Sternberg, R.W., 1976, Measurements of boundary-layer flow and boundary roughness over Campeche Bank, Yucatan, *Marine Geology*, 20: M25-M31.

Sternberg, R.W., Kineke, G.C., and R. Johnson, 1991, An instrument system for profiling suspended sediment and fluid and flow conditions in shallow marine environments, *Continental Shelf Research* 11: 109-122.

Tennekes, H., and J.L. Lumley, 1972, *A first course in turbulence*, MIT Press, Cambridge, Mass.

Thompson, C.E.L., Amos, C.L., Jones, T.E.R., and J. Chaplin, 2003, The manifestation of fluid-transmitted bed shear stress in a smooth annular flume – a comparison of methods, *Journal of Coastal Research* 19(4): 1094-1103.

U.S. Geological Survey, 2015, National Water Information System data available on the World Wide Web for Old Lyme, CT (USGS Water Data for the Nation), accessed July 20, 2015, at URL http://waterdata.usgs.gov/ct/nwis/uv?site_no=01194796.

U.S. Geological Survey, 2015, National Water Information System data available on the World Wide Web for Thompsonville, CT (USGS Water Data for the Nation), accessed July 20, 2015, at URL http://waterdata.usgs.gov/ct/nwis/uv?site_no=01184000.

Vanoni, V.A., 1964, Measurements of critical shear stress for entraining fine sediments in a boundary layer: *Calif. Inst. Technol.*, W.M. Keck Lab. Of Hydraulics and

Water Resources, Rept. KH-R-7, 47 pp.

Vincent, C.E., and J.G. Harvey, 1976, Roughness length in the turbulent Ekman layer above the sea bed, *Marine Geology*, 22: M75-M81.

Wentworth, C.K., 1922, A scale of grade and class terms for clastic sediments, *The Journal of Geology* 30(5): 377-392.

Wiberg, P., and J.D. Smith, 1987, Calculations of the critical shear stress for motion of uniform and heterogeneous sediments, *Water Resources Research* 23(8): 1471-1480.

Woodruff, J.D., Martini, A.P., Elzidani, E.Z.H., Naughton, T.J., Kekacs, D.J., and D.G. MacDonald, 2013, Off-river waterbodies on tidal river: Human impact on rates of infilling and the accumulation of pollutants, *Geomorphology*, 184(2012): 38-50.

Wright, L.D., 1995, *Morphodynamics of Inner Continental Shelves*, CRC Press, Boca Raton.

Yalin, M.S., 1972, *Mechanics of Sediment Transport*, Pergamon Press, University of Minnesota.

8. Figures

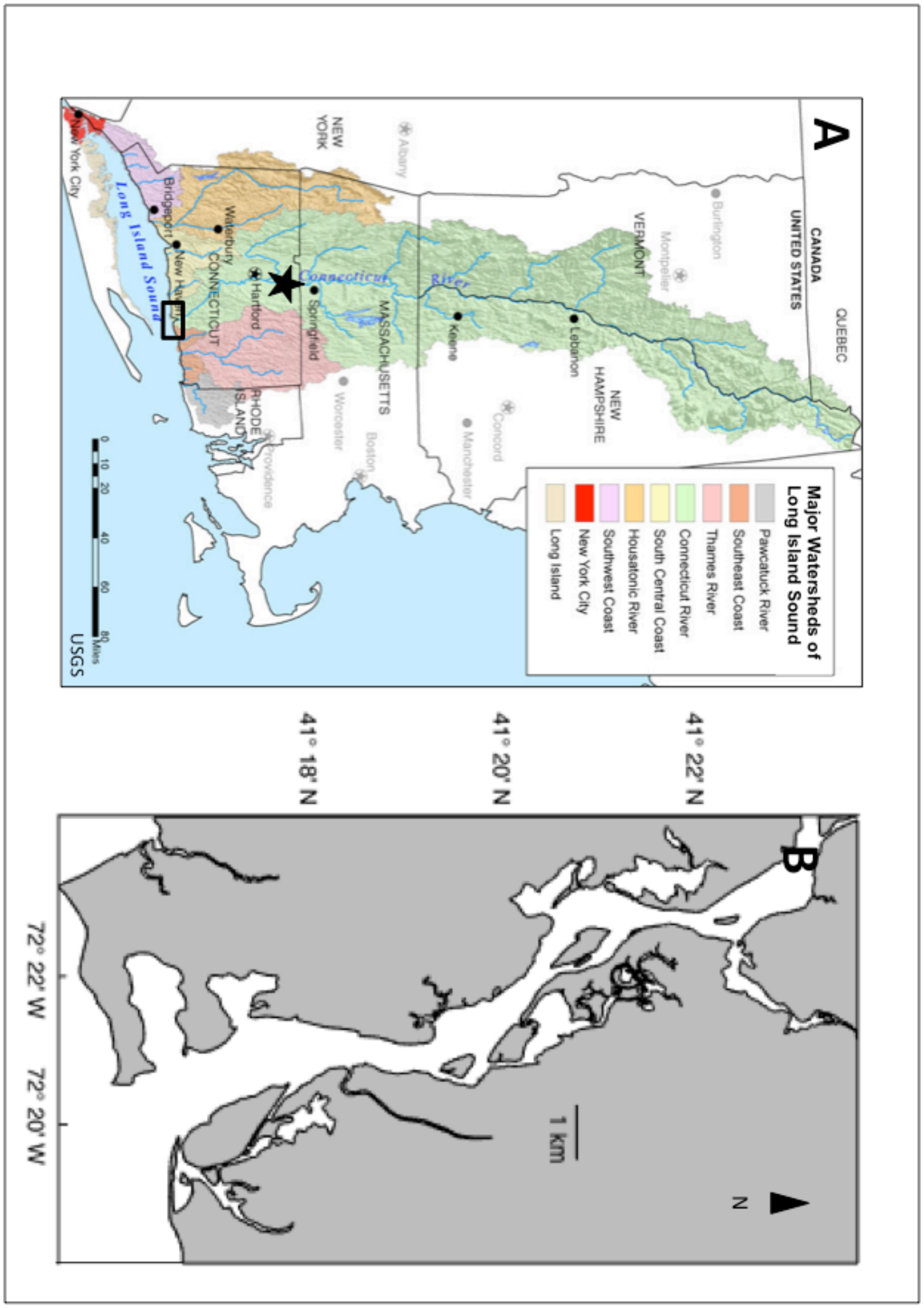

Figure 1: Site map. (A) the Connecticut River watershed with the study site marked with a box (courtesy of the USGS); (B) the Connecticut River estuary study area. The star in panel A marks the location of the USGS Thompsonville gauging station.

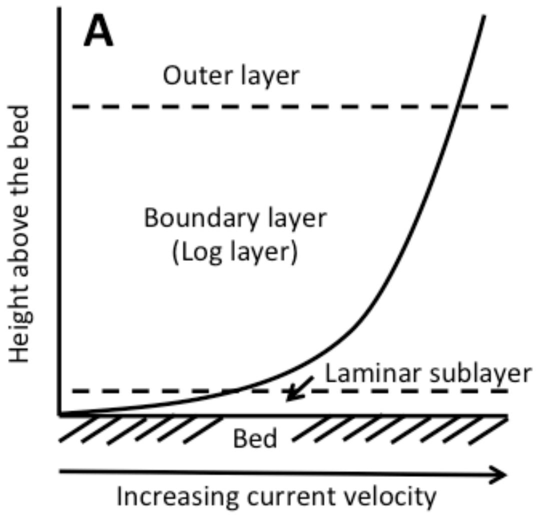

Figure 2: Idealized mean velocity profile showing the laminar sublayer, log layer, and outer layer, adapted from Dyer (1986). (A) Smooth turbulent flow. (B) Rough turbulent flow.

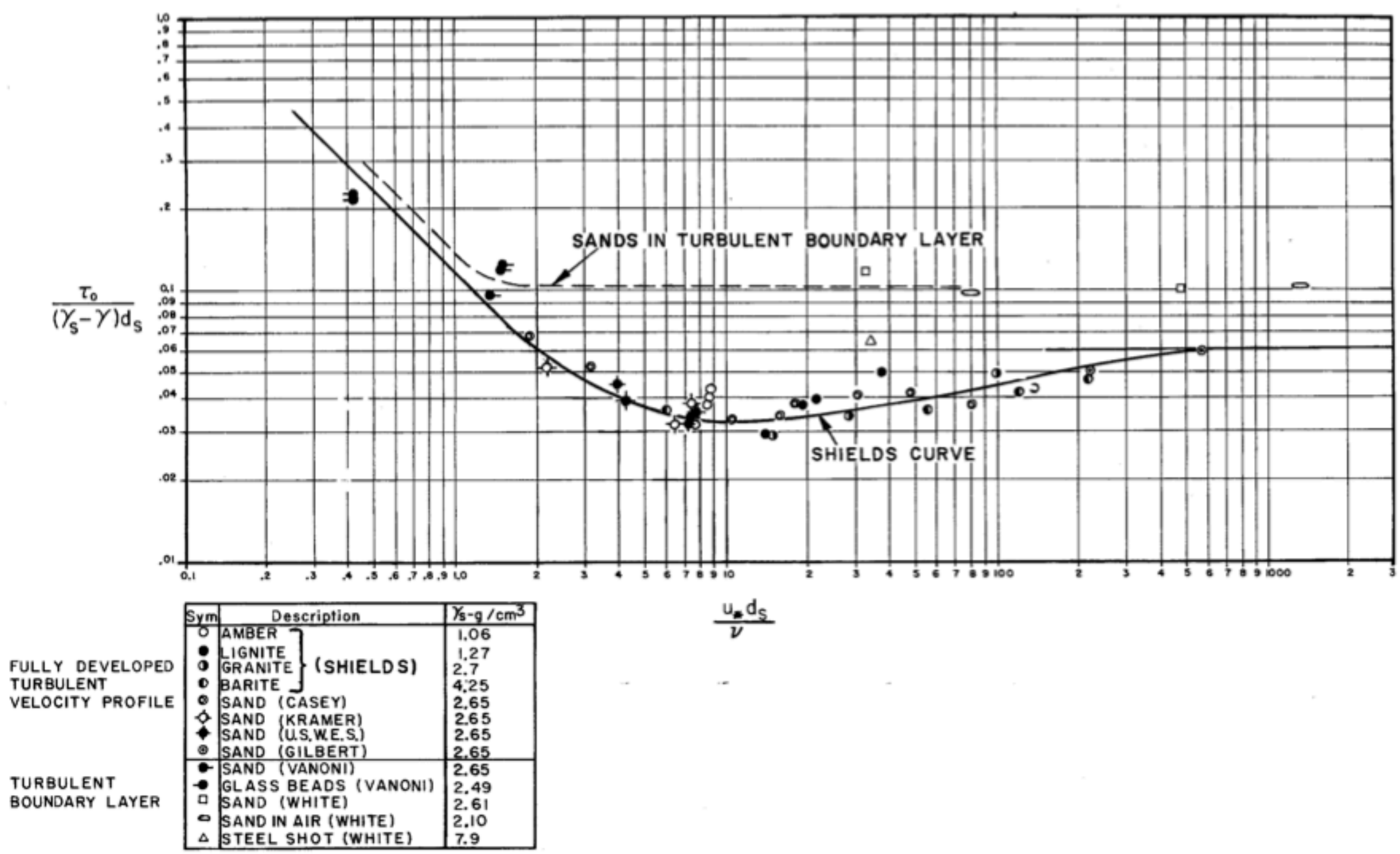

Figure 3: Shields diagram taken from Vanoi (1964). The black line shows the curve determined by Shields (1936) and data from a variety of studies are superimposed on the curve to show that there is considerable scatter in these measurements.

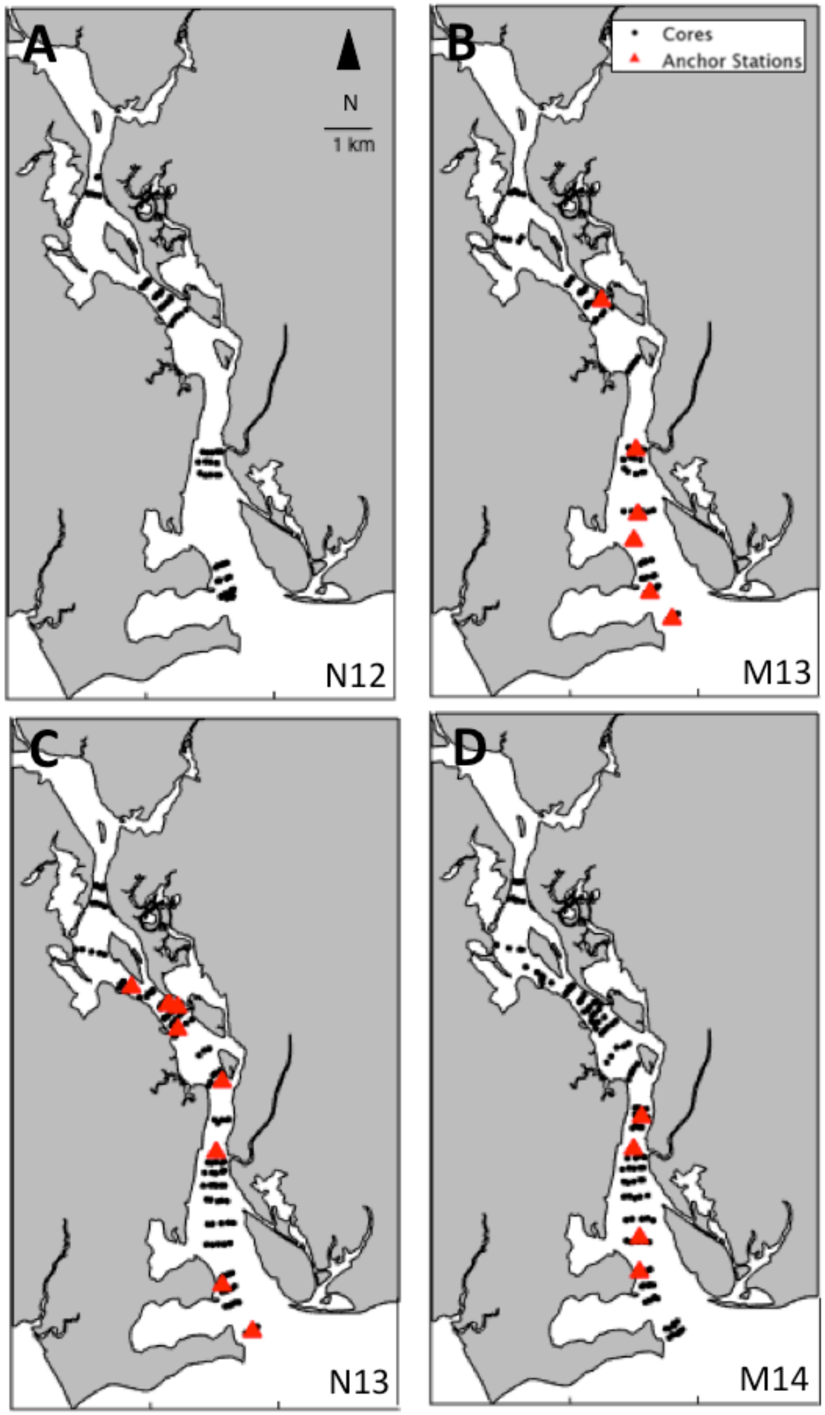

Figure 4: Sampling scheme for the four field excursions from November 2012 (N12), May 2013 (M13), November 2013 (N13), and May 2014 (M14). Bottom sediment sampling increased over the field seasons for increased resolution. Cores are samples taken using a HAPS corer (Figure 6) and at anchor stations, a suite of of water column data was collected, including velocity and suspended-sediment

concentration.

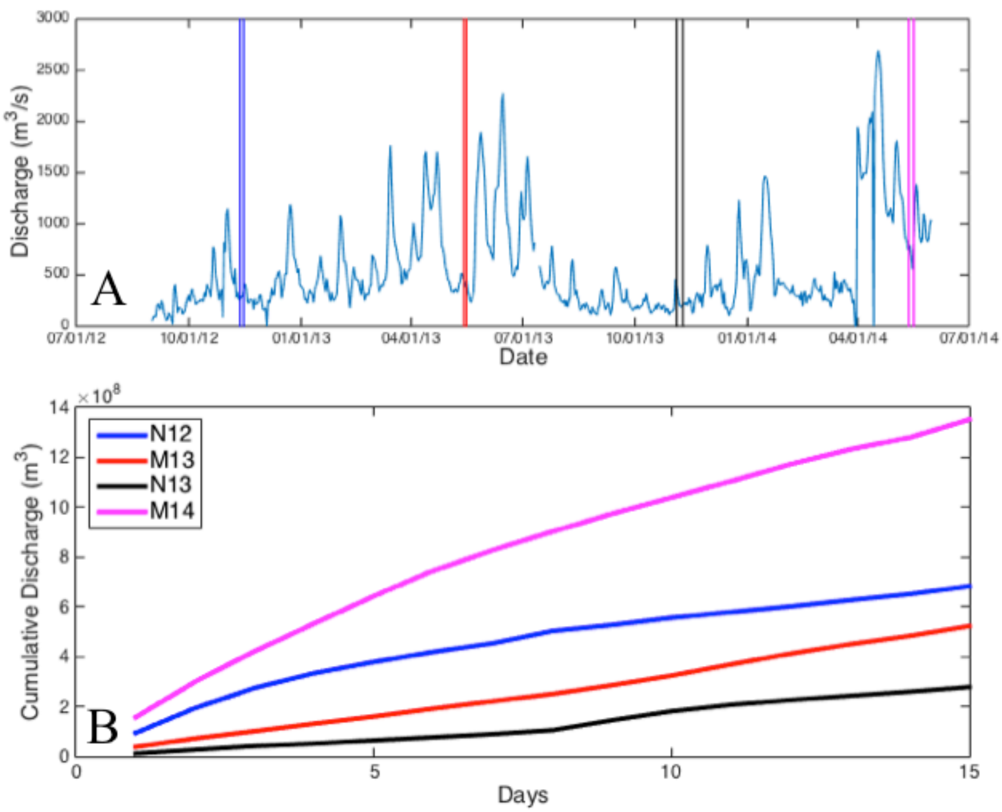

Figure 5: (A) Discharge of the Connecticut River over the span of the study, with sampling periods highlighted (USGS gauging station at Thompsonville, CT). (B) Cumulative discharge for two weeks prior to the respective study period. The discharge preceeding the M14 survey was greater than twice that of the other surveys.

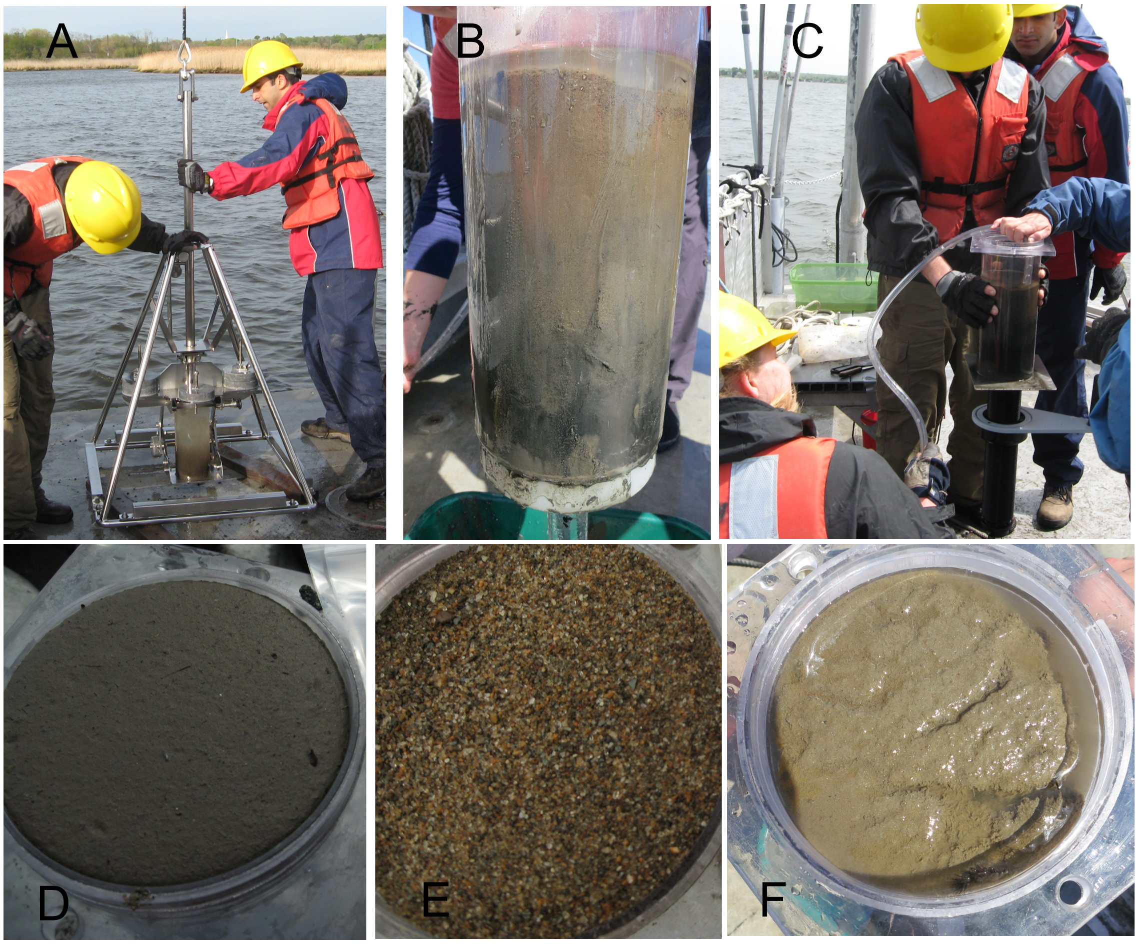

Figure 6: The HAPS corer (KC Denmark, A) shallow cores were retrieved (B) and then extruded (C). The corer samples the top ~20 cm and is effective in a range of bottom types, e.g. sand with a mud drape (D), well-sorted medium sand (E), and unconsolidated mud (F).

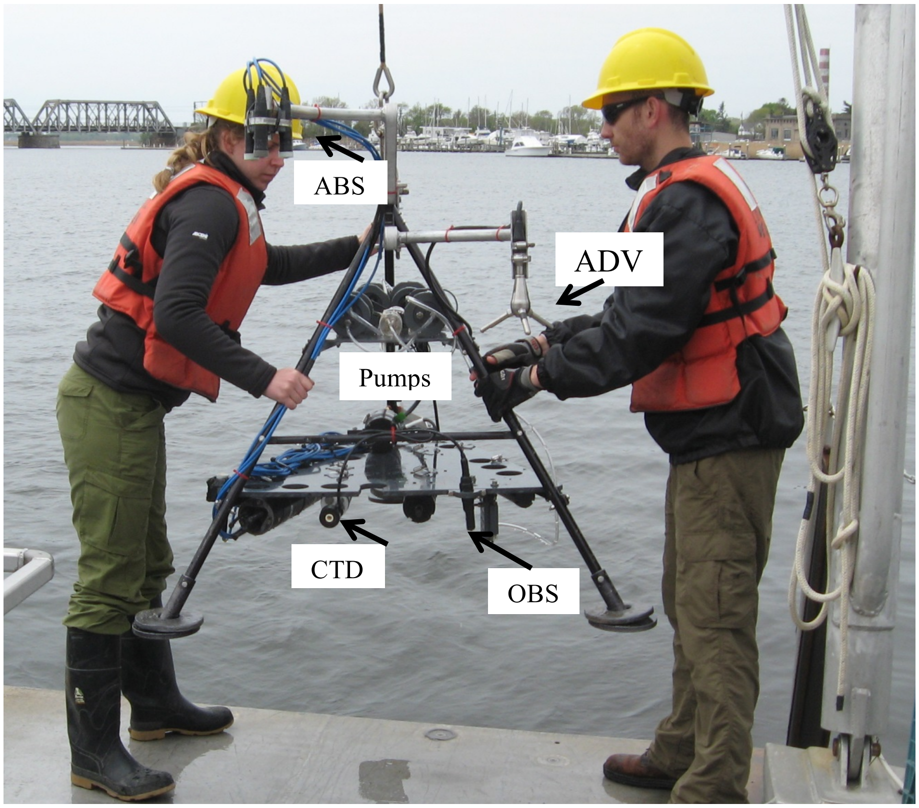

Figure 7: Tripod with CTD, ADV, ABS, OBS, and pump system after Sternberg et al. (1991). Photo courtesy of G.C. Kineke.

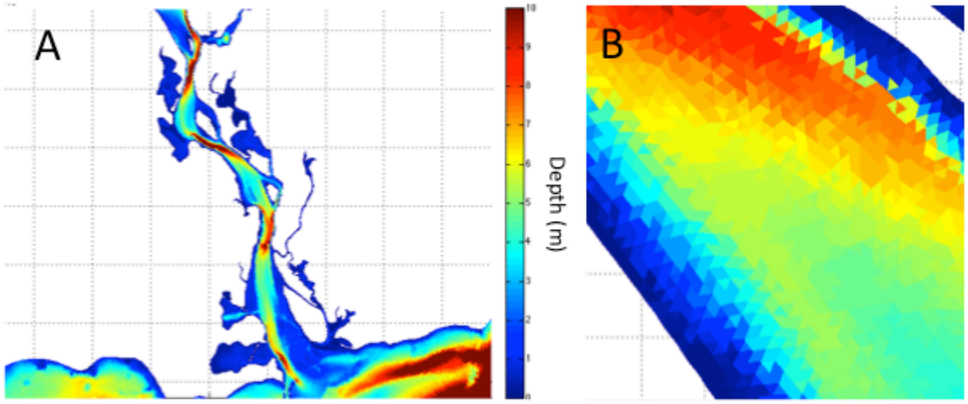

Figure 8: Model domain for the Connecticut River estuary with detailed bathymetry input (A). The FVCOM model uses triangular grid cells (B). (Ralston, *pers. comm.*)

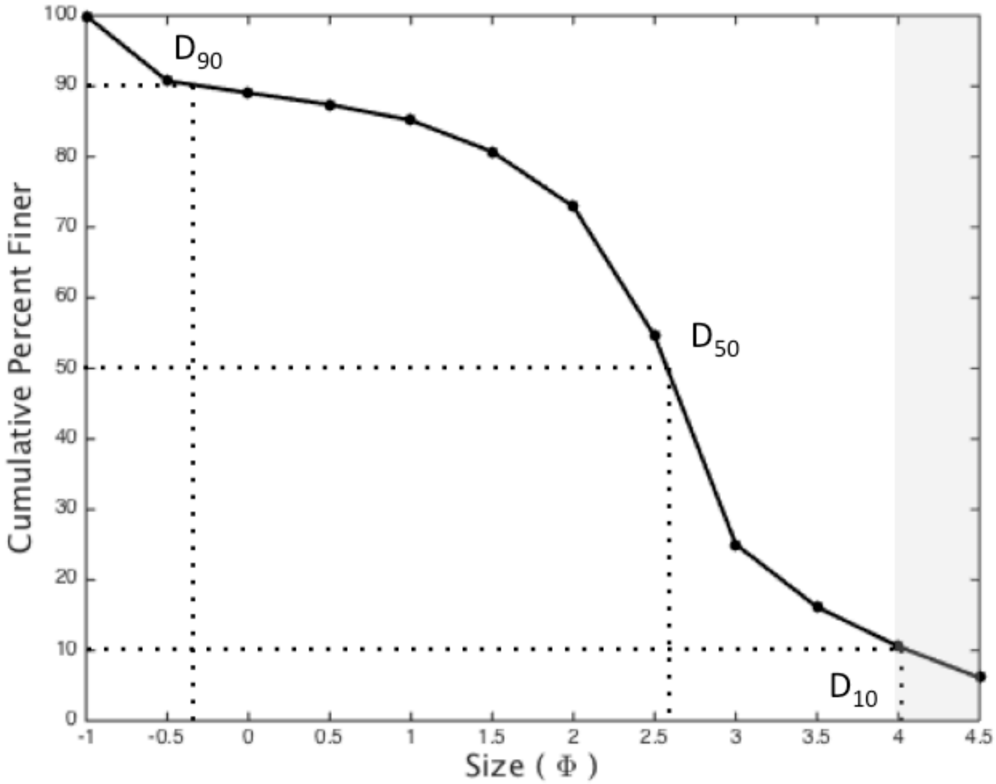

Figure 9: Example grain-size distribution for one of the samples from the present study. The graphical Folk and Ward method can be used to determine median grain size, the D_{50}, and any other percentiles. The grey shaded area is that not resolved by sieving with the Ro-Tap.

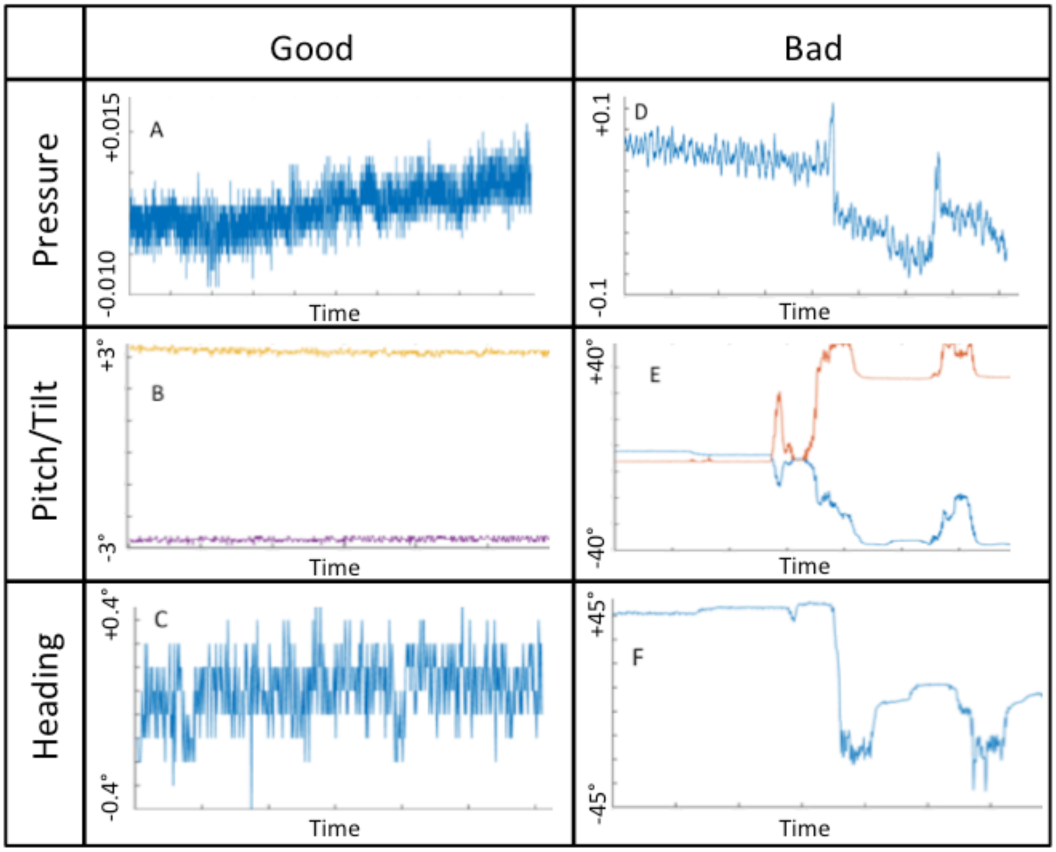

Figure 10: Examples of good data (A-C) and bad data (D-F) for the different requirements for the shear stress calculations. The pressure record from the ADV must be steady (A, not D), the pitch and tilt must be steady (B, not E), and heading must also be steady (C, not F).

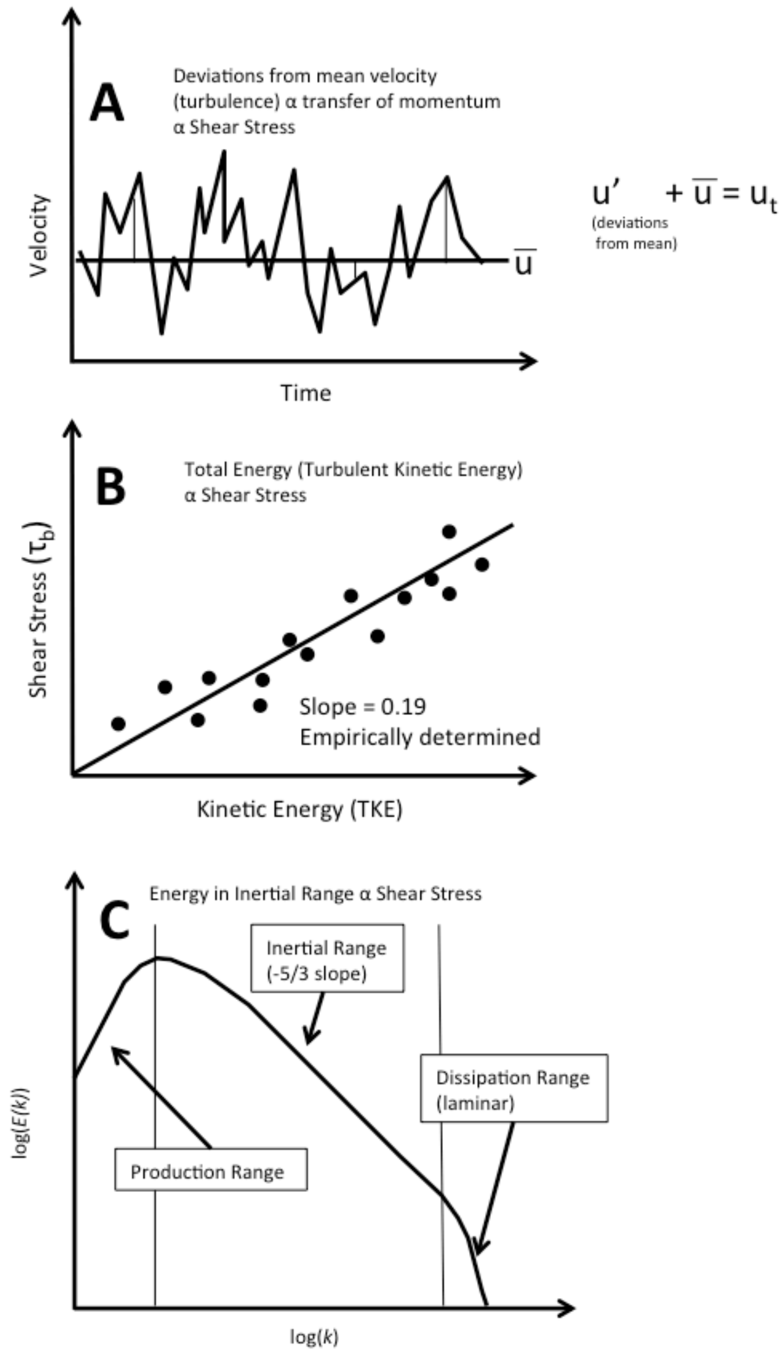

Figure 11: (A) Deviations in the mean velocities create a transfer in momentum (Reynolds stress method). (B) Total kinetic energy is proportional to the shear stress, which was determined empirically using independent measures of energy and shear stress (Kim et al. 2000; TKE method). (C) Inertial range of the energy spectra of the velocity is proportional to shear stress (ID method)

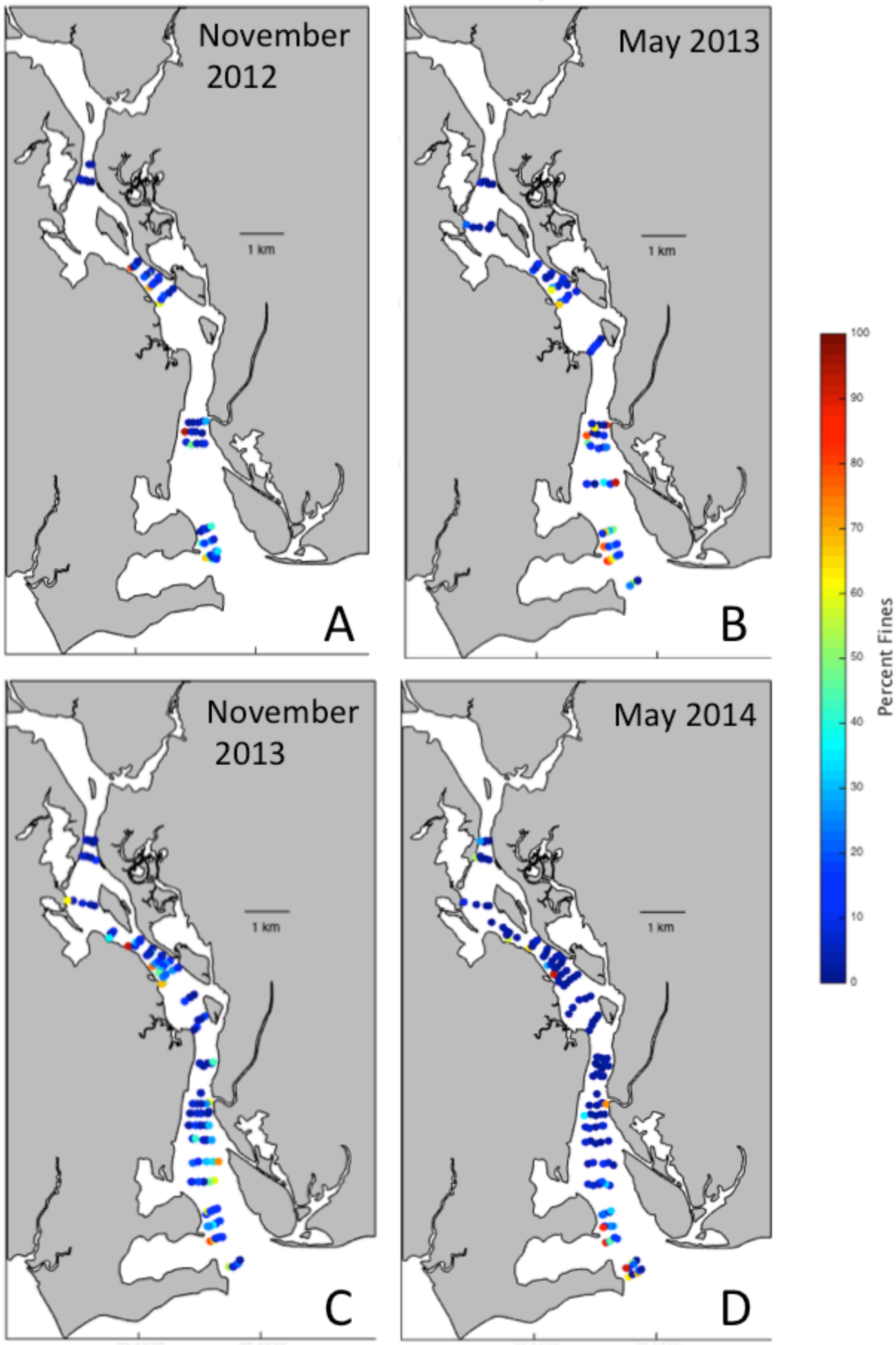

Figure 12: Percent fine sediments (<63 microns) throughout the estuary over the four sampling periods. Brighter colors denote higher percentages.

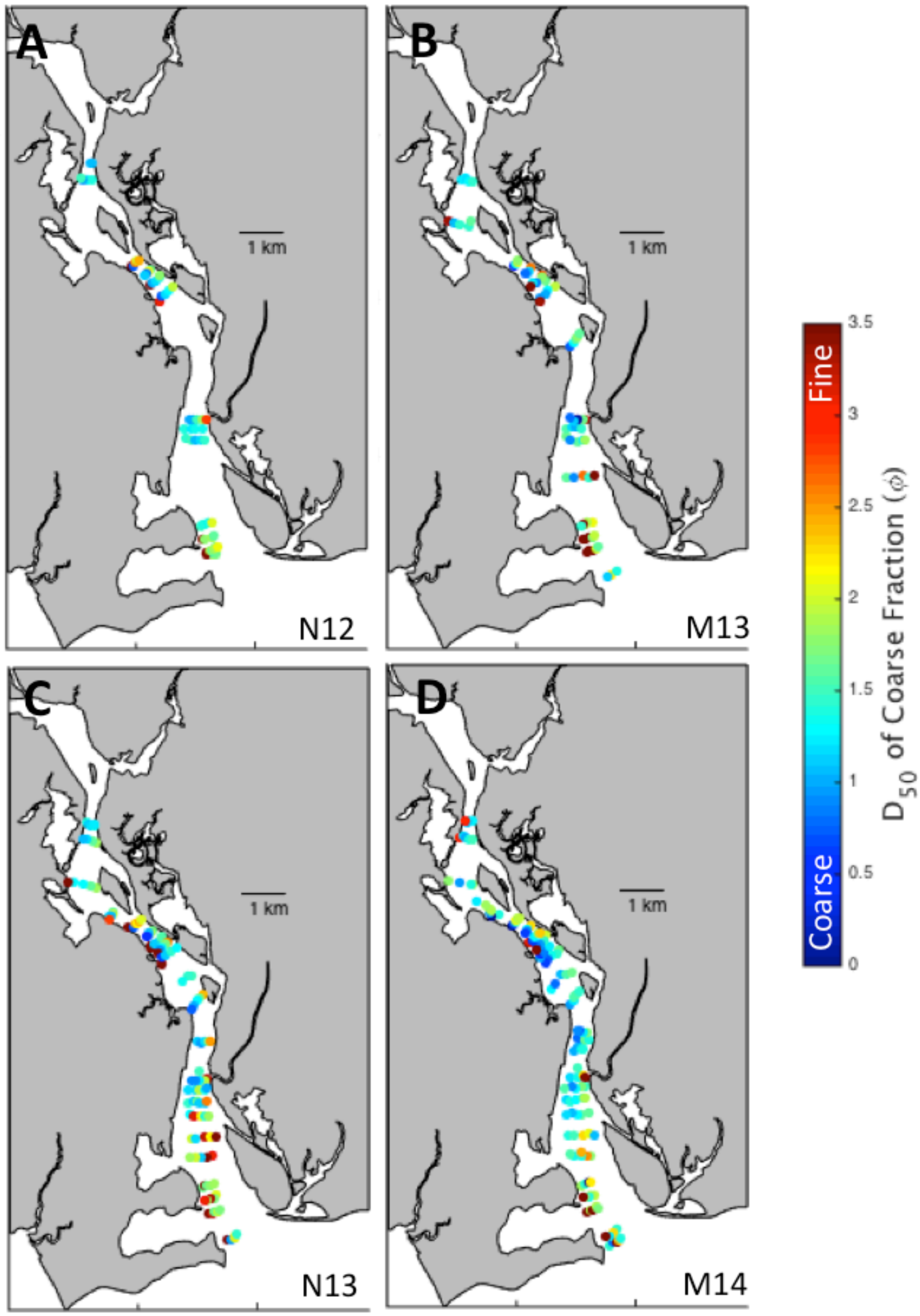

Figure 13: The median grain size, D_{50}, of the coarse fraction throughout the estuary over the four sampling periods.

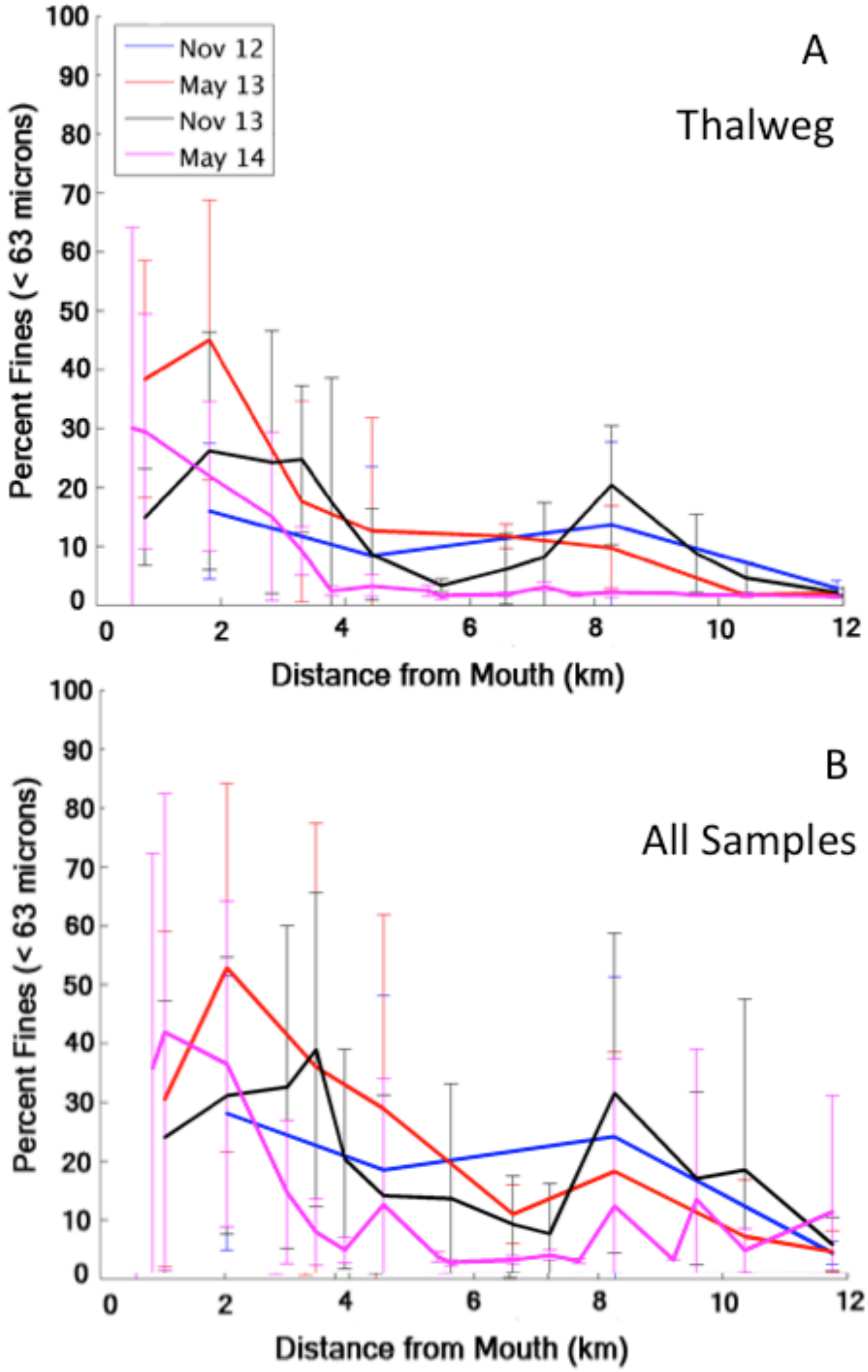

Figure 14: Percent fines (<63 microns) along-channel for all cores in the center of the channel (across-channel stations 2-4) (A) and in the whole estuary (B) in all field seasons. Error bars are standard deviations.

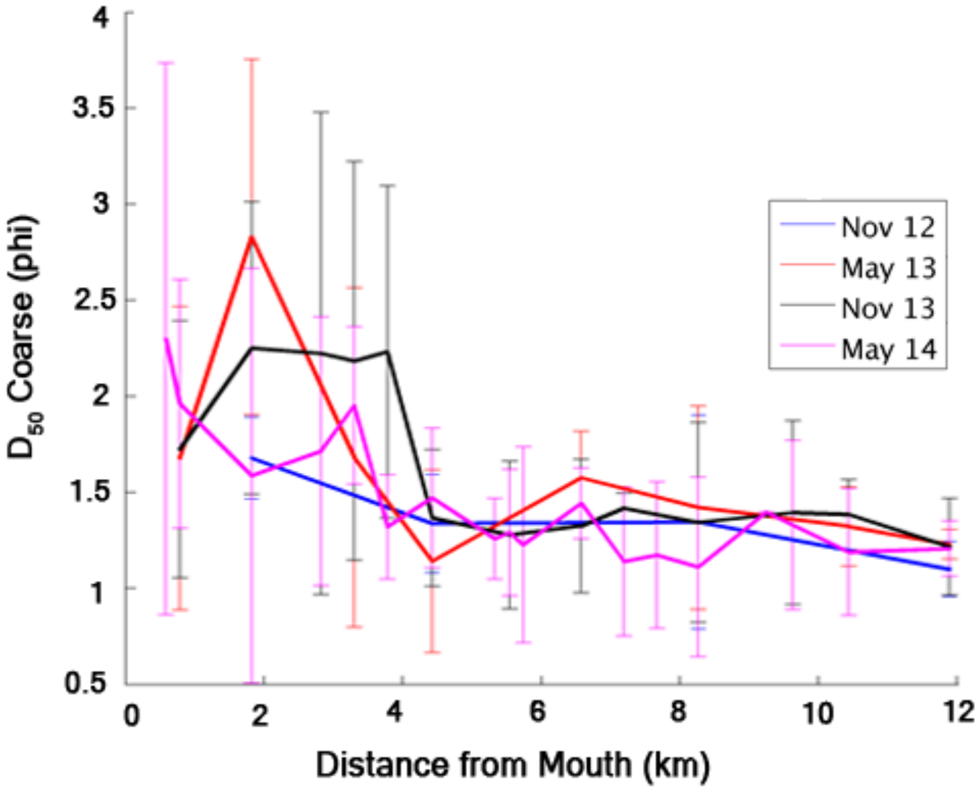

Figure 15: D_{50} of the coarse fraction of sediment (>63 microns) along-channel for all cores in the center of the channel (across-channel stations 2-4) in all field seasons. Error bars are the standard deviation.

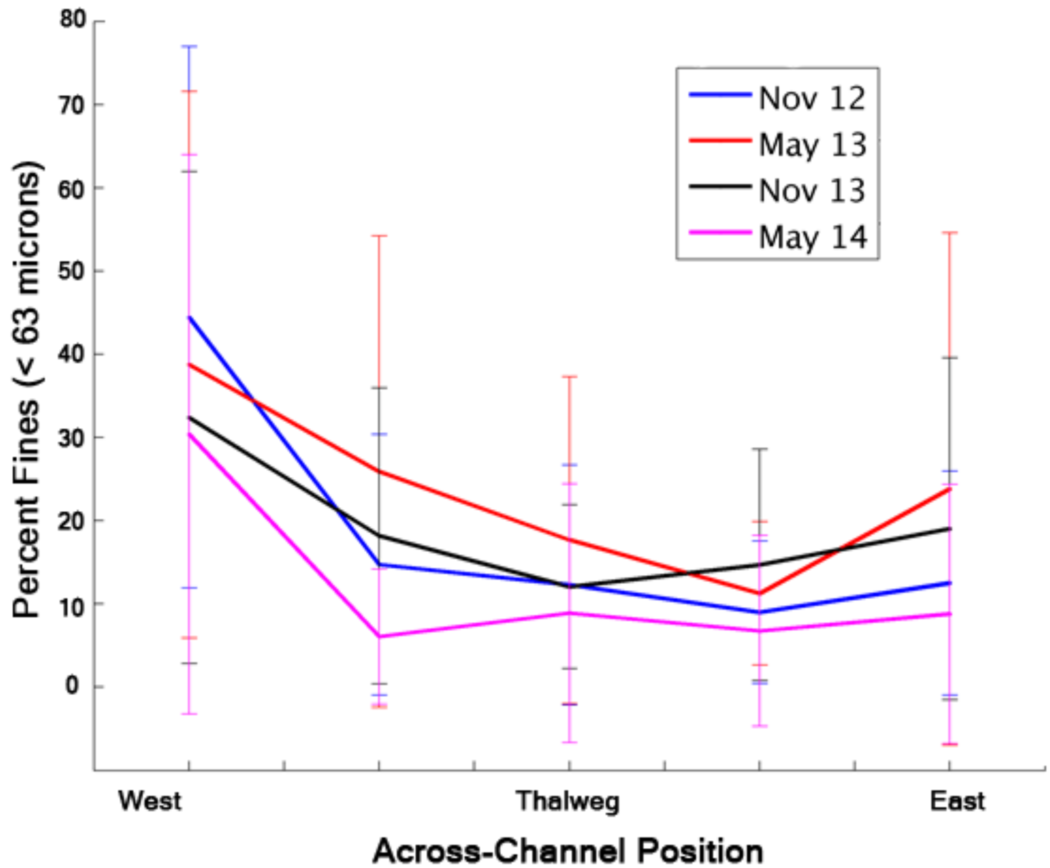

Figure 16: Across-channel percent fines (<63 microns) for all stations across-channel for all field seasons using all cores. There are significantly more fines on the western side of the channel compared to the center of the channel ($p<0.001$).

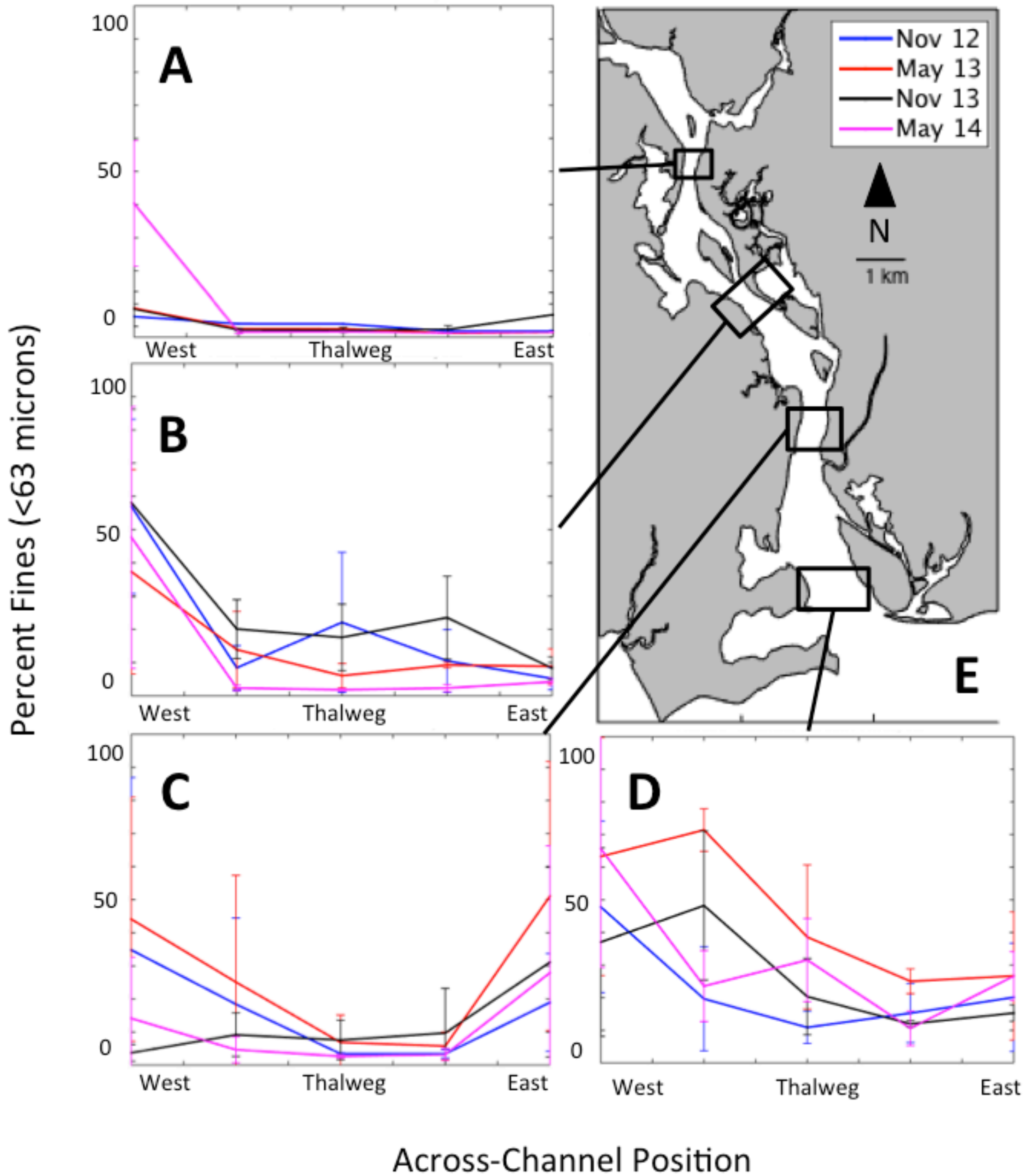

Figure 17: Across-channel percent fines (<63 microns) for all stations across-channel for all field seasons using all cores in four areas in the estuary.

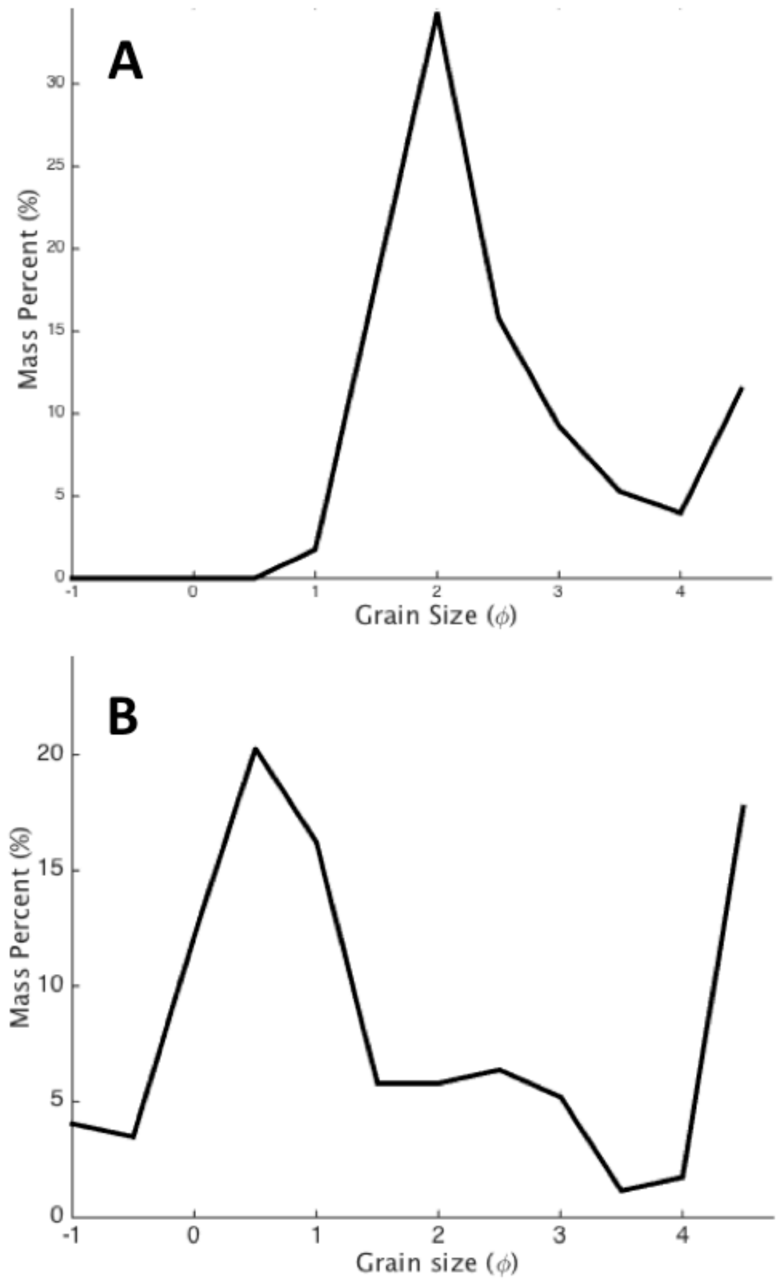

Figure 18: (A) Sample with unimodal sediment distribution from the center of the channel ~12 km from the mouth. (B) Sample bimodal sediment distribution from the center of the channel ~2 km from the mouth, with a mode in medium sand and a mode in silts/clays. The fraction at 4.5ϕ is the cumulative mass percent of all sediment finer than 4ϕ.

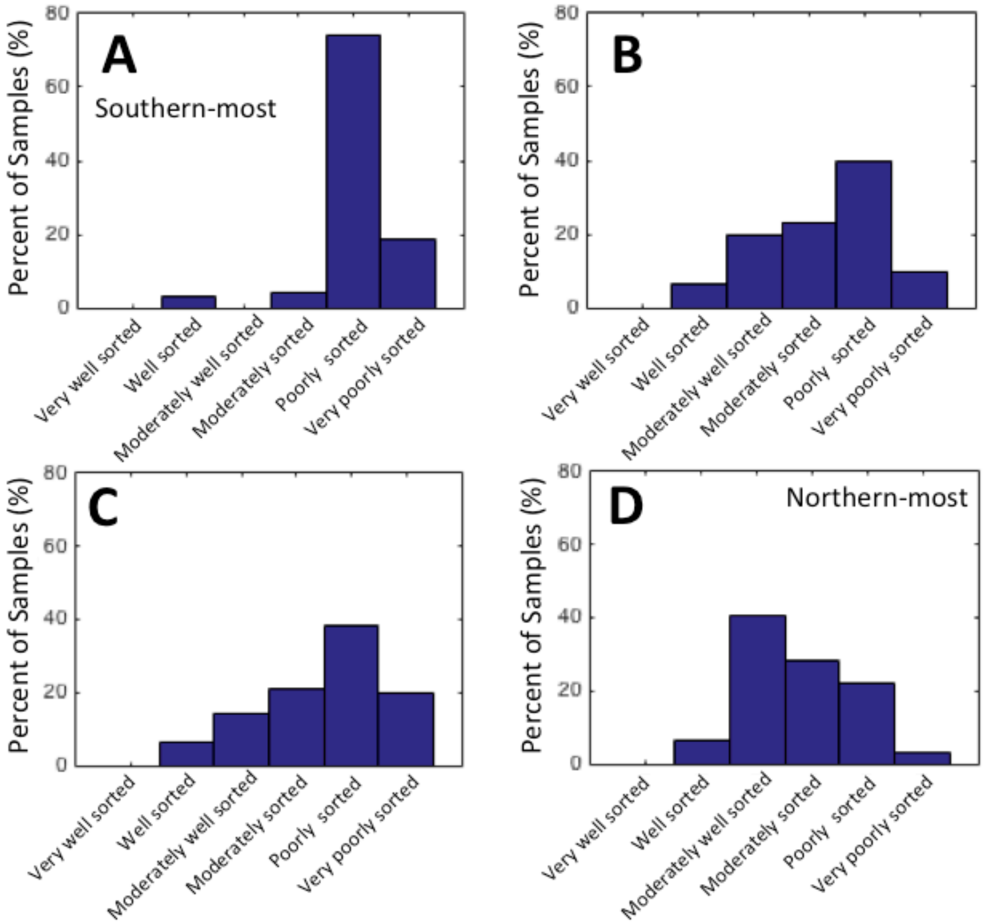

Figure 19: Grain size sorting from bottom sediment samples separated by sampling area (See location in Figure 17). The x-axis ranges from very-well sorted to very-poorly sorted. Sorting increases with increasing distance from the mouth.

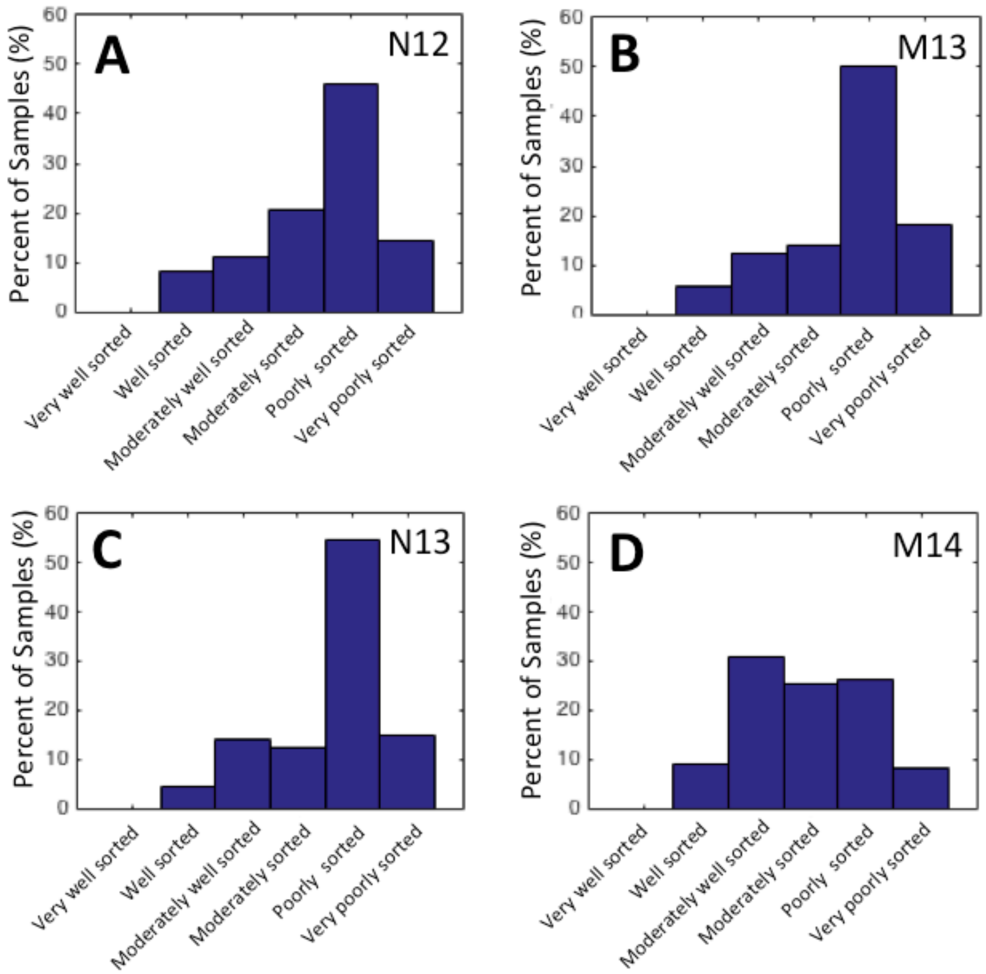

Figure 20: Grain size sorting from bottom sediment samples by field season. The x-axis ranges from very-well sorted to very-poorly sorted. M14 sediment was the most sorted.

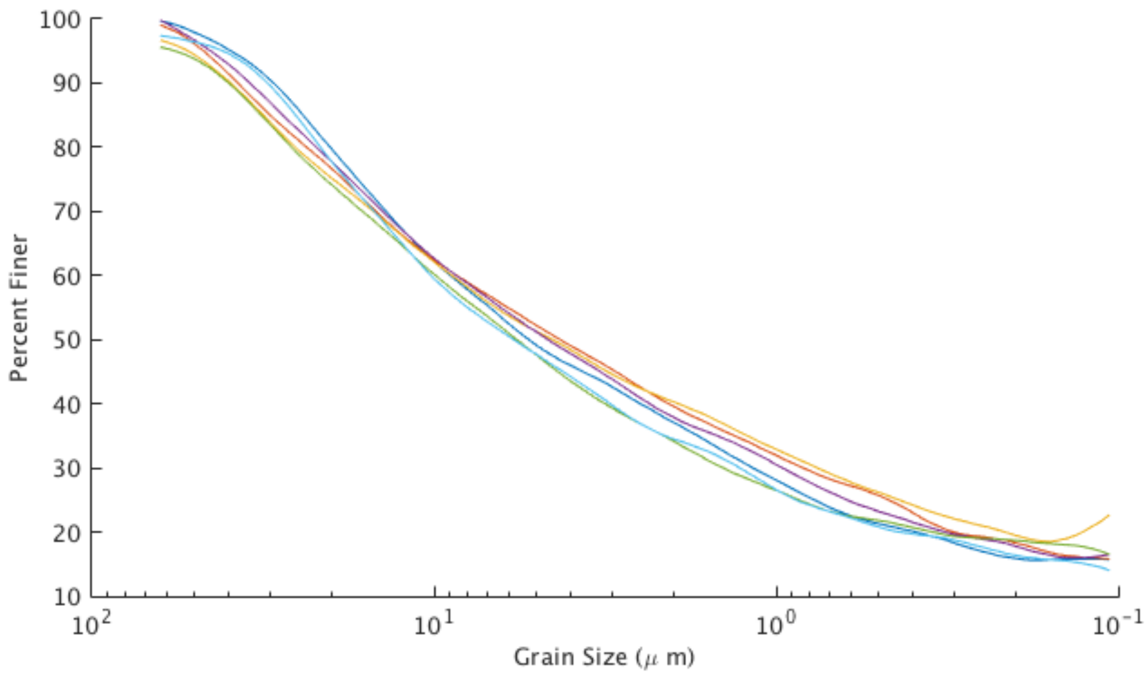

Figure 21: Examples of grain size distribution for the fine fraction of the samples determined using the SediGraph. The D_{50} of this fraction is 5-10 µm.

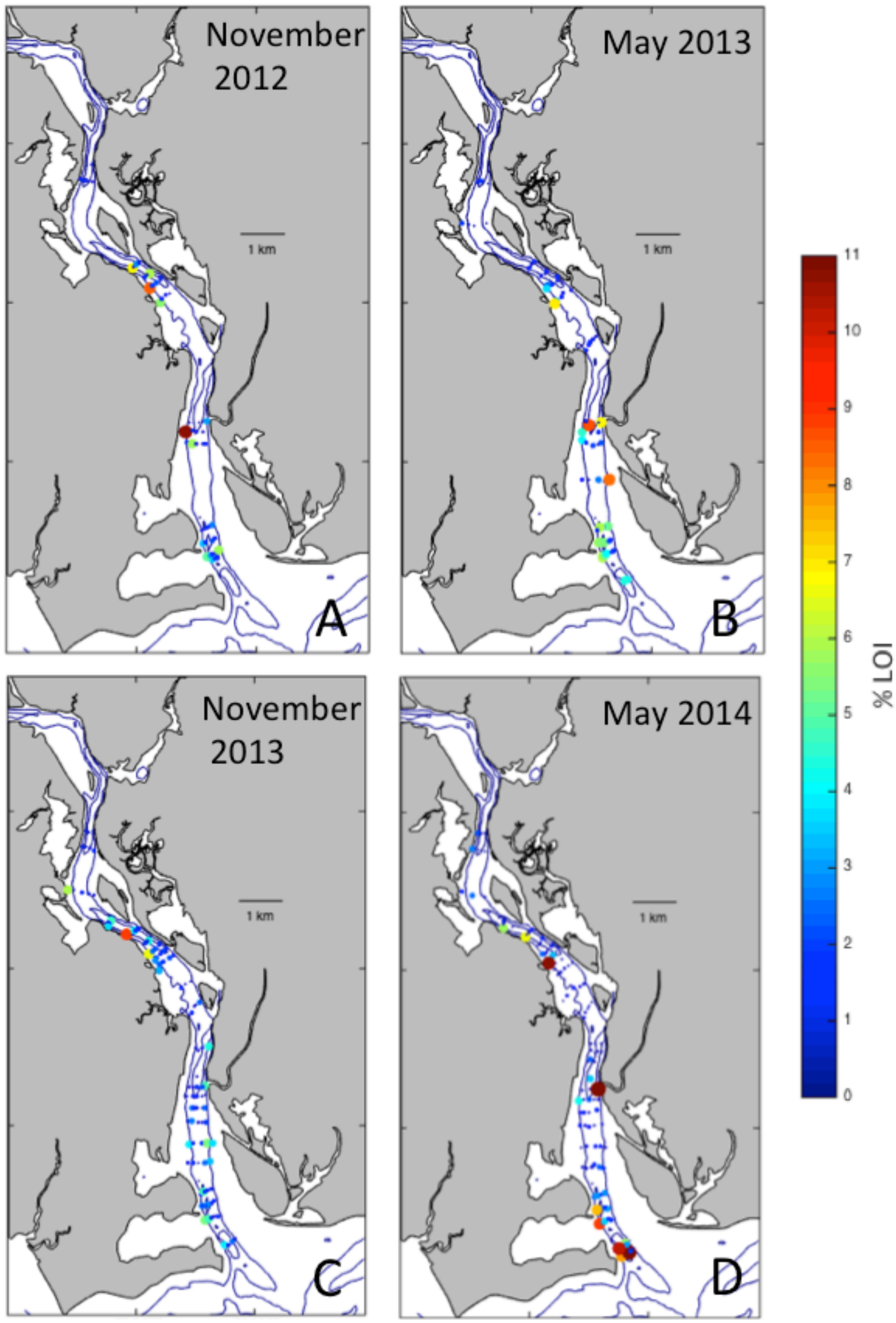

Figure 22: Organic matter distribution, represented by LOI, throughout the estuary over the four field experiments.

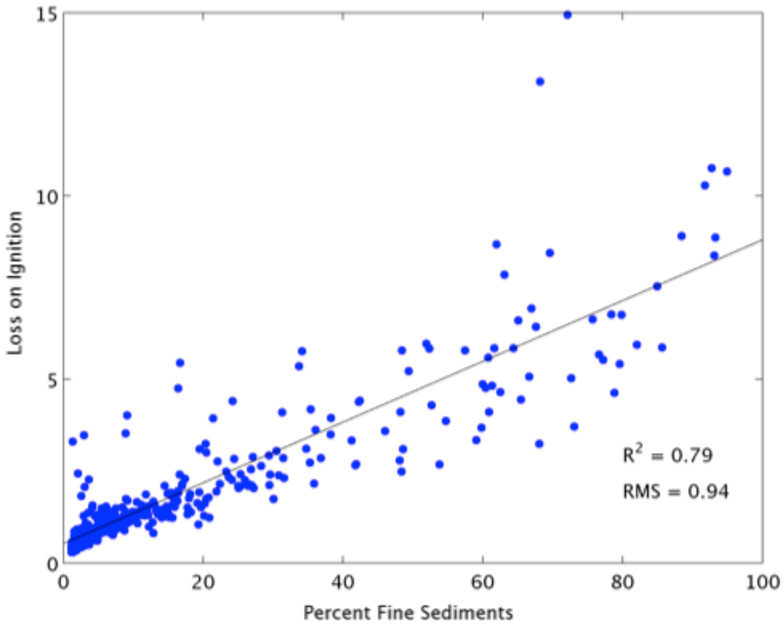

Figure 23: Percent organic matter, determined from loss on ignition, versus percent fines(<63 microns). Organic matter increases with increasing amounts of fine sediments. (n=383, p=0.042, Slope=0.083, Offset=0.53)

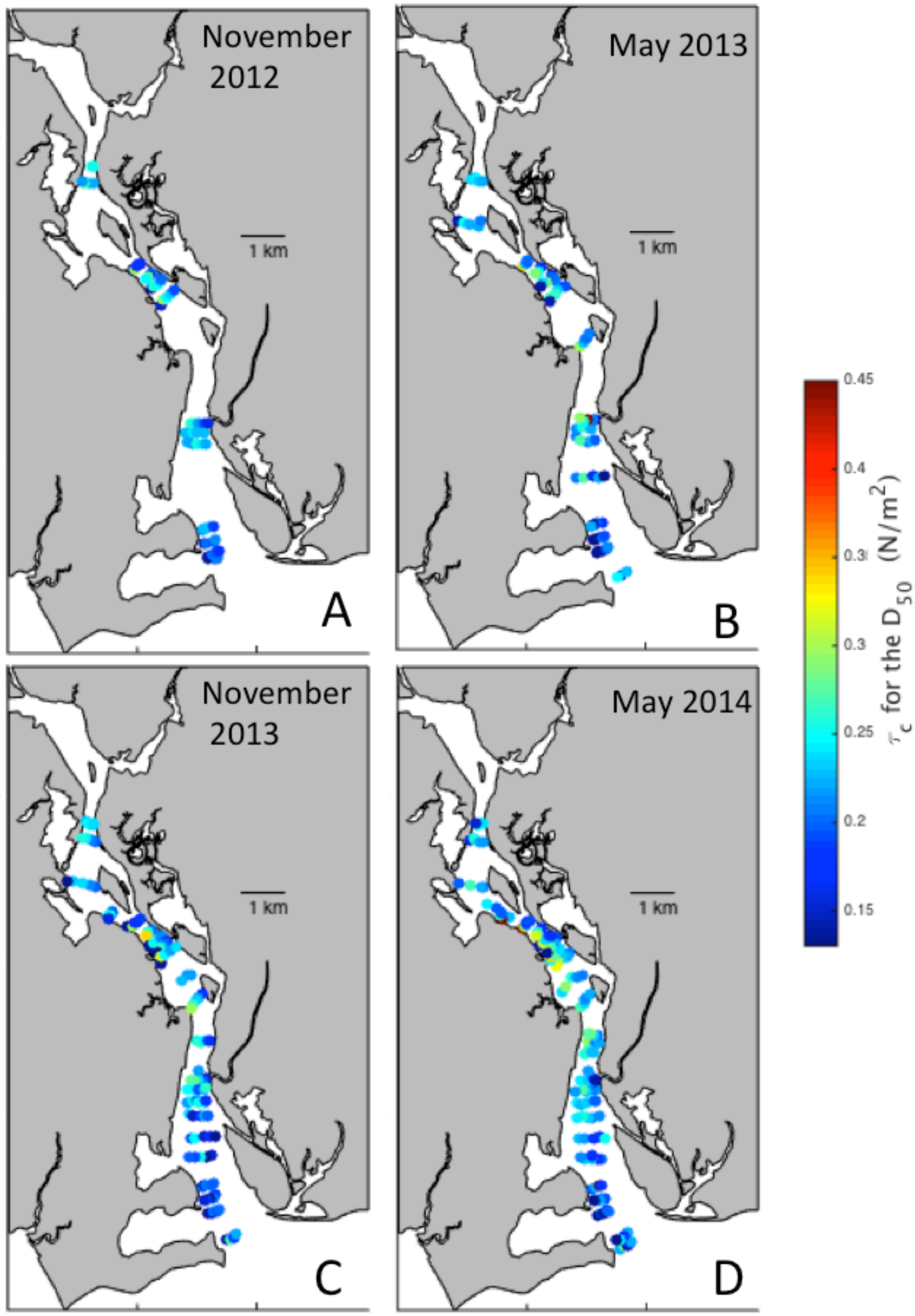

Figure 24: Critical Shear Stress for the D50 of the coarse fraction for all field seasons determined by an empirical formulation of the Shields criteria.

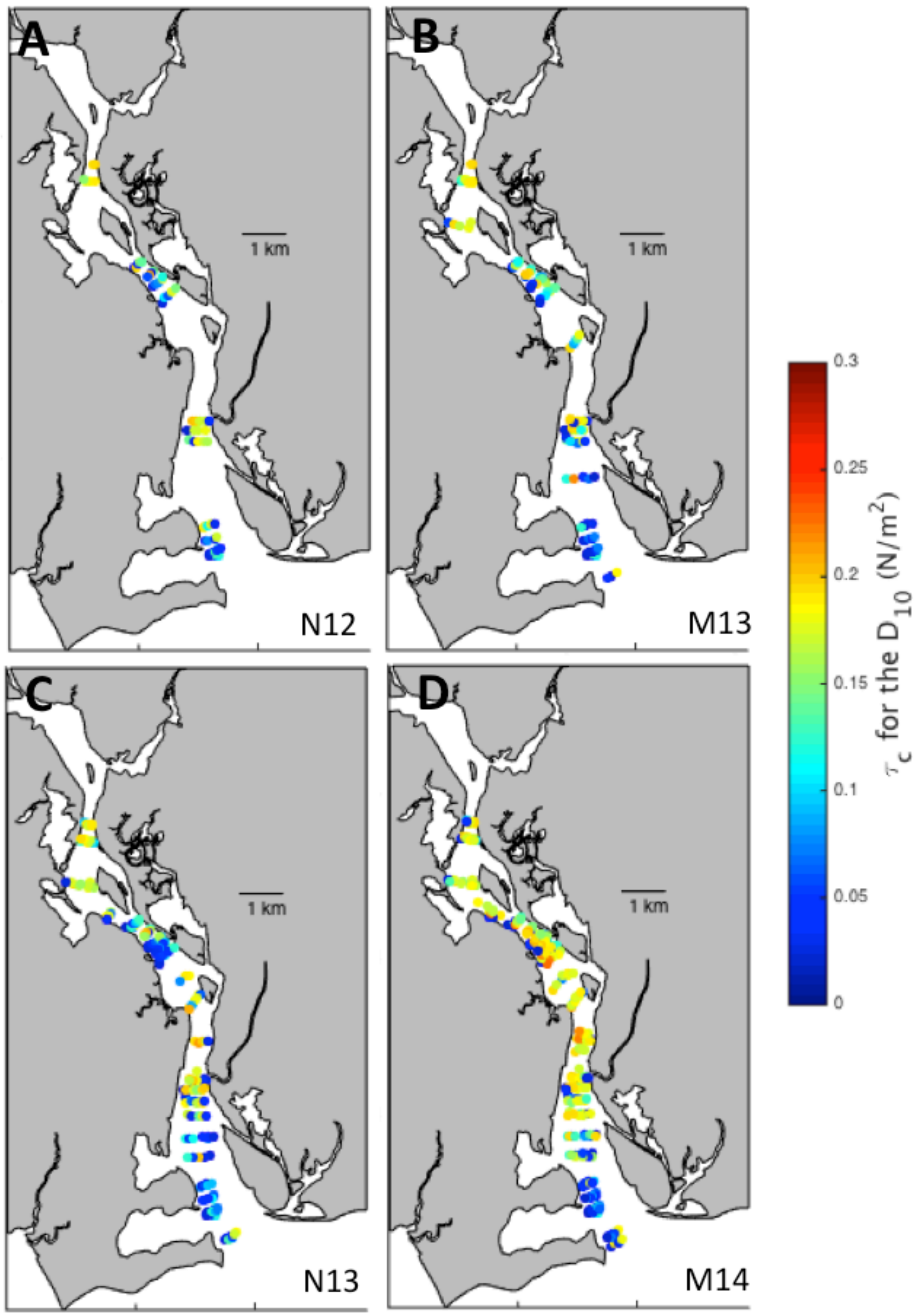

Figure 25: Critical shear stress for the D_{10} of the coarse fraction for all field seasons determined by an empirical formulation of the Shields criteria.

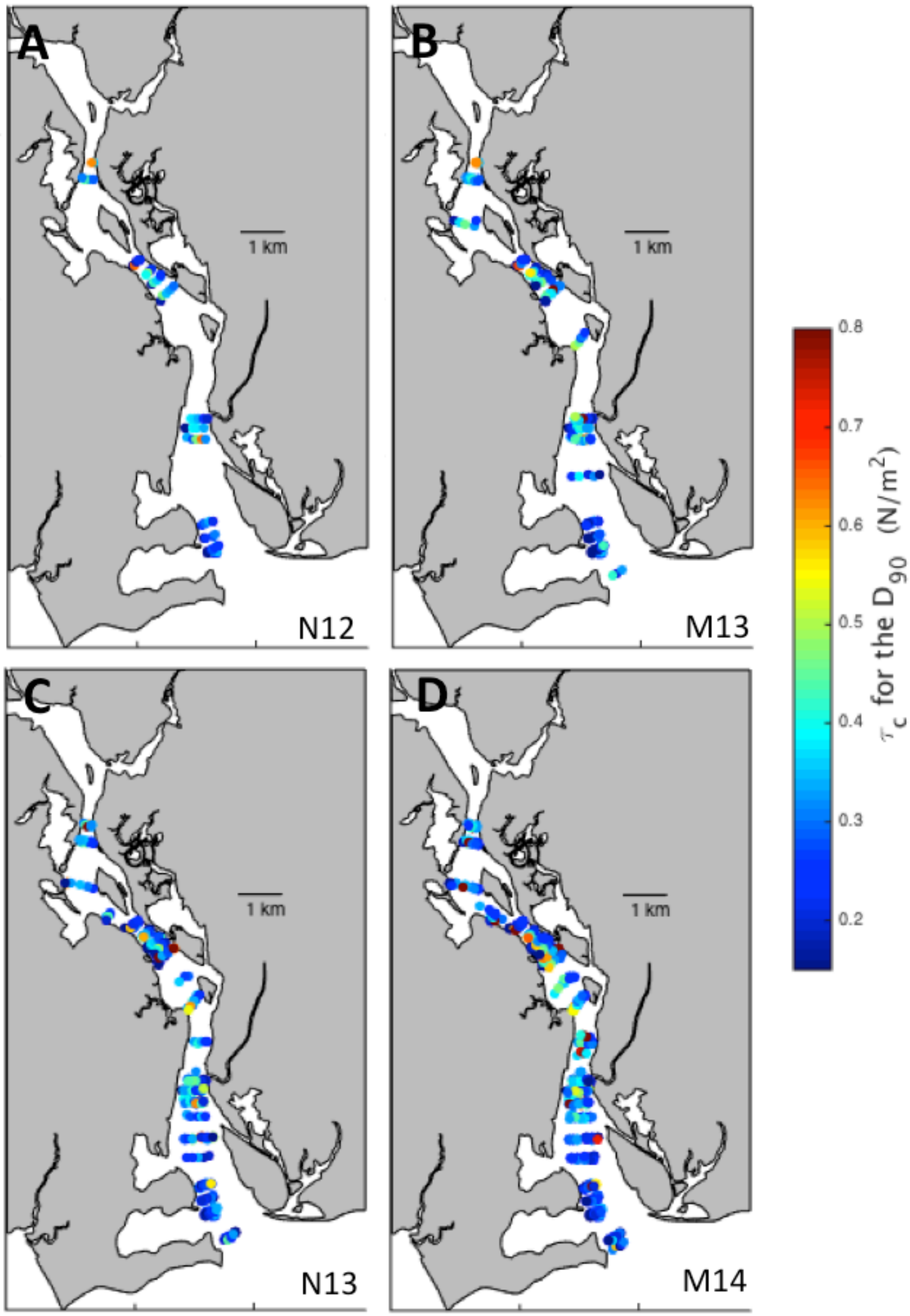

Figure 26: Critical shear stress for the D_{90} for all field seasons determined by an empirical formulation of the Shields criteria.

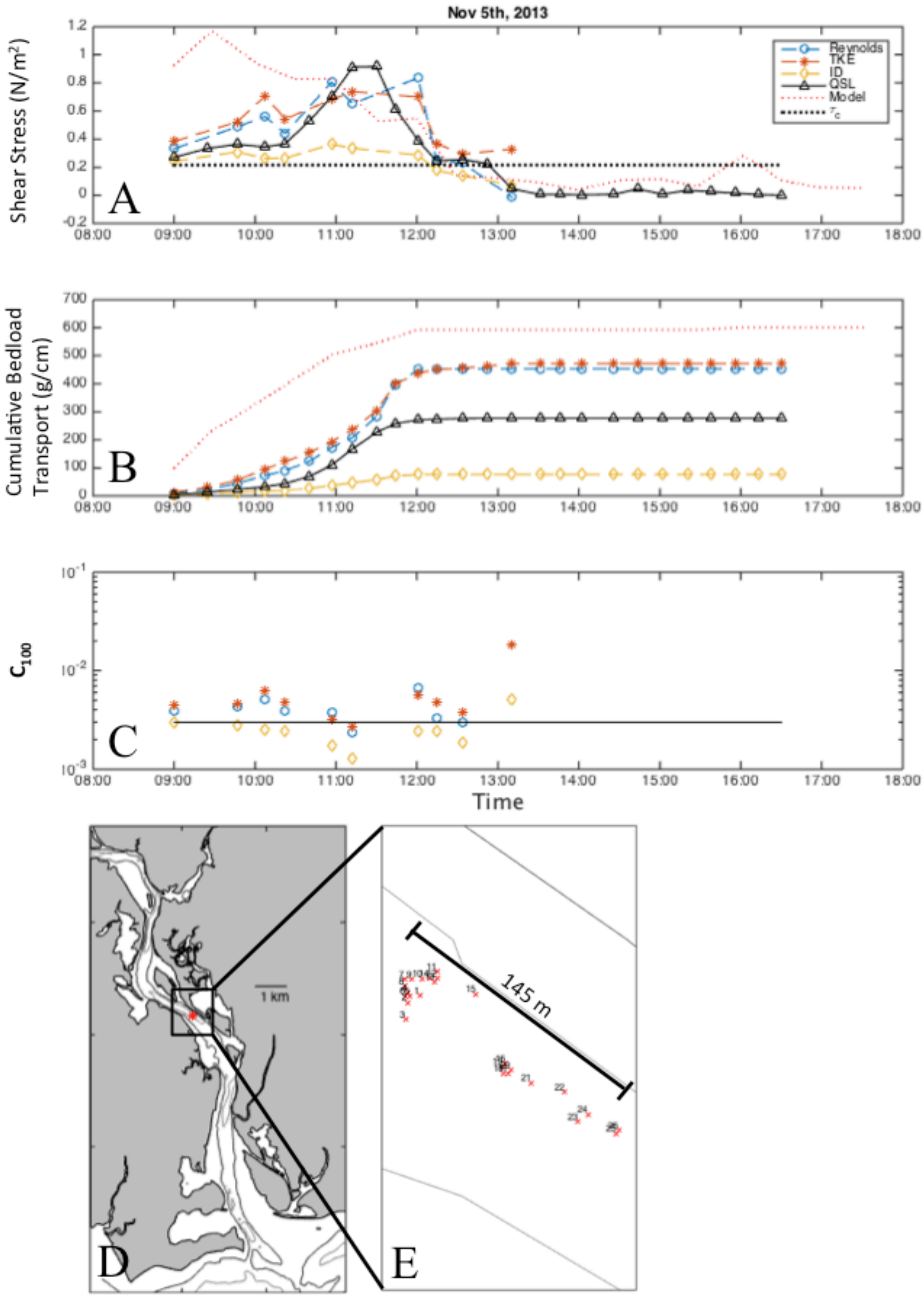

Figure 27: (A) Critical shear stress, determined using sediment grain size and Shields criteria, compared to observed shear stress, using Reynolds, TKE, ID, and QSL methods, and model calculations of shear stress for November 6th 2013 with associated model data. (B) Cumulative bedload transport calculated using Reynolds, TKE, ID, QSL and model shear stresses. (C) Drag coefficients calculated using Reynolds, TKE, and ID methods in relation to the common 3×10^{-3} drag coefficient. (D) Location of measurements (E) and individual casts (numbers refer to order of measurements).

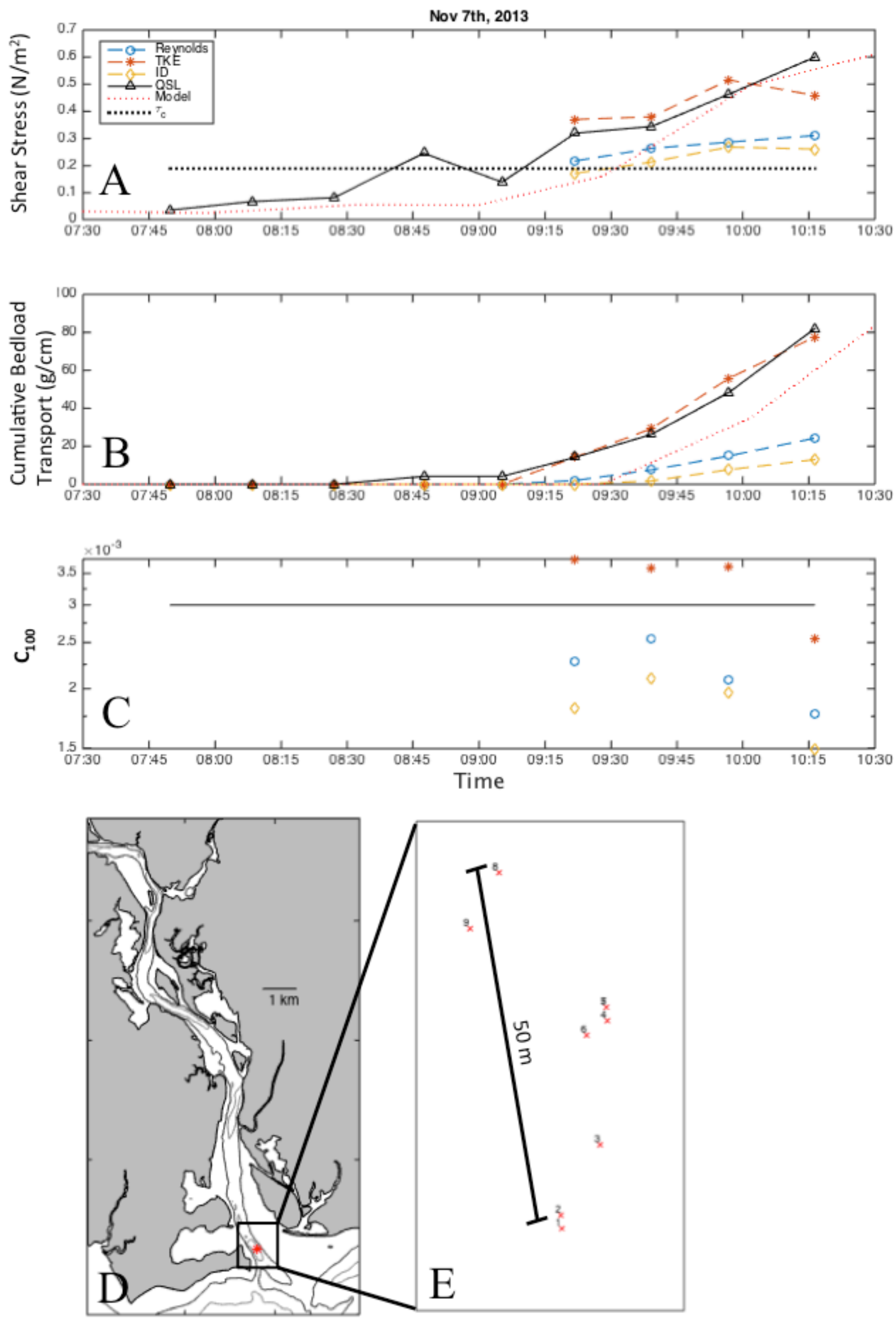

Figure 28: (A) Critical shear stress, determined using sediment grain size and Shields criteria, compared to observed shear stress, using Reynolds, TKE, ID, and QSL methods, and model calculations of shear stress for November 7th 2013 with associated model data. (B) Cumulative bedload transport calculated using Reynolds, TKE, ID, QSL and model shear stresses. (C) Drag coefficients calculated using Reynolds, TKE, and ID methods in relation to the common 3×10^{-3} drag coefficient. (D) Location of measurements (E) and individual casts (numbers refer to order of measurements).

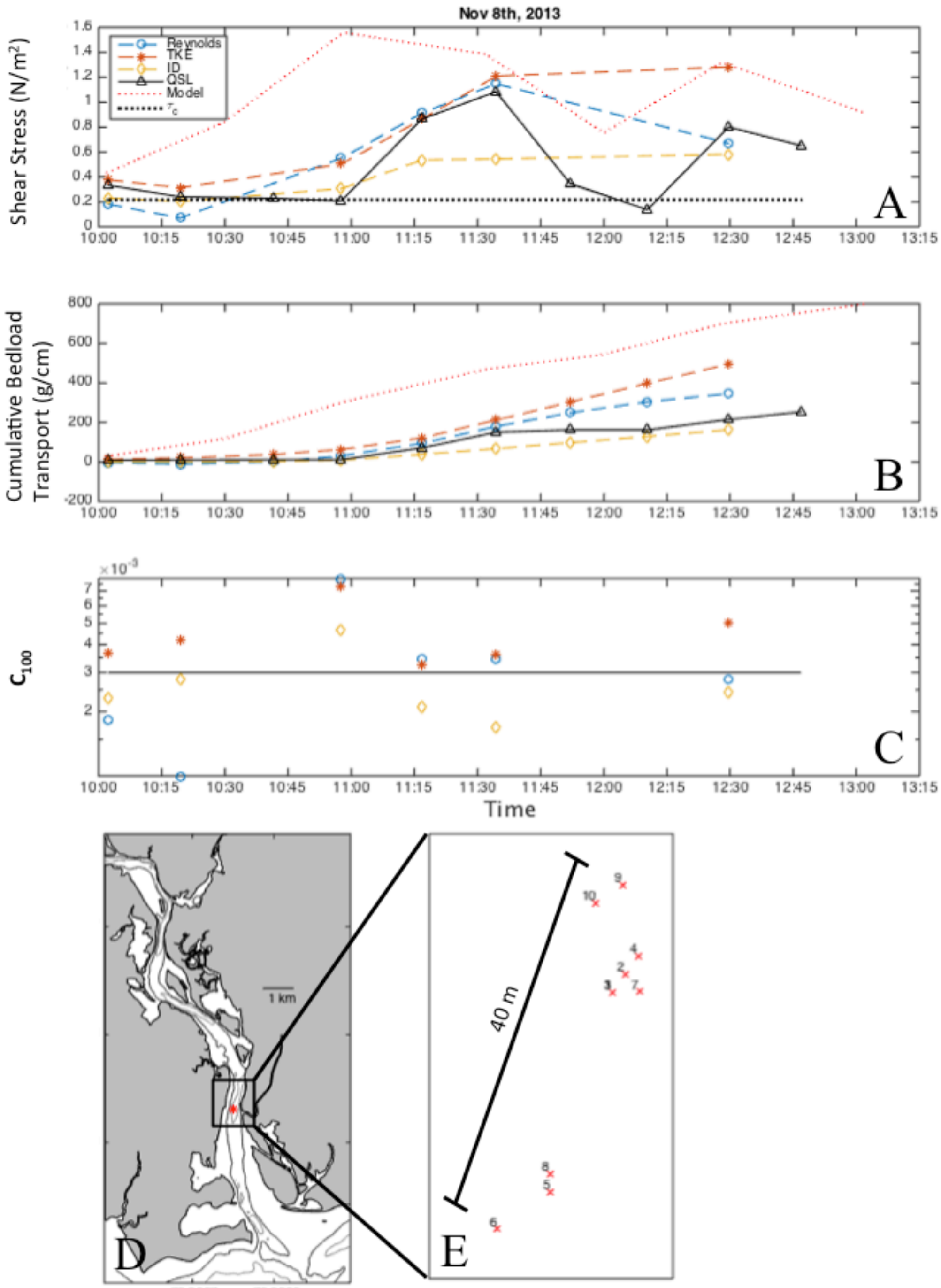

Figure 29: (A) Critical shear stress, determined using sediment grain size and Shields criteria, compared to observed shear stress, using Reynolds, TKE, ID, and QSL methods, and model calculations of shear stress for November 8th 2013 with associated model data. (B) Cumulative bedload transport calculated using Reynolds, TKE, ID, QSL and model shear stresses. (C) Drag coefficients calculated using Reynolds, TKE, and ID methods in relation to the common 3×10^{-3} drag coefficient. (D) Location of measurements (E) and individual casts (numbers refer to order of measurements).

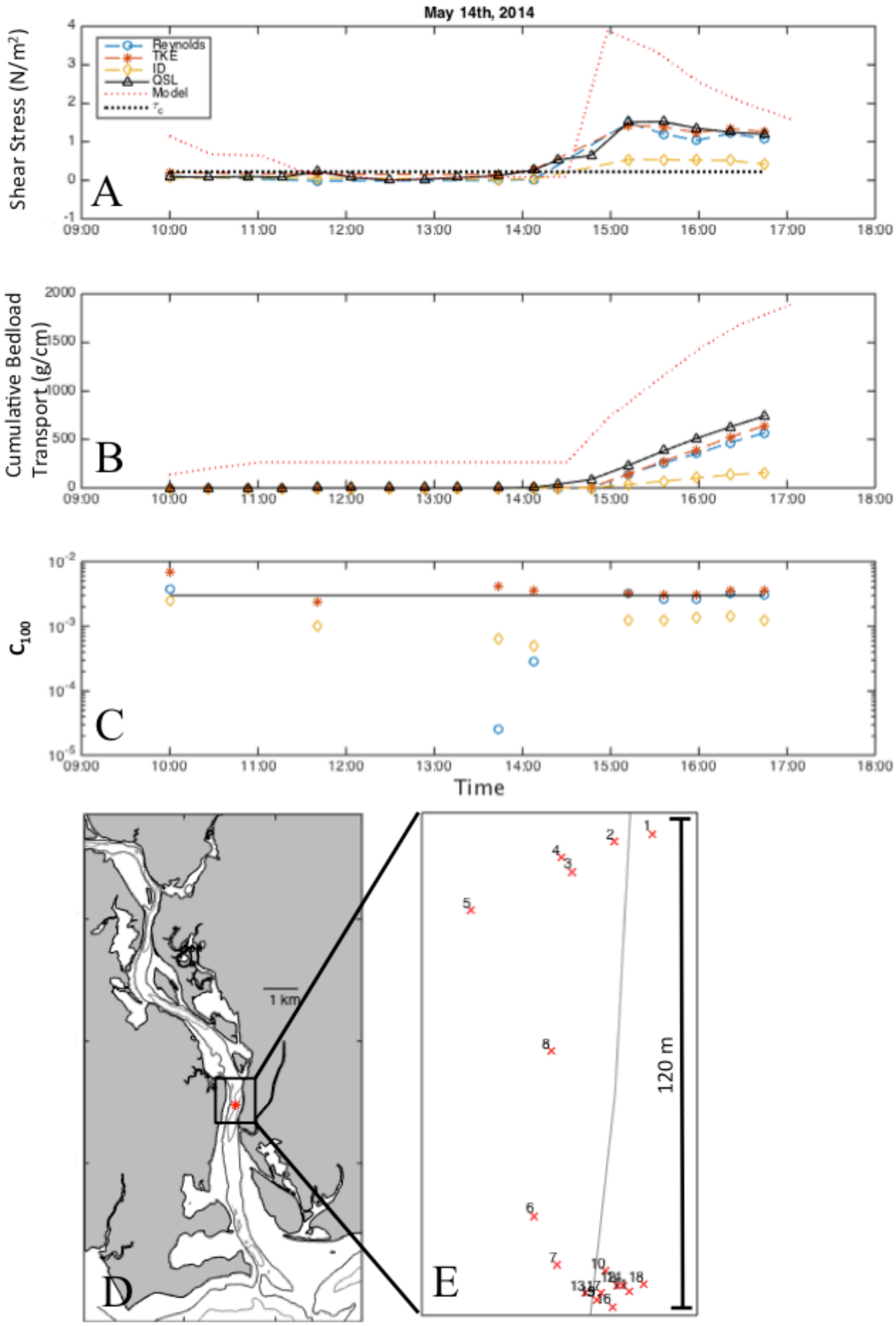

Figure 30: (A) Critical shear stress, determined using sediment grain size and Shields criteria, compared to observed shear stress, using Reynolds, TKE, ID, and QSL methods, and model calculations of shear stress for May 14th 2013 with associated model data. (B) Cumulative bedload transport calculated using Reynolds, TKE, ID, QSL and model shear stresses. (C) Drag coefficients calculated using Reynolds, TKE, and ID methods in relation to the common 3×10^{-3} drag coefficient. (D) Location of measurements (E) and individual casts (numbers refer to order of measurements).

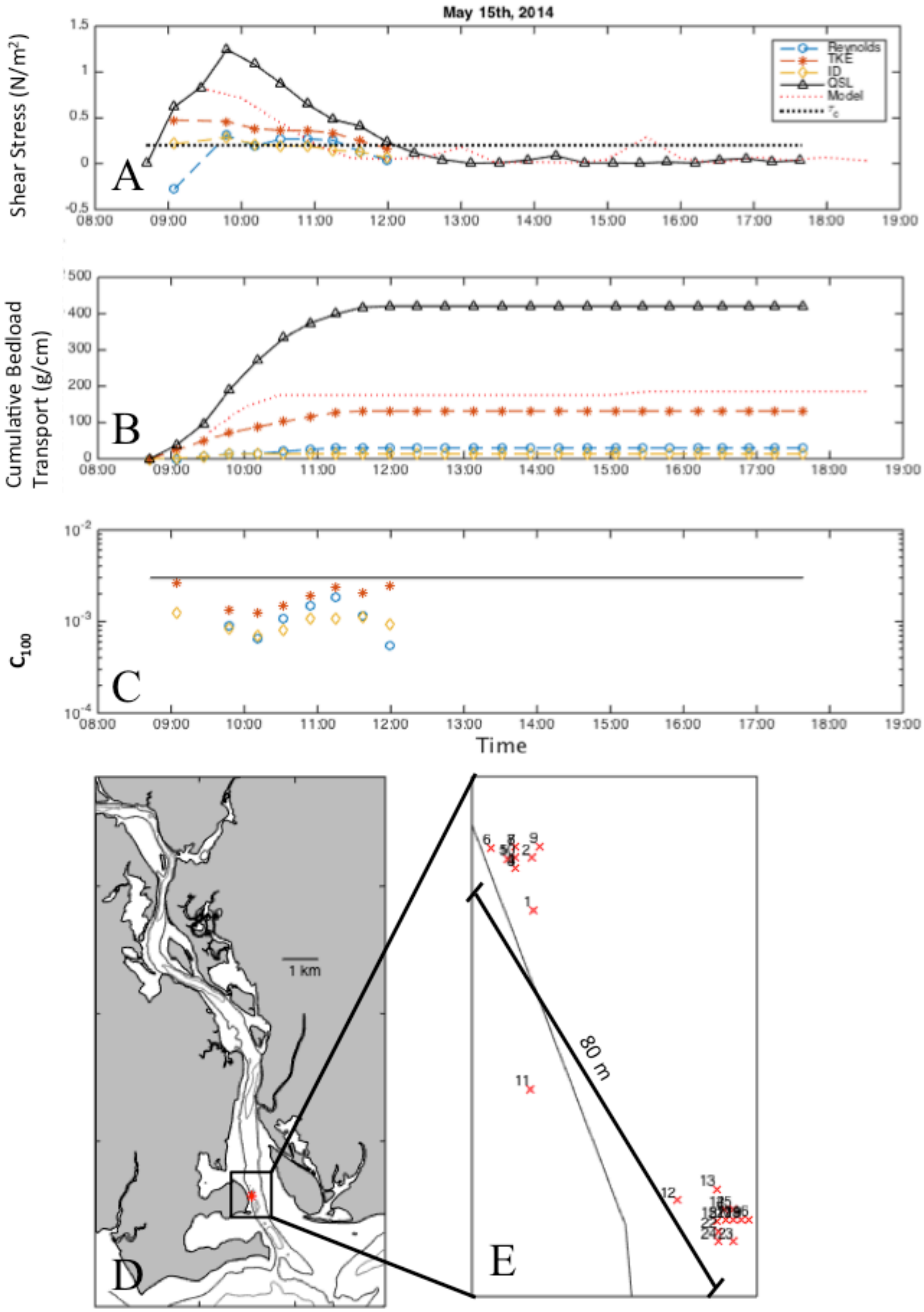

Figure 31: (A) Critical shear stress, determined using sediment grain size and Shields criteria, compared to observed shear stress, using Reynolds, TKE, ID, and QSL methods, and model calculations of shear stress for May 15th 2013 with associated model data. (B) Cumulative bedload transport calculated using Reynolds, TKE, ID, QSL and model shear stresses. (C) Drag coefficients calculated using Reynolds, TKE, and ID methods in relation to the common 3×10^{-3} drag coefficient. (D) Location of measurements (E) and individual casts (numbers refer to order of measurements).

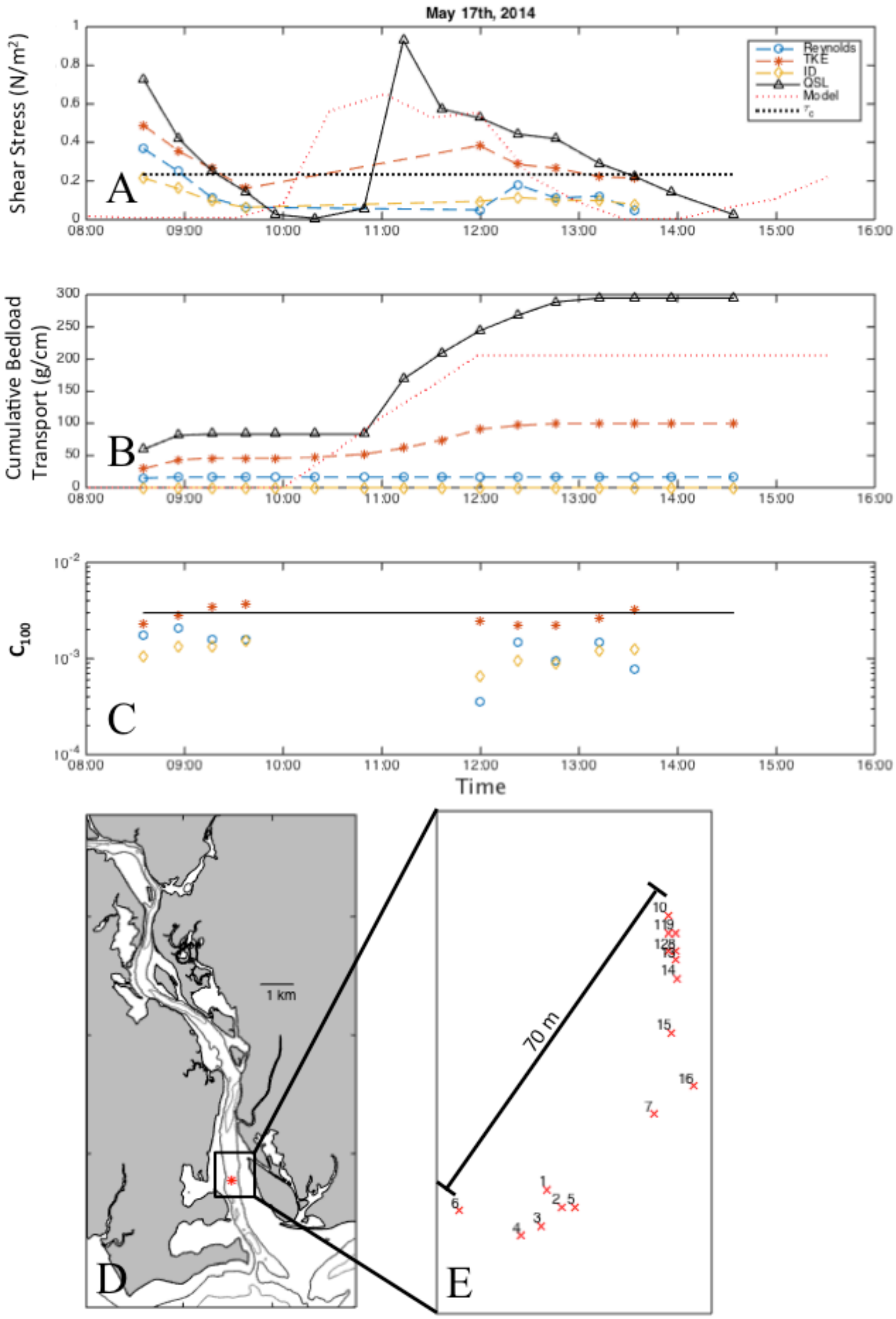

Figure 32: (A) Critical shear stress, determined using sediment grain size and Shields criteria, compared to observed shear stress, using Reynolds, TKE, ID, and QSL methods, and model calculations of shear stress for May 17th 2013 with associated model data. (B) Cumulative bedload transport calculated using Reynolds, TKE, ID, QSL and model shear stresses. (C) Drag coefficients calculated using Reynolds, TKE, and ID methods in relation to the common 3×10^{-3} drag coefficient. (D) Location of measurements (E) and individual casts (numbers refer to order of measurements).

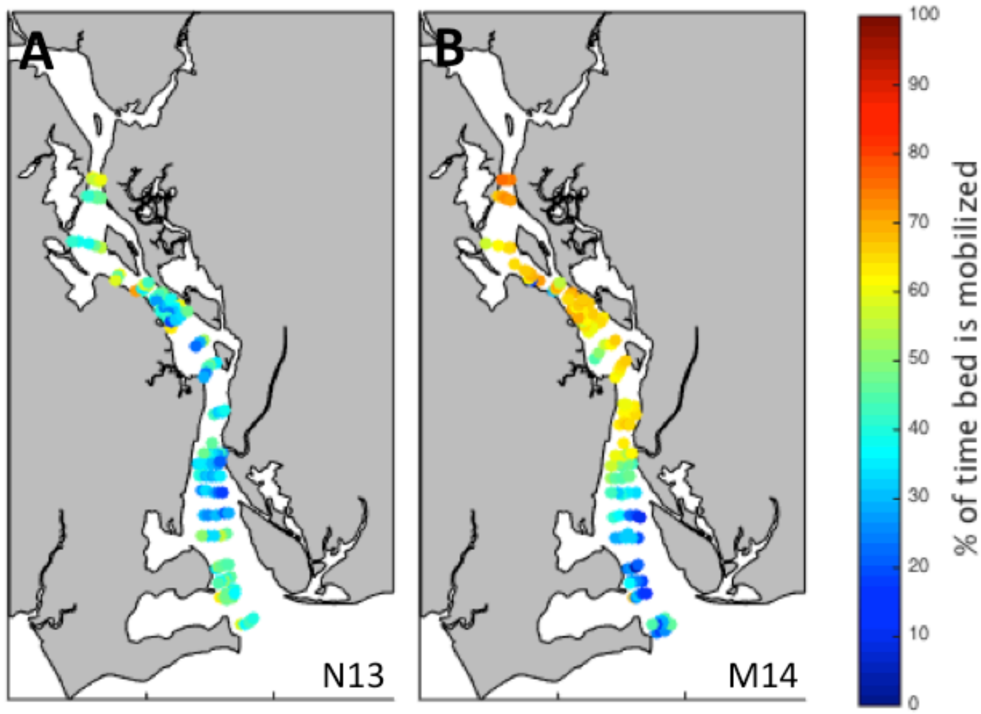

Figure 33: Percent of the time during the model run in November 2013 (A) and in May 2014 (B) that the bed (D_{50}) was mobilized ($\tau_b > \tau_c$). τ_c values are determined using the bottom sediment samples and Shields criteria.

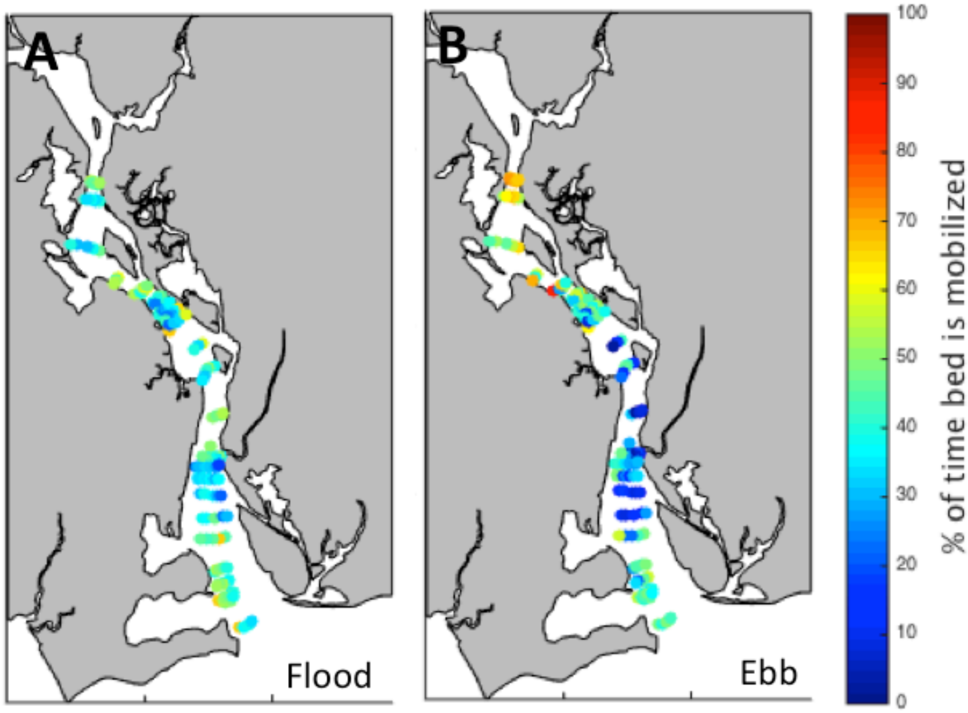

Figure 34: Percent of the time during the model run in November 2013 during the flood (A) and during the ebb (B) that the bed (D_{50}) was mobilized ($\tau_b > \tau_c$). τ_c values are determined using the bottom sediment samples and an empirical formulation of the Shields criteria.

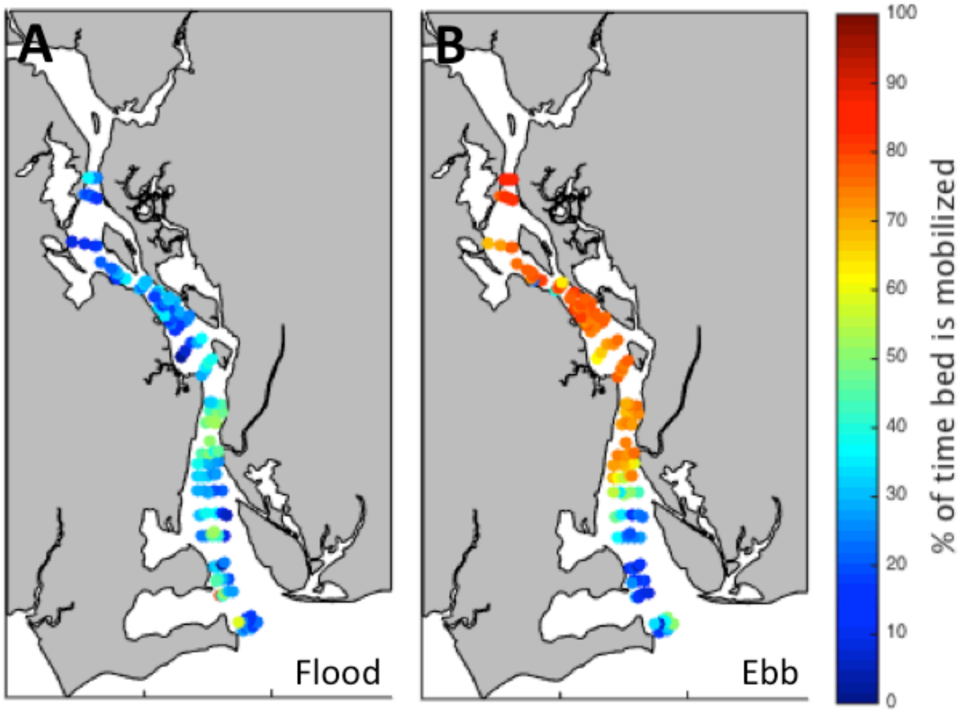

Figure 35: Percent of the time during the model run in May 2014 during the flood (A) and during the ebb (B) that the bed (D_{50}) was mobilized ($\tau_b > \tau_c$). τ_c values are determined using the bottom sediment samples and an empirical formulation of the Shields criteria.

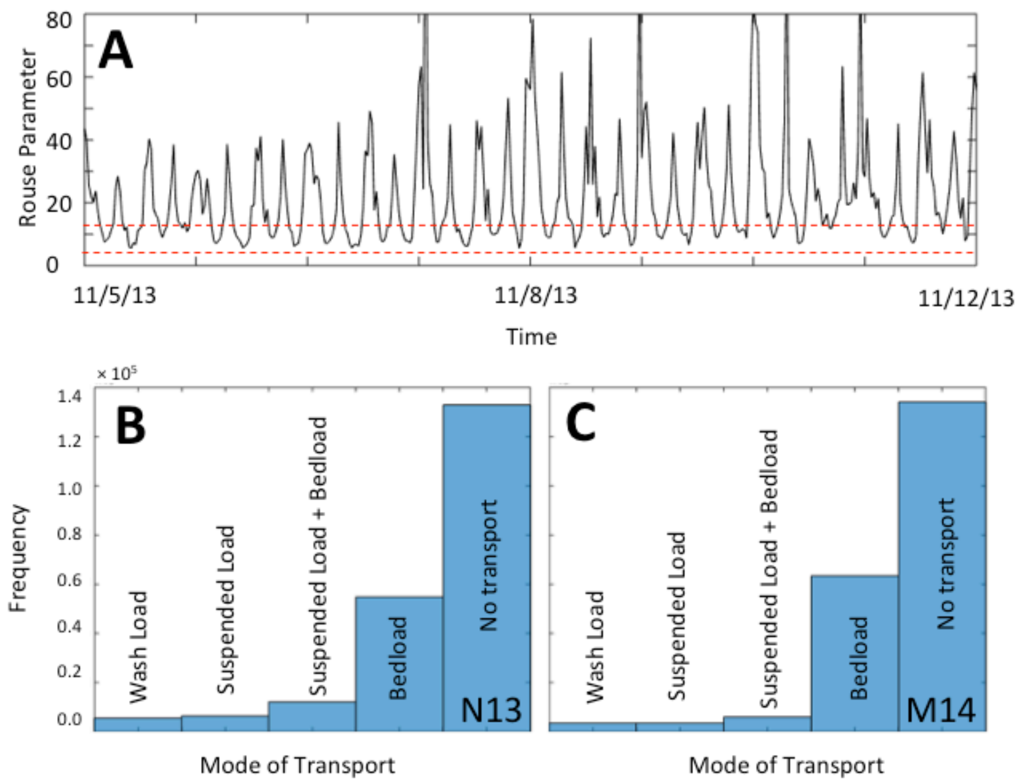

Figure 36: Rouse parameter for the D_{50} histogram for model runs. (A) Example time series of Rouse parameter for one core location in N13 ~2 km from the mouth in the center of the channel. Bottom dashed red line indicates boundary between bedload and suspended load, upper red line indicates boundary between bedload and no transport. (B) N13 and (C) M14 distributions of the Rouse parameter. Frequency is the number of times that a Rouse parameter within the given range was observed during each model run.

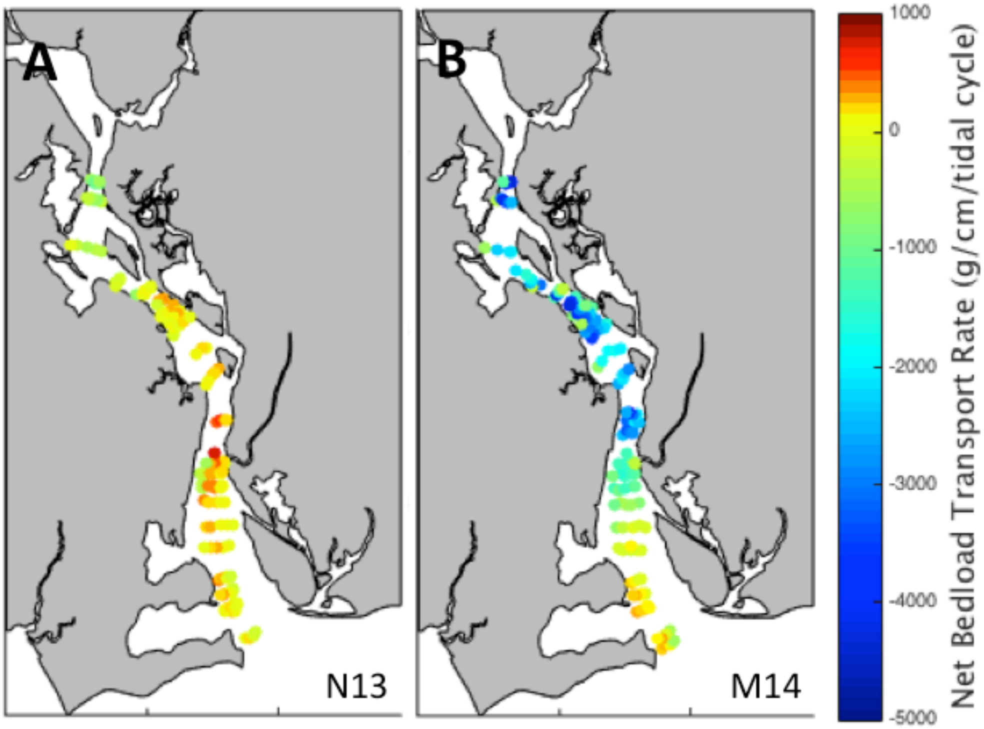

Figure 37: Tidally averaged bedload transport rate for November 2013 (A) and May 2014 (B) using model shear stress data and sediment sample grain sizes (D_{50}). Negative indicates ebb-directed transport.

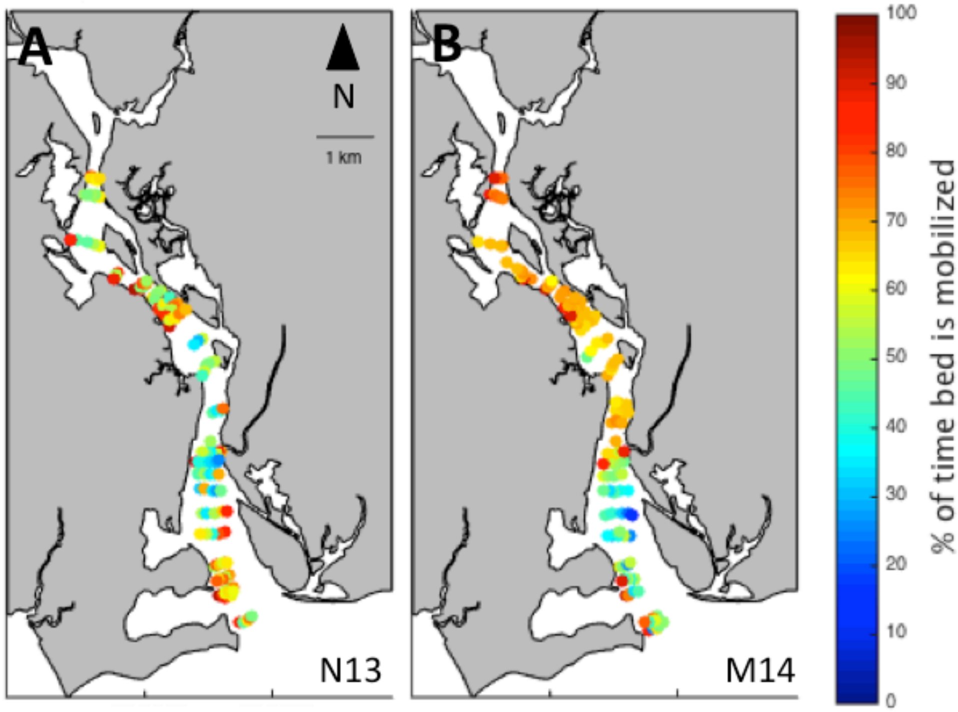

Figure 38: Percent of the time during the model run in November 2013 (A) and in May 2014 (B) that the D_{10} was mobilized ($\tau_b > \tau_c$). τ_c values are determined using the bottom sediment samples and an empirical formulation of the Shields criteria.

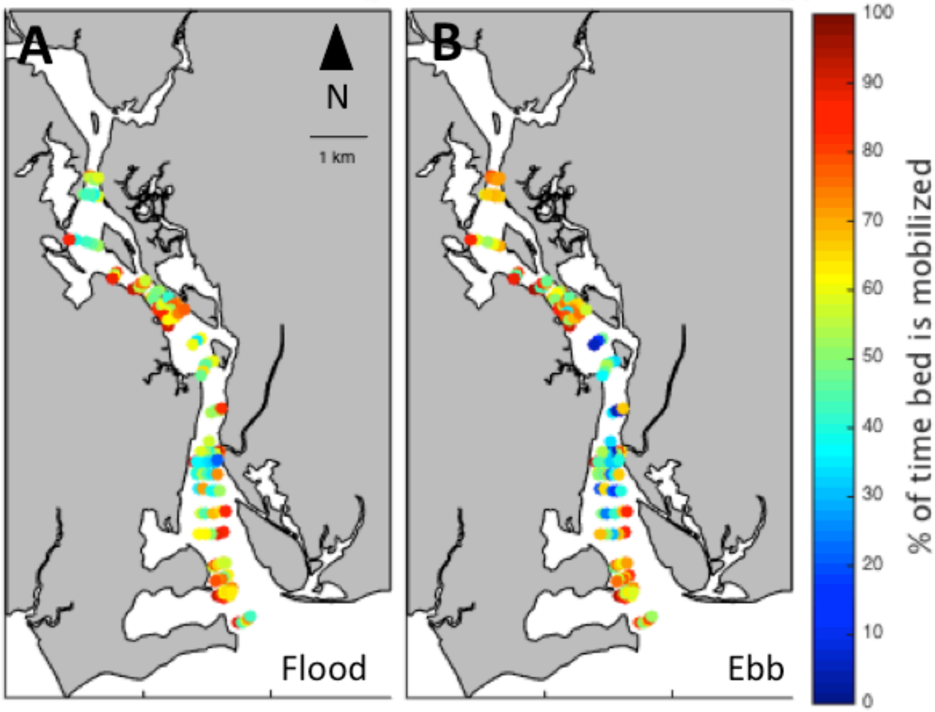

Figure 39: Percent of the time during the model run in November 2013 during the flood (A) and during the ebb (B) that the D_{10} was mobilized ($\tau_b > \tau_c$). τ_c values are determined using the bottom sediment samples and an empirical formulation of the Shields diagram.

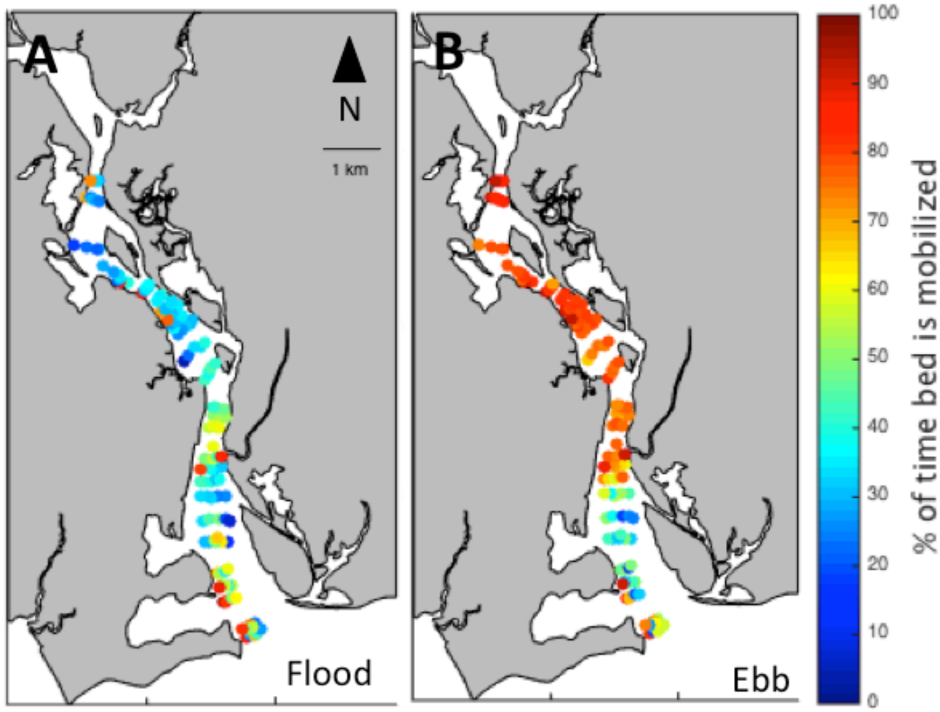

Figure 40: Percent of the time during the model run in May 2014 during the flood (A) and during the ebb (B) that the D_{10} was mobilized ($\tau_b > \tau_c$). τ_c values are determined using the bottom sediment samples and an empirical formulation of the Shields criteria.

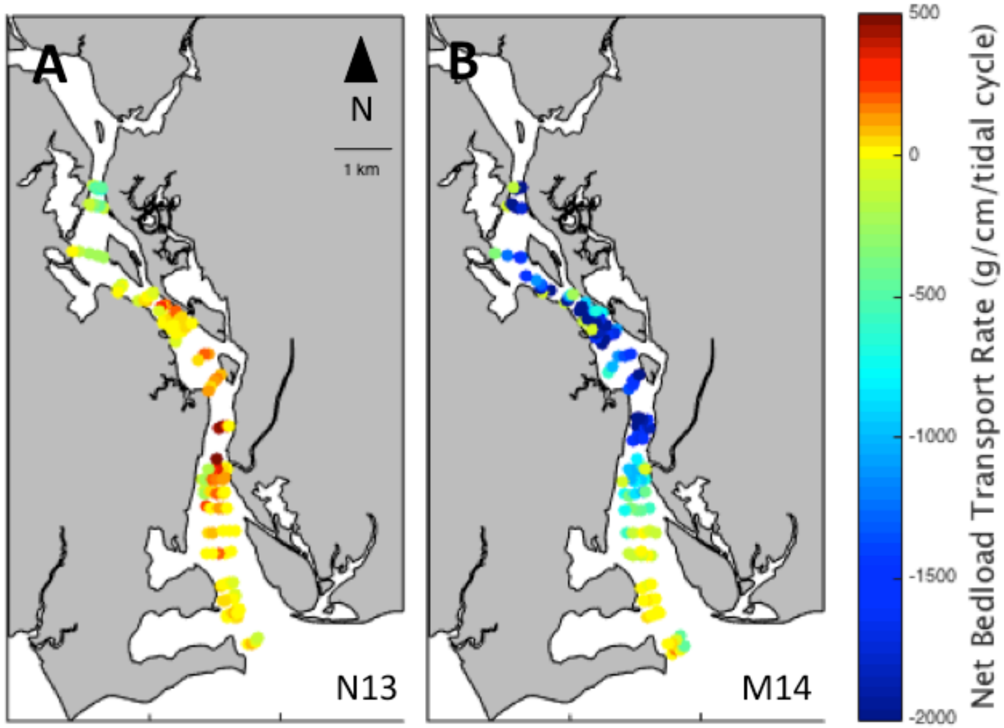

Figure 41: Tidally averaged bedload for November 2013 (A) and May 2014 (B) using model shear stress data and sediment sample grain sizes (D_{10}). The D_{10} is a proxy for the size fraction of the mud drape.

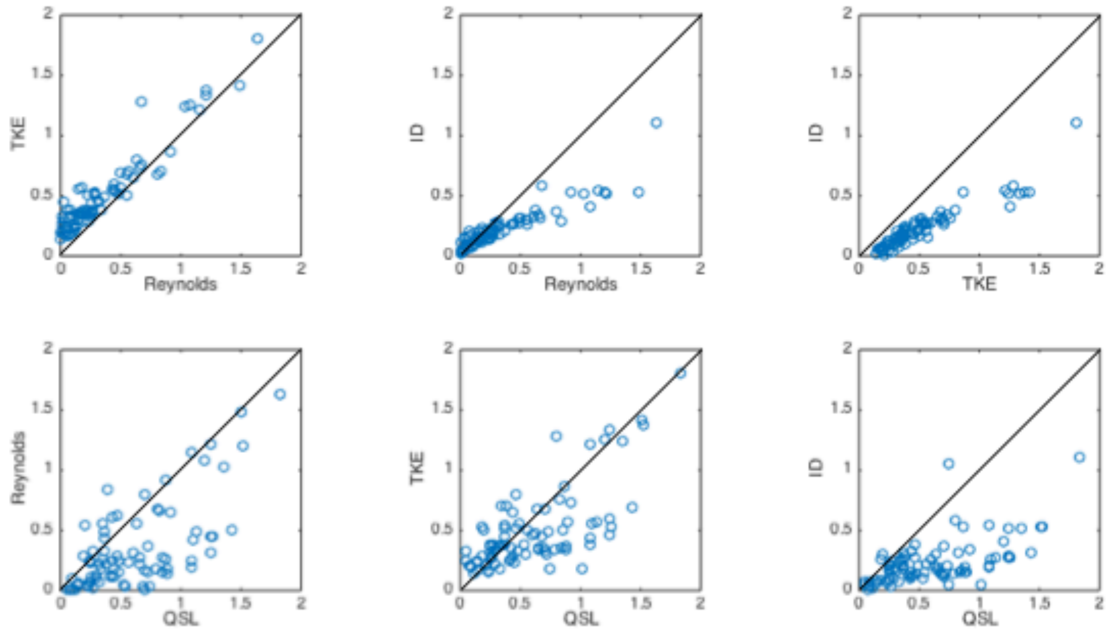

Figure 42: Comparison of Reynolds, TKE, ID and QSL methods for calculating shear stress. The solid black line on each plot is a 1:1 relationship.

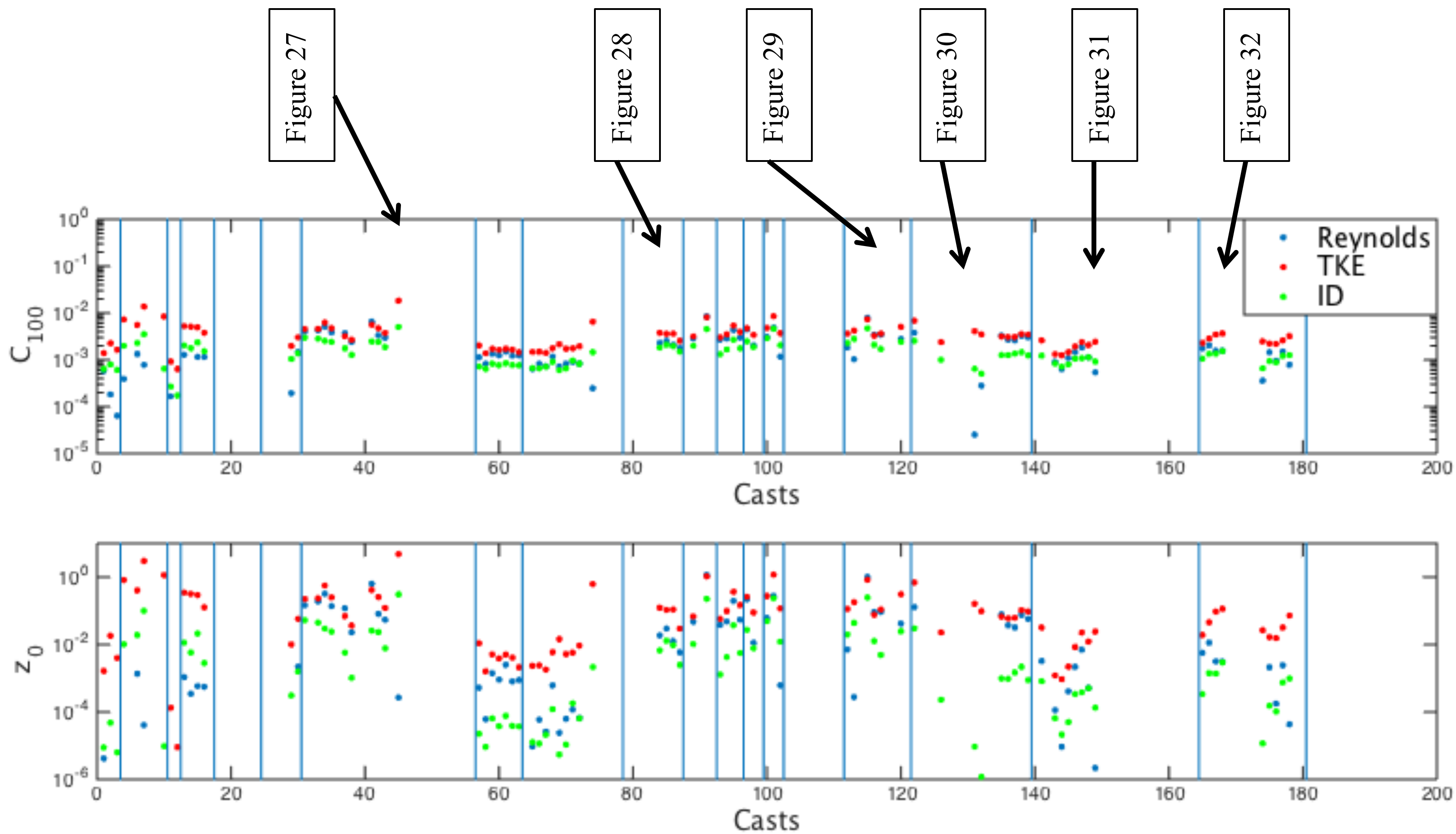

Figure 43: Drag coefficient at 1 mab and the corresponding z_0 for all anchor station measurements over field seasons M13, N13, and M14. Vertical lines indicate a change in time and/or location. See corresponding Figures 27-32 for locations.

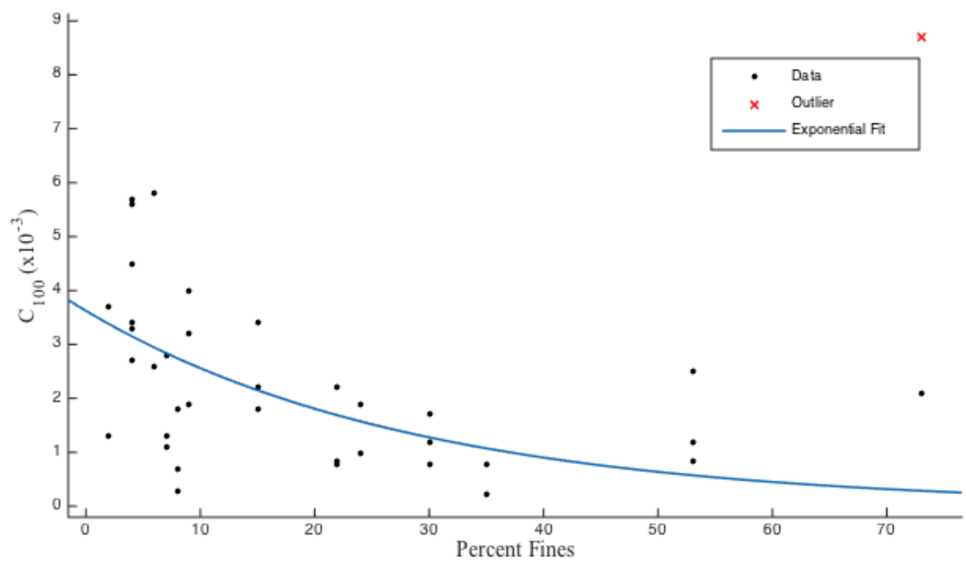

Figure 44: Drag coefficient at 1 mab versus percent fine sediments with one outlier removed. The data are expressed with an exponential fit (n=36, R^2=0.13, p=0.0332). Data were averaged by anchor station location for each method.

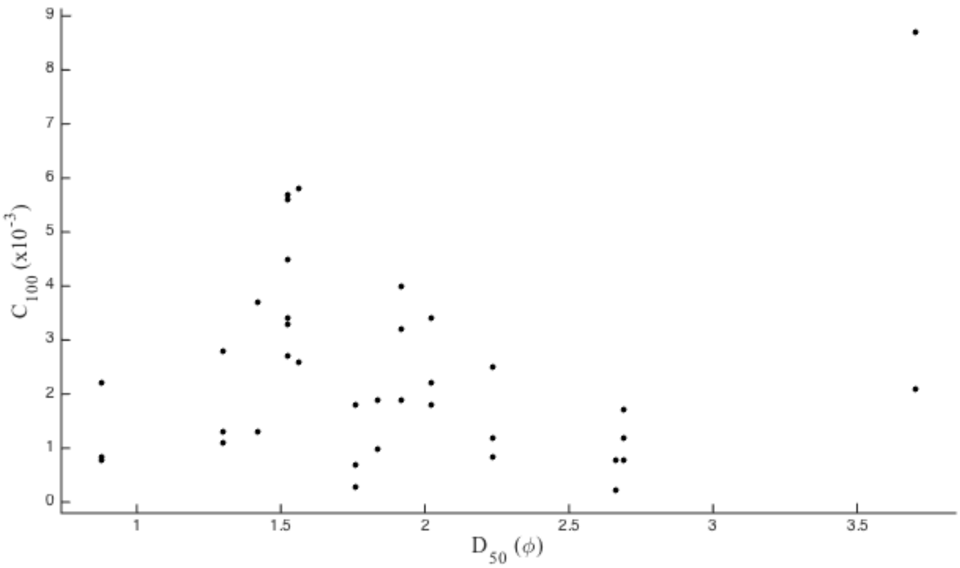

Figure 45: D50 versus drag coefficient has no trend.

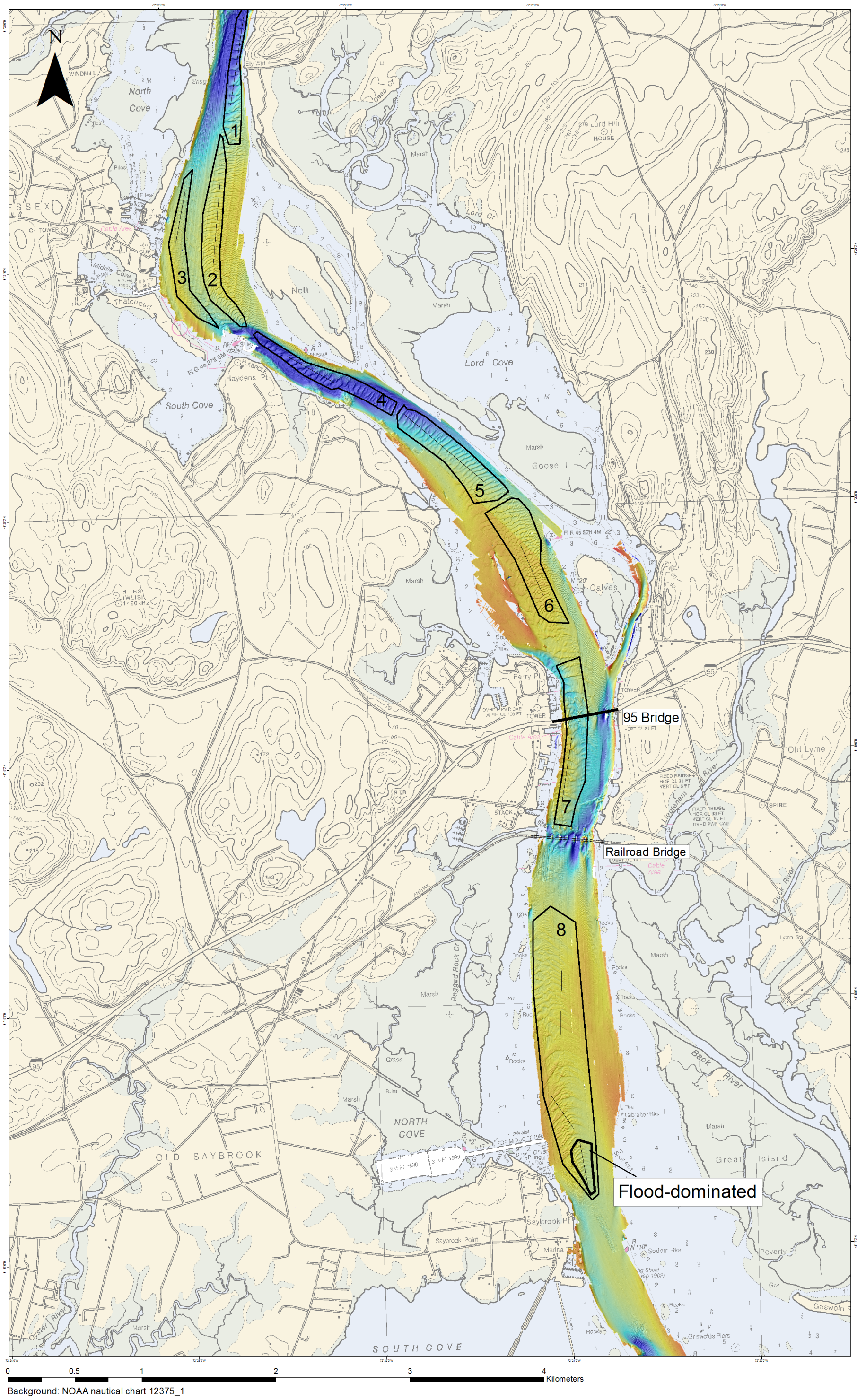

Figure 46: Bedform fields (BFF) 1-8 from north to south. The only flood-dominated section of bedforms is in BFF8 in the southern most region. Transects are marked by lines within the BFFs. Bathymetry data courtesy USGS.

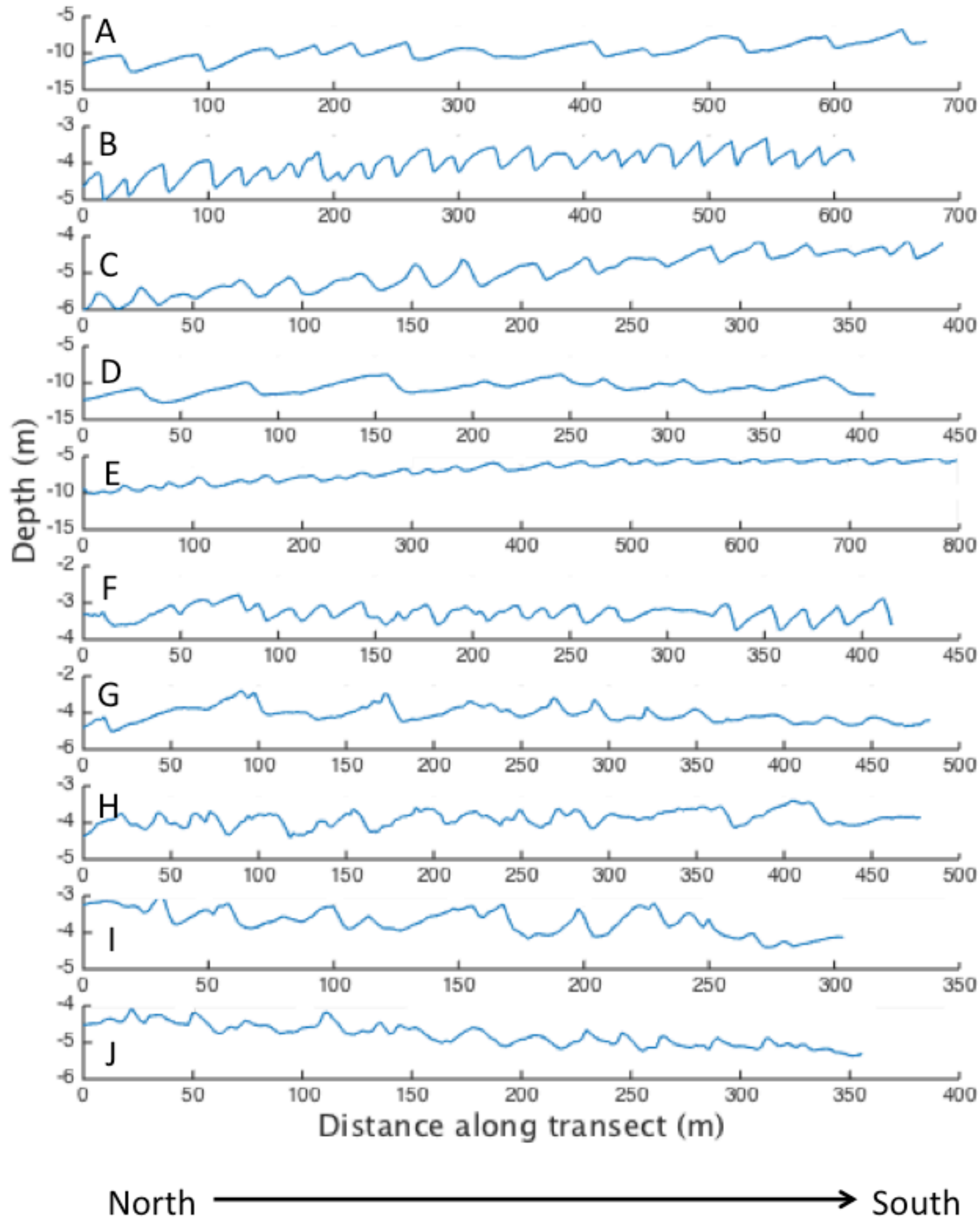

Figure 47: Bedform profiles from Fall 2012 USGS bathymetry survey for each BFF (1-8), with three profiles from BFF8. Profiles are marked in Figure 42. All transects are from north to south. All of the transects have ebb-dominated bedforms except the southern-most transect in BFF8.

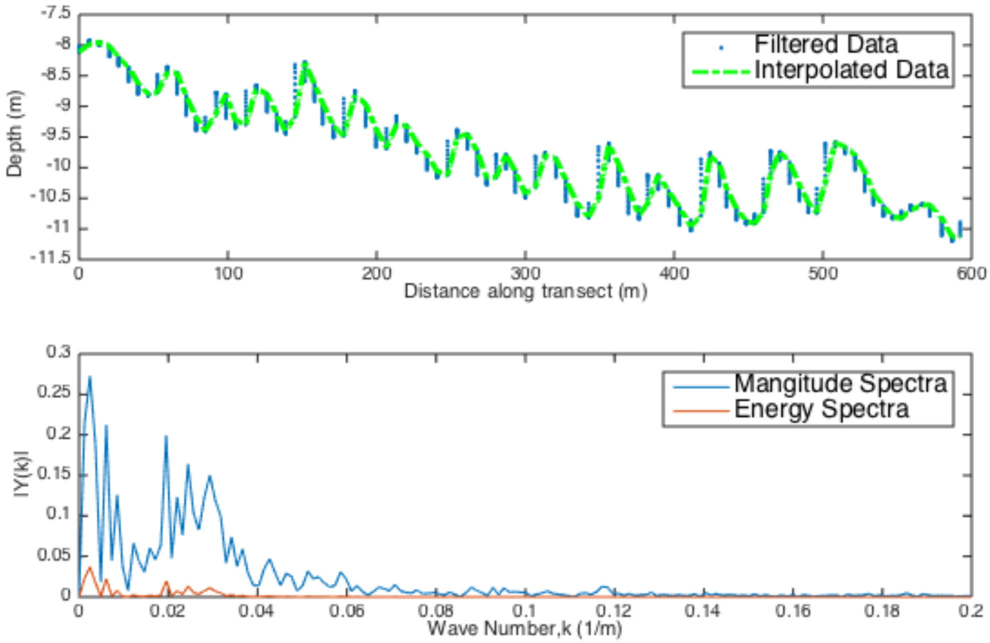

Figure 48: Example of processed data from echosounder surveys. BFF4 transect from N13 shown from north to south, with corresponding spectra used to determine the component waveforms.

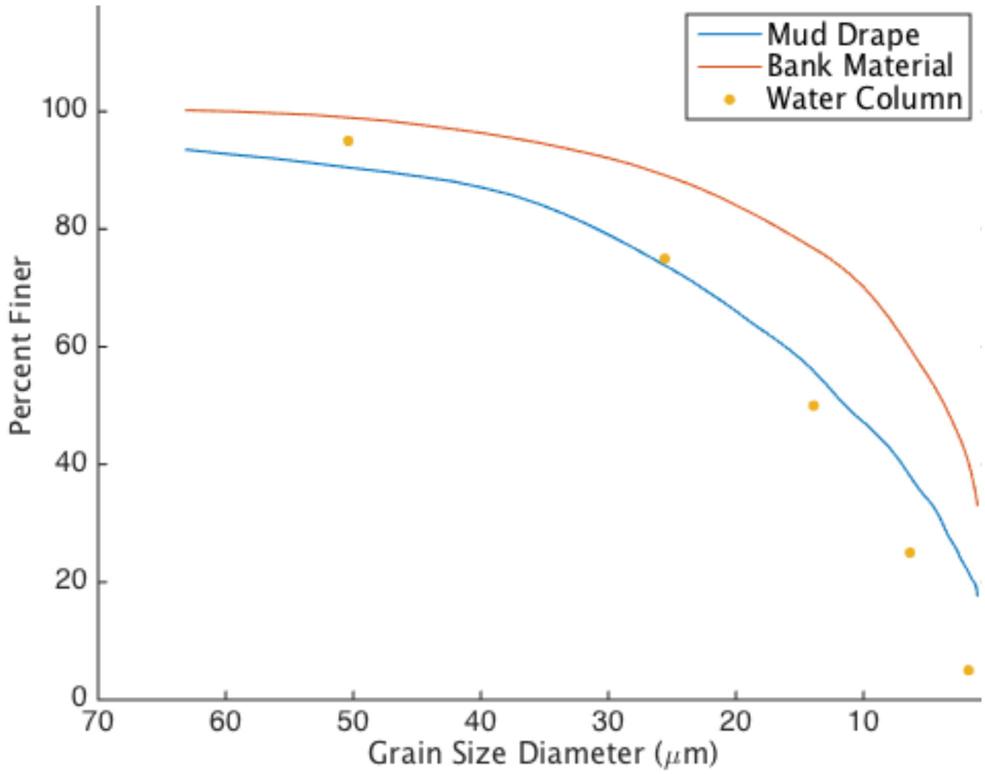

Figure 49: Grain size distribution of the fine fraction from a mud drape, a core taken from the side of the channel, and the mean grain size distribution in the water column. Water column distribution sized using a Coulter counter (*pers. comm. Milligan*).

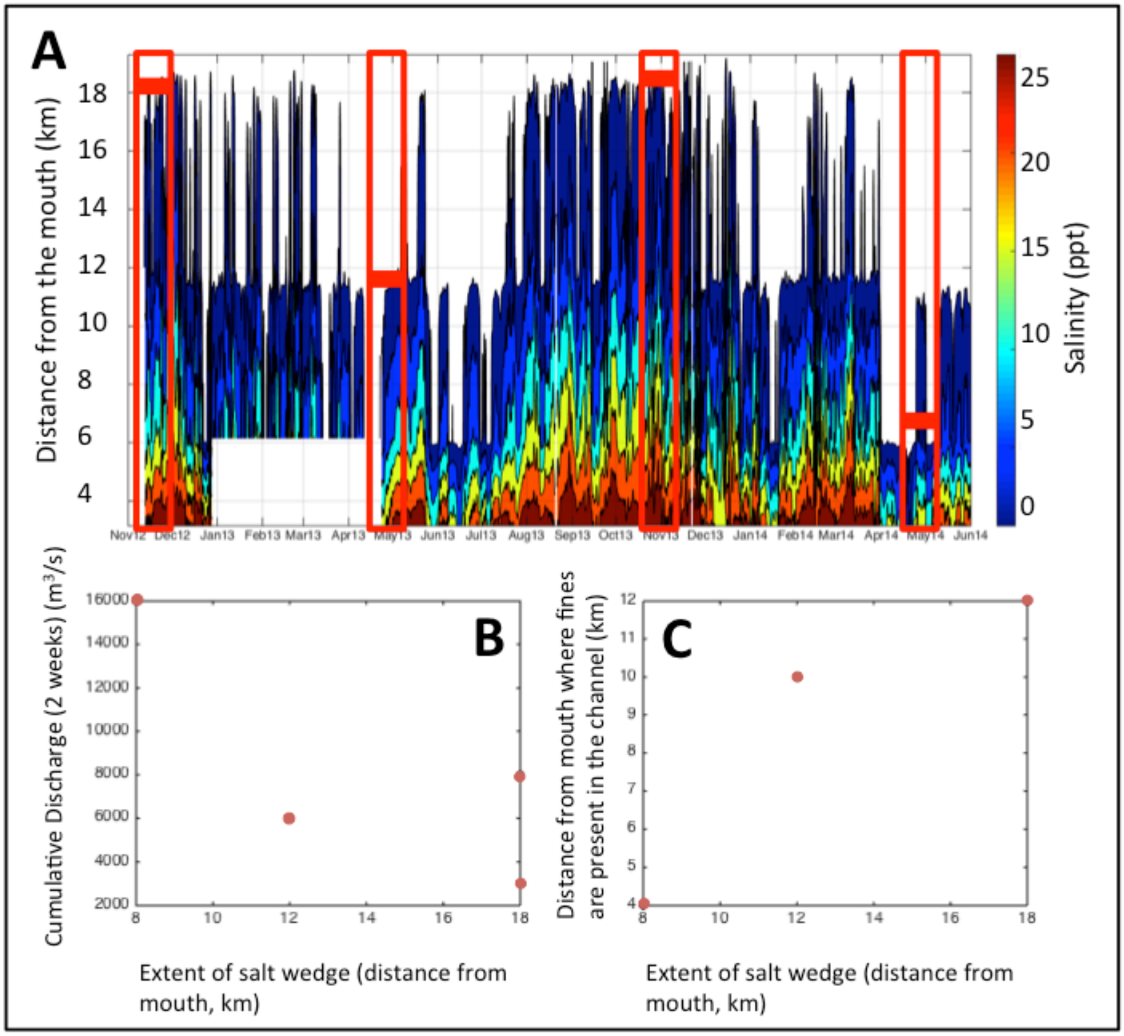

Figure 50: (A) Salinity throughout the estuary from N12 through M14 (*pers. comm. Wehof*). (B) Cumulative discharge (see Figure 5) versus extent of salt wedge (panel A). (C) Distance from the mouth that there are fine sediments in the channel (see Figure 14A) versus extent of salt wedge (panel A). Salinity measurements were taken using moored CTDs for a companion paper to the present study. Red boxes in (A) indicate sampling periods, and the red bar within the boxes indicates the average extent of the salt wedge during the sampling period.

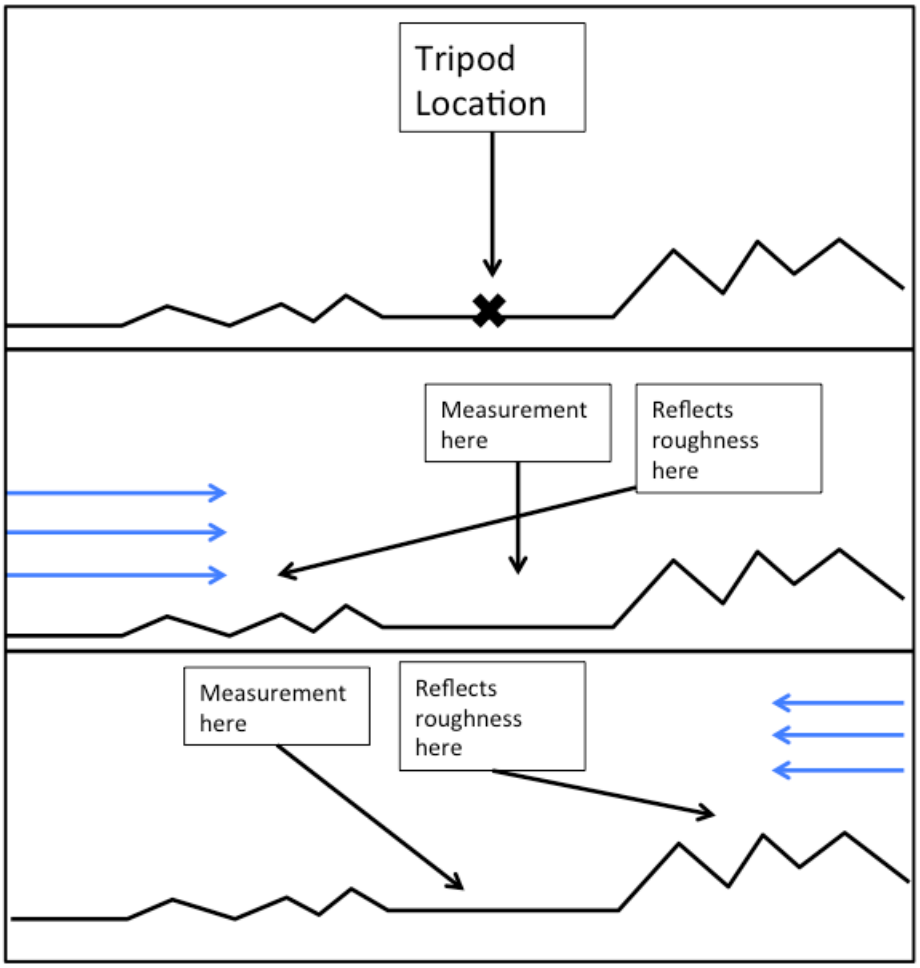

Figure 51: Schematic demonstrating that the measured flow reflects the bed it flowed over prior to the measurement. The measurement does not reflect the roughness of the bed immediately below the area sampled.

Table 1: From Soulsby (1983) showing the different calculated drag coefficients and roughness for different bottom types and configurations from multiple studies. The variation factor shown is for the roughness length. These values come from a variety of different studies (Lesser, 1951; Bowden and Fairbairn, 1956; Charnock, 1959; Sternberg, 1968; Dyer, 1970; Channon and Hamilton, 1971; Dyer, 1972; McCave, 1973; Vincent and Harvey, 1973; Sternberg, 1976; Heathershaw et al., 1979; Dyer, 1980 all in Heathershaw, 1981 and Soulsby, 1983).

Bottom Type	z_0 (cm)	Variation Factor	C_{100}	No. of observations
Mud	0.02	--	0.0022	1
Mud/sand	0.07	4.1	0.0030	3
Silt/sand	0.005	--	0.0016	1
Sand (unrippled)	0.04	2.0	0.0026	7
Sand (rippled)	0.6	1.3	0.0061	6
Sand/shell	0.03	4.5	0.0024	2
Sand/gravel	0.03	6.7	0.0024	7
Mud/sand/gravel	0.03	3.0	0.0024	2
Gravel	0.3	1.6	0.0047	4

Table 2: Percent organic matter for all field seasons, determined using LOI.

Field Season	Mean	Standard Deviation
Nov 12	2.1388	2.1089
May 13	2.3556	2.0999
Nov 13	1.9506	1.5487
May 14	1.6998	2.4192

Table 3: Grain size, bed composition, and calculated drag coefficient and roughness length from the ADV data using the Reynolds, TKE and ID methods. These values are compared to a roughness length calculated using *k'_b*.

Season	Cast ID	D_{50} (Coarse)	fines (%)	C_{100} Rey	TKE	ID	z0 (cm) Rey	TKE	ID	z_0 (via k'_b)
M13	1-3	1.76	8	.276	1.8	.6808	0.0000014	0.0079	0.000021	13.33
M13	4-10	3.701	73	--	8.7	2.1	0.00035	1.34	0.032	6.67
M13	11-12	2.665	35	--	.7786	.2206	$7.8*10^{-13}$	$7.1*10^{-5}$	$7.0*10^{-10}$	6.67
M13	**13-17**	**--**	**--**	**--**	**4.8**	**1.9**	0.00064	0.27	0.010	---
M13	18-24	0.087	2	--	--	--	---	---	---	0.0059
M13	25-30	2.237	53	.829	2.5	1.2	0.0011	0.0339	0.00095	---
N13	**1-26**	**1.5616**	**6**	**--**	**5.8**	**2.6**	0.172	0.7007	0.052	13.34
N13	**27-33**	**2.6872**	**30**	**1.2**	**1.7**	**.763**	0.00101	0.00466	0.000041	6.67
N13	**34-48**	**0.879**	**22**	**.765**	**2.2**	**.827**	0.000108	0.074	0.000288	13.34
N13	**49-57**	**2.023**	**15**	**2.2**	**3.4**	**1.8**	0.0168	0.092	0.0079	---
N13	58-62	1.521	4	5.7	5.6	3.3	0.60	0.56	0.118	0.0025
N13	**63-66**	**1.92**	**9**	**3.2**	**4.0**	**1.9**	0.084	0.167	0.012	13.36
N13	67-69	--	--	3.3	4.1	2.2	0.116	0.175	0.017	---
N13	70-72	--	--	3.0	5.7	3.2	0.113	0.524	0.099	---
N13	73-81	1.5616	6	--	--	--	---	---	---	13.34

N13	**82-91**	**1.521**	**4**	**3.4**	**4.5**	**2.7**	0.207	0.27	0.059	0.0025
M14	**1-18**	**1.421**	**2**	**--**	**3.7**	**1.3**	0.0454	0.152	0.00409	16.67
M14	**19-43**	**1.8374**	**24**	**--**	**1.9**	**.9696**	0.00169	0.013	0.00029	6.67
M14	**44-59**	**1.2998**	**7**	**1.3**	**2.8**	**1.1**	0.0031	0.049	0.0009	6.67
M14	60-63	1.4793	3	--	--	--	---	---	---	0.0026

Table 4: Bedform fields (BFFs) identified in Figure 42. BFFs identified by Horne and Patton (1989) are indicated. The dominant wavelengths of the BFFs using the USGS survey and the echosounder surveys are reported in meters. * indicates that there were multiple dominant wavelengths determined from the Fourier transform.

BFF	Horne and Patton 1989	USGS	Echosounder
1		63.98	---
2	X	44.52	---
3		26.82	---
4		56.66	51.20
5	X	31.99	31.73
6		18.93*	22.75*
7	X	102.2*	117.0*
8a	X	42.64*	45.52*
8b		73.05*	81.57*
8c	X	31.95*	---

Appendix A: Sediment Data

A.1 Core Locations and Indices

Core ID	Latitude (N)	Longitude (W)
1	41.27953	72.34770
2	41.27912	72.34637
3	41.27935	72.34588
4	41.27930	72.34500
5	41.27967	72.34495
6	41.28082	72.34492
7	41.34052	72.36618
8	41.34072	72.36560
9	41.34117	72.36527
10	41.34138	72.36493
11	41.34172	72.36442
12	41.34192	72.36425
13	41.33633	72.36145
14	41.33678	72.36063
15	41.33733	72.35978
16	41.33795	72.35867
17	41.33845	72.35863
18	41.33972	72.36102
19	41.33918	72.36145
20	41.33910	72.36212
21	41.33847	72.36280
22	41.30793	72.35155
23	41.30777	72.35037
24	41.30775	72.34908
25	41.30795	72.34770
26	41.30790	72.34673
27	41.33305	72.35868
28	41.33390	72.35813
29	41.33463	72.35725
30	41.33512	72.35612

31	41.33593	72.35468
32	41.30602	72.35282
33	41.30605	72.35087
34	41.30595	72.34968
35	41.30567	72.34800
36	41.28518	72.34912
37	41.28557	72.34853
38	41.28568	72.34782
39	41.28585	72.34703
40	41.28610	72.34617
41	41.28252	72.34880
42	41.28263	72.34815
43	41.28298	72.34632
44	41.28332	72.34552
45	41.27950	72.34793
46	41.27977	72.34697
47	41.27958	72.34790
48	41.27993	72.34693
49	41.28008	72.34637
50	41.28032	72.34547
51	41.28090	72.34460
52	41.30378	72.35245
53	41.30333	72.35107
54	41.30342	72.34975
55	41.30335	72.34815
56	41.30332	72.34728
57	41.35920	72.37828
58	41.35897	72.37745
59	41.35882	72.37635
60	41.35922	72.37918
61	41.35943	72.37968
62	41.36245	72.37645
63	41.36242	72.37687
64	41.27962	72.34765
65	41.27968	72.34773

66	41.28000	72.34698
67	41.28022	72.34643
68	41.28057	72.34513
69	41.28102	72.34452
70	41.33718	72.35683
71	41.33585	72.35432
72	41.33508	72.35638
73	41.33437	72.35707
74	41.33365	72.35853
75	41.33310	72.35895
76	41.33858	72.35792
77	41.33790	72.35798
78	41.33698	72.35937
79	41.33690	72.36058
80	41.33620	72.36105
81	41.30307	72.34942
82	41.30335	72.34788
83	41.30340	72.34723
84	41.30417	72.35235
85	41.30358	72.35153
86	41.30598	72.35257
87	41.30635	72.35065
88	41.30613	72.34970
89	41.30583	72.34803
90	41.30780	72.34698
91	41.30790	72.34790
92	41.30788	72.34937
93	41.30742	72.35042
94	41.30830	72.35112
95	41.33990	72.36100
96	41.33928	72.36145
97	41.33910	72.36230
98	41.33880	72.36247
99	41.34057	72.36585
100	41.34090	72.36538

101	41.34150	72.36490
102	41.34187	72.36440
103	41.27475	72.34120
104	41.27540	72.33970
105	41.27443	72.34210
106	41.28258	72.34878
107	41.28255	72.34825
108	41.28275	72.34732
109	41.28292	72.34588
110	41.28310	72.34530
111	41.28613	72.34598
112	41.28588	72.34740
113	41.28573	72.34798
114	41.28577	72.34833
115	41.28540	72.34892
116	41.29582	72.35285
117	41.29578	72.35078
118	41.29590	72.34833
119	41.29558	72.34652
120	41.29588	72.34513
121	41.32312	72.35067
122	41.32405	72.34988
123	41.32467	72.34930
124	41.32515	72.34862
125	41.32598	72.34782
126	41.35035	72.38387
127	41.34995	72.38205
128	41.34973	72.38055
129	41.34933	72.37798
130	41.35017	72.37720
131	41.35890	72.37965
132	41.35928	72.37878
133	41.35917	72.37833
134	41.35878	72.37768
135	41.35853	72.37635

136	41.34057	72.36785
137	41.34067	72.36600
138	41.34135	72.36553
139	41.34140	72.36503
140	41.34162	72.36445
141	41.34198	72.36435
142	41.33980	72.36122
143	41.33918	72.36168
144	41.33877	72.36233
145	41.33923	72.36203
146	41.33842	72.36267
147	41.33643	72.36162
148	41.33633	72.36155
149	41.33680	72.36057
150	41.33742	72.35972
151	41.33812	72.35870
152	41.33837	72.35868
153	41.33737	72.35672
154	41.33680	72.35762
155	41.33612	72.35850
156	41.33553	72.35933
157	41.33487	72.35983
158	41.33297	72.35870
159	41.33270	72.35892
160	41.33397	72.35862
161	41.33450	72.35772
162	41.33522	72.35597
163	41.33592	72.35450
164	41.28513	72.34887
165	41.28547	72.34835
166	41.28553	72.34782
167	41.28577	72.34697
168	41.28603	72.34600
169	41.28347	72.34538
170	41.28295	72.34623

171	41.28273	72.34717
172	41.28277	72.34720
173	41.28257	72.34805
174	41.28243	72.34872
175	41.28247	72.34865
176	41.27955	72.34797
177	41.27963	72.34690
178	41.27990	72.34630
179	41.28025	72.34537
180	41.28025	72.34447
181	41.27415	72.34288
182	41.27418	72.34185
183	41.27457	72.34063
184	41.27498	72.34048
185	41.27533	72.33985
186	41.30332	72.35275
187	41.30335	72.35090
188	41.30340	72.35007
189	41.30325	72.34947
190	41.30322	72.34807
191	41.30322	72.34723
192	41.36280	72.37838
193	41.36270	72.37803
194	41.36235	72.37742
195	41.36210	72.37657
196	41.36265	72.37627
197	41.35863	72.37607
198	41.35908	72.37730
199	41.35933	72.37842
200	41.35940	72.37875
201	41.35932	72.37947
202	41.34922	72.37657
203	41.34953	72.37793
204	41.34982	72.37997
205	41.35037	72.38240

206	41.35032	72.38405
207	41.34387	72.37192
208	41.34352	72.37212
209	41.34323	72.37273
210	41.34302	72.37255
211	41.34252	72.37297
212	41.33010	72.35018
213	41.32980	72.35150
214	41.32888	72.35287
215	41.32580	72.34757
216	41.32528	72.34877
217	41.32488	72.34933
218	41.32360	72.35002
219	41.32290	72.35062
220	41.31617	72.34932
221	41.31557	72.34845
222	41.31607	72.34737
223	41.31603	72.34605
224	41.31613	72.34568
225	41.30795	72.34710
226	41.30762	72.34778
227	41.30785	72.34925
228	41.30767	72.35040
229	41.30782	72.35142
230	41.30587	72.35233
231	41.30582	72.35043
232	41.30572	72.34943
233	41.30592	72.34778
234	41.30613	72.34710
235	41.30060	72.35203
236	41.30052	72.35100
237	41.30020	72.34912
238	41.30030	72.34810
239	41.30017	72.34678
240	41.29572	72.35188
241	41.29575	72.35068

242	41.29583	72.34833
243	41.29590	72.34655
244	41.29583	72.34525
245	41.29192	72.34625
246	41.29172	72.34778
247	41.29178	72.34937
248	41.29167	72.35093
249	41.29178	72.35247
250	41.30987	72.34922
251	41.27223	72.34190
252	41.27275	72.34095
253	41.27293	72.33962
254	41.27335	72.33925
255	41.27377	72.33842
256	41.27538	72.33967
257	41.27493	72.34067
258	41.27462	72.34050
259	41.27402	72.34185
260	41.27400	72.34275
261	41.27937	72.34780
262	41.27958	72.34687
263	41.27972	72.34638
264	41.28032	72.34537
265	41.28000	72.34463
266	41.28263	72.34553
267	41.28275	72.34637
268	41.28260	72.34688
269	41.28268	72.34812
270	41.28242	72.34860
271	41.28507	72.34888
272	41.28518	72.34822
273	41.28533	72.34785
274	41.28558	72.34675
275	41.28578	72.34628
276	41.29110	72.34632

277	41.29125	72.34752
278	41.29142	72.34938
279	41.29120	72.35097
280	41.29152	72.35222
281	41.29557	72.35217
282	41.29573	72.35063
283	41.29565	72.34810
284	41.29578	72.34663
285	41.29532	72.34520
286	41.30023	72.34640
287	41.30003	72.34837
288	41.29977	72.34977
289	41.30020	72.35115
290	41.30015	72.35255
291	41.30308	72.35245
292	41.30287	72.35137
293	41.30303	72.34985
294	41.30333	72.34812
295	41.30333	72.34747
296	41.30570	72.34730
297	41.30568	72.34808
298	41.30560	72.34973
299	41.30573	72.35098
300	41.30553	72.35275
301	41.30767	72.35137
302	41.30768	72.34917
303	41.30805	72.34788
304	41.30777	72.34692
305	41.30997	72.34927
306	41.31522	72.34735
307	41.31557	72.34765
308	41.31603	72.34870
309	41.31615	72.34903
310	41.31583	72.34673
311	41.31353	72.34983
312	41.31400	72.34892

313	41.31363	72.34790
314	41.31360	72.34735
315	41.31562	72.34575
316	41.31722	72.34608
317	41.31730	72.34748
318	41.31752	72.34828
319	41.31748	72.34895
320	41.32305	72.35048
321	41.32410	72.34985
322	41.32472	72.34937
323	41.32530	72.34895
324	41.32608	72.34793
325	41.32657	72.35595
326	41.32777	72.35480
327	41.32943	72.35325
328	41.32962	72.35142
329	41.33013	72.35017
330	41.33465	72.35323
331	41.33403	72.35420
332	41.33347	72.35537
333	41.33278	72.35647
334	41.33218	72.35718
335	41.33318	72.35853
336	41.33423	72.35890
337	41.33455	72.35785
338	41.33547	72.35623
339	41.33788	72.35717
340	41.33700	72.35755
341	41.33627	72.35868
342	41.33572	72.35947
343	41.33472	72.35970
344	41.33663	72.36152
345	41.33683	72.36058
346	41.33753	72.36000
347	41.33827	72.35892
348	41.33855	72.35843

349	41.33998	72.36130
350	41.33923	72.36192
351	41.33880	72.36228
352	41.33852	72.36260
353	41.34023	72.36615
354	41.34072	72.36562
355	41.34107	72.36500
356	41.34143	72.36517
357	41.34163	72.36442
358	41.34185	72.36422
359	41.34248	72.36973
360	41.34232	72.37220
361	41.34307	72.37225
362	41.34333	72.37212
363	41.34367	72.37180
364	41.34398	72.37227
365	41.34463	72.37337
366	41.34573	72.37623
367	41.34913	72.37700
368	41.34922	72.37768
369	41.34952	72.38050
370	41.35023	72.38370
371	41.35923	72.38013
372	41.35933	72.37900
373	41.35892	72.37850
374	41.35882	72.37775
375	41.35860	72.37647
376	41.36243	72.37660
377	41.36248	72.37695
378	41.36242	72.37748
379	41.36238	72.37793
380	41.36263	72.37870
381	41.29128	72.34908
382	41.29160	72.34908
383	41.29188	72.34860

A.2 Grain Size Distributions

Core ID	Date	Hr.	Min.	-1 Φ	-0.5 Φ	0 Φ	0.5 Φ	1 Φ	1.5 Φ	2 Φ	2.5 Φ	3 Φ	3.5 Φ	4 Φ	% Fine
1	11/12/2012	10	19	0.00	0.00	0.00	0.00	0.00	0.00	0.00	0.00	0.00	3.29	35.39	61.31
2	11/12/2012	10	45	0.00	0.00	0.64	1.27	4.46	11.46	15.92	9.55	3.82	3.82	10.83	38.23
3	11/12/2012	10	56	0.00	0.55	1.09	1.64	4.37	14.74	28.38	11.46	4.37	4.91	12.55	15.94
4	11/12/2012	11	4	0.00	0.58	1.73	2.31	5.77	17.87	32.29	9.23	5.19	4.61	9.23	11.20
5	11/12/2012	11	24	1.67	1.67	2.23	4.45	7.79	18.37	29.50	8.91	5.57	4.45	6.12	9.27
6	11/12/2012	11	36	1.57	1.05	2.62	4.71	10.48	19.38	25.67	13.09	3.14	2.10	7.33	8.86
7	11/13/2012	6	54	0.00	0.00	0.00	0.00	0.00	0.00	0.00	1.88	3.75	4.69	11.26	78.41
8	11/13/2012	7	10	3.60	4.12	8.24	16.99	30.38	21.63	6.69	3.60	2.06	0.00	0.00	2.68
9	11/13/2012	7	27	0.00	0.00	0.00	1.06	12.70	40.22	34.40	7.41	1.59	0.00	0.00	2.61
10	11/13/2012	7	43	0.00	0.00	0.00	0.00	0.00	1.24	8.05	24.78	31.60	6.82	3.10	24.41
11	11/13/2012	7	58	0.00	0.00	0.00	0.00	1.70	14.76	31.79	30.66	14.19	3.97	0.00	2.92
12	11/13/2012	8	10	0.00	0.00	0.00	0.00	0.00	8.58	14.10	26.97	29.42	12.26	5.52	3.16
13	11/13/2012	8	23	0.00	0.00	0.00	0.00	0.00	0.00	0.00	0.00	4.20	8.40	17.85	69.55
14	11/13/2012	8	29	0.00	1.12	5.02	12.82	23.42	13.94	3.90	3.90	6.69	4.46	8.36	16.36
15	11/13/2012	8	33	0.00	0.58	2.89	7.51	24.26	24.26	12.13	4.62	4.04	1.73	3.47	14.50
16	11/13/2012	8	40	0.00	0.00	0.54	2.68	13.94	36.45	31.09	7.50	2.14	0.00	0.00	5.67
17	11/13/2012	9	28	0.00	0.00	0.00	1.15	6.34	23.07	26.53	17.88	10.96	2.88	1.15	10.04
18	11/13/2012	9	43	0.00	0.00	0.00	0.64	9.01	27.67	25.10	12.87	12.23	3.22	1.29	7.97
19	11/13/2012	9	50	0.00	0.00	0.00	0.00	1.78	8.02	11.58	7.13	5.35	4.46	9.80	51.88
20	11/13/2012	9	58	3.09	2.06	4.64	13.39	36.58	27.30	7.73	1.03	0.52	0.52	0.00	3.15
21	11/13/2012	10	6	0.00	0.00	3.72	12.23	21.81	10.64	4.79	5.32	10.64	5.32	6.38	19.15
22	11/13/2012	16	57	0.00	0.00	2.75	11.01	33.04	37.44	11.01	1.10	1.10	0.00	0.00	2.54
23	11/13/2012	17	1	0.00	0.00	1.68	11.21	33.62	35.86	14.01	1.68	0.00	0.00	0.00	1.96
24	11/13/2012	17	4	0.00	0.00	2.60	6.25	14.58	23.43	31.25	11.98	3.12	1.56	1.56	3.66
25	11/13/2012	17	9	0.00	0.00	0.00	0.00	0.53	15.26	46.83	26.83	6.31	1.05	0.00	3.19
26	11/13/2012	17	16	0.00	0.00	0.00	0.00	1.86	3.71	6.81	11.14	17.95	15.48	13.62	29.42
27	11/14/2012	6	58	0.00	0.00	0.00	0.00	1.78	1.78	3.57	3.57	7.13	8.92	12.48	60.76
28	11/14/2012	7	1	0.00	1.63	7.06	20.10	33.14	15.21	3.26	1.09	2.17	1.09	3.80	11.45
29	11/14/2012	7	6	2.34	0.00	1.75	5.85	21.06	29.24	9.94	2.34	1.75	1.17	5.26	19.29
30	11/14/2012	7	14	1.70	0.00	1.13	4.52	21.48	32.78	23.74	6.78	2.83	1.13	0.00	3.91
31	11/14/2012	7	23	3.24	0.54	1.08	2.16	5.39	10.25	26.97	22.65	15.64	5.39	2.16	4.54
32	11/14/2012	7	52	0.00	0.00	0.00	0.00	0.00	3.39	1.69	0.00	0.00	0.00	0.00	94.92
33	11/14/2012	7	59	0.00	1.58	3.70	7.92	19.55	33.81	19.55	4.23	2.11	1.06	1.58	4.91
34	11/14/2012	8	4	1.48	1.97	2.46	5.91	17.72	25.11	24.61	10.34	3.94	1.48	1.48	3.51
35	11/14/2012	8	7	1.10	1.10	2.21	5.52	17.67	30.37	28.16	8.83	2.76	0.00	0.00	2.27
36	11/14/2012	8	57	0.00	0.00	0.00	0.00	4.87	43.80	40.76	4.87	1.22	0.00	0.00	4.49
37	11/14/2012	9	0	0.00	0.00	0.00	1.59	11.16	45.69	32.94	3.72	1.59	0.00	0.00	3.30
38	11/14/2012	9	3	0.00	0.00	0.00	3.41	14.33	36.16	19.78	4.09	2.73	3.41	5.46	10.63
39	11/14/2012	9	6	0.98	1.47	2.44	4.88	15.14	33.70	26.86	5.86	1.47	0.00	2.44	4.75
40	11/14/2012	9	11	0.00	0.00	0.63	1.26	2.53	5.06	18.33	18.33	6.32	1.90	3.79	41.84
41	11/14/2012	9	19	0.00	0.00	0.00	0.00	0.00	0.00	0.00	1.38	4.15	8.99	44.24	41.24
42	11/14/2012	9	23	0.00	0.00	0.00	1.65	7.71	18.73	28.64	6.06	4.41	4.96	13.22	14.62
43	11/14/2012	9	33	0.00	0.00	1.19	2.38	6.55	15.48	17.26	5.95	2.98	2.38	20.83	25.00
44	11/14/2012	9	37	0.00	0.00	1.59	3.70	11.10	22.73	34.36	16.92	1.59	0.00	1.59	6.44
45	11/14/2012	9	44	0.00	0.00	0.00	0.00	0.00	0.00	0.00	0.00	0.00	2.21	32.36	65.43
46	11/14/2012	9	47	0.00	0.52	2.09	4.71	10.99	22.51	31.93	8.38	3.66	3.66	4.19	7.35
47	11/14/2012	10	15	0.00	0.00	0.00	0.00	0.00	0.00	0.00	0.00	0.00	4.17	29.20	66.63
48	11/14/2012	10	26	0.00	0.00	0.60	2.42	6.04	10.27	16.32	7.86	4.23	4.83	12.69	34.74
49	11/14/2012	10	30	0.00	0.00	1.16	2.90	9.85	24.34	27.24	9.27	8.69	5.22	5.22	6.10
50	11/14/2012	10	44	1.09	0.00	0.54	2.17	5.44	15.22	24.46	5.98	4.35	4.35	16.31	20.10
51	11/14/2012	10	48	0.00	0.00	0.00	0.62	3.73	9.94	15.53	11.81	1.86	0.62	21.75	34.14
52	11/14/2012	11	9	2.14	1.07	1.60	4.27	15.49	24.57	23.50	8.55	6.41	3.20	2.14	7.07
53	11/14/2012	11	17	0.77	0.00	0.77	2.31	8.47	13.85	9.24	3.08	2.31	2.31	8.47	48.43
54	11/14/2012	11	22	0.54	3.21	5.35	12.31	24.08	25.68	17.66	5.89	2.14	0.00	0.00	3.16
55	11/14/2012	11	28	2.75	4.95	7.15	9.90	15.41	20.91	20.91	8.25	3.85	0.00	1.10	4.80
56	11/14/2012	11	34	0.00	0.00	1.73	4.60	13.23	29.91	29.34	9.78	2.30	0.58	0.00	8.54
57	11/15/2012	12	57	3.54	2.02	4.55	9.60	23.24	26.28	13.64	6.57	4.04	1.52	1.01	3.99
58	11/15/2012	13	51	0.00	0.00	1.09	5.45	21.78	35.94	24.51	6.54	2.72	0.00	0.00	1.97
59	11/15/2012	13	57	0.00	0.00	0.00	1.04	13.47	41.97	34.72	6.22	1.04	0.00	0.00	1.55
60	11/15/2012	14	4	0.00	1.11	4.99	13.87	32.17	24.96	10.54	4.44	2.77	1.11	0.00	4.03
61	11/15/2012	14	19	0.00	0.00	0.56	3.91	13.40	29.59	31.83	6.70	3.91	2.79	1.12	6.20
62	11/15/2012	14	45	0.00	0.00	1.59	8.46	32.24	38.58	14.80	2.11	0.53	0.00	0.00	1.70
63	11/15/2012	14	51	4.50	3.50	5.50	9.50	21.50	30.00	17.50	4.50	1.00	0.50	0.00	2.00
64	5/14/2013	10	6	0.00	0.00	0.00	0.00	0.00	0.00	0.00	0.00	0.00	1.71	16.27	82.02
65	5/14/2013	10	15	0.00	0.00	0.00	0.00	0.00	0.00	0.00	0.00	0.00	0.00	14.35	85.65
66	5/14/2013	10	26	0.00	0.00	0.00	0.00	0.00	0.00	0.00	0.00	0.00	2.88	24.48	72.64
67	5/14/2013	10	35	0.00	0.00	0.63	0.63	2.52	2.52	1.89	0.63	1.26	3.79	25.24	60.87
68	5/14/2013	11	9	0.00	0.00	0.00	0.00	2.33	12.80	25.03	12.22	3.49	4.66	18.62	20.85
69	5/14/2013	11	16	2.36	2.36	3.54	5.31	8.85	14.76	21.25	12.39	2.95	1.77	8.85	15.60
70	5/14/2013	15	42	0.00	0.00	0.00	2.32	9.28	23.78	31.90	19.72	5.80	1.16	1.16	4.88
71	5/14/2013	15	58	4.10	1.17	1.17	1.76	4.69	11.13	24.60	23.43	11.13	6.44	3.51	6.87
72	5/14/2013	16	4	10.52	0.00	0.00	3.68	15.78	24.71	15.78	6.84	6.84	3.68	3.16	9.03
73	5/14/2013	16	14	0.64	1.28	2.55	8.30	32.54	29.99	8.30	2.55	1.28	0.00	1.28	11.31
74	5/14/2013	16	21	0.63	1.26	4.43	13.28	22.13	13.91	4.43	5.69	5.06	2.53	6.32	20.35
75	5/14/2013	16	37	0.00	0.00	0.00	1.00	1.00	0.00	3.01	2.00	5.01	6.01	15.03	66.94
76	5/14/2013	16	41	0.00	0.00	0.00	0.00	0.00	1.24	5.60	21.77	28.61	14.30	13.68	14.80
77	5/14/2013	17	25	0.00	0.00	0.52	2.09	7.85	19.37	30.37	18.32	8.90	2.62	1.57	8.38
78	5/14/2013	17	33	1.44	1.92	5.28	15.83	35.03	23.51	8.16	1.92	0.96	0.48	0.00	5.47
79	5/14/2013	17	39	0.00	1.91	4.45	9.55	16.55	8.91	3.18	6.36	6.36	4.45	11.45	26.82
80	5/14/2013	17	49	0.00	0.00	0.00	0.00	0.00	0.00	0.00	0.82	5.74	11.48	22.14	59.81
81	5/15/2013	9	21	1.17	0.58	2.34	4.68	11.69	15.78	25.13	13.44	4.09	1.17	3.51	16.42
82	5/15/2013	9	33	0.97	0.97	4.36	8.72	18.40	29.06	24.70	6.78	1.45	0.00	0.00	4.60

83	5/15/2013	9	41	0.00	0.00	0.00	0.00	3.27	14.50	32.75	15.90	7.02	1.40	2.81	22.35
84	5/15/2013	13	58	0.00	0.00	0.00	0.76	7.62	14.48	9.91	3.81	4.57	2.29	8.38	48.18
85	5/15/2013	14	7	0.00	1.05	4.71	15.16	28.23	26.67	9.93	1.57	0.00	0.00	1.05	11.64
86	5/15/2013	14	20	0.00	0.00	0.00	0.00	3.53	5.89	7.06	1.18	0.00	0.00	3.53	78.81
87	5/15/2013	14	32	0.47	1.88	3.76	7.52	23.02	36.65	19.73	3.76	1.41	0.00	0.00	1.80
88	5/15/2013	14	40	0.00	0.50	4.02	13.08	31.19	30.69	14.09	3.02	0.50	0.00	0.50	2.40
89	5/15/2013	14	45	0.00	1.08	2.17	4.88	13.56	25.50	26.58	11.93	2.71	0.00	1.08	10.49
90	5/15/2013	14	52	0.00	0.00	0.00	0.00	0.00	0.00	1.92	2.88	3.84	2.88	8.64	79.85
91	5/15/2013	15	1	0.00	0.00	0.00	0.00	3.07	25.05	52.66	15.34	1.53	0.00	0.00	2.34
92	5/15/2013	15	8	8.41	16.82	21.03	15.89	10.75	8.41	9.34	4.67	2.34	0.47	0.00	1.88
93	5/15/2013	15	15	1.06	2.12	3.17	4.23	6.35	9.52	7.40	2.12	0.00	0.00	2.12	61.93
94	5/15/2013	15	24	0.00	2.00	8.51	19.52	30.53	21.02	9.51	2.50	1.00	0.00	0.00	5.41
95	5/15/2013	15	59	0.00	0.00	0.00	0.00	0.00	0.00	4.98	32.11	37.65	11.07	4.98	9.21
96	5/15/2013	16	8	0.00	0.50	2.01	6.04	24.67	38.26	22.66	3.02	0.00	0.00	0.00	2.83
97	5/15/2013	16	15	1.59	1.06	3.71	11.13	29.68	32.34	12.72	3.18	1.06	0.00	0.00	3.53
98	5/15/2013	16	21	3.16	3.16	5.79	14.75	32.66	25.81	6.85	2.11	1.05	0.00	0.00	4.66
99	5/15/2013	16	28	4.06	3.48	12.17	20.28	16.22	5.79	5.79	6.37	5.21	1.16	1.74	17.74
100	5/15/2013	16	40	0.00	0.51	0.51	2.06	19.05	40.16	22.14	7.72	2.57	0.51	0.00	4.74
101	5/15/2013	16	48	0.00	0.00	1.10	3.86	11.59	16.55	11.04	23.73	21.52	3.86	2.21	4.55
102	5/15/2013	16	54	0.00	0.00	0.00	0.00	4.66	21.54	31.44	17.47	8.15	2.91	3.49	10.34
103	5/16/2013	13	3	0.00	0.00	0.00	0.00	0.73	4.37	12.39	12.39	1.46	1.46	14.57	52.63
104	5/16/2013	13	16	0.00	0.52	1.55	5.18	16.06	34.19	30.56	8.81	1.04	0.00	0.00	2.10
105	5/16/2013	13	22	0.52	1.57	4.18	9.93	18.30	14.12	5.75	2.09	0.52	2.61	16.21	24.19
106	5/16/2013	13	43	0.00	0.00	0.00	0.00	0.00	0.00	0.00	0.00	0.00	0.84	22.55	76.62
107	5/16/2013	13	54	0.00	0.00	0.00	0.00	0.00	0.95	2.85	0.47	0.95	3.80	13.77	77.21
108	5/16/2013	14	2	0.00	0.00	0.00	0.00	0.00	0.00	0.00	0.00	2.25	15.77	65.32	16.67
109	5/16/2013	14	9	0.55	1.11	1.11	3.32	7.74	16.02	17.68	4.97	2.21	2.76	16.58	25.95
110	5/16/2013	14	15	0.00	1.01	1.51	3.02	6.03	11.57	21.12	11.06	7.54	8.05	14.08	15.02
111	5/16/2013	14	23	0.00	0.65	0.65	1.30	1.95	5.19	12.33	11.68	3.89	1.30	11.68	49.37
112	5/16/2013	14	30	1.18	0.00	0.59	2.35	8.23	15.88	10.00	2.35	2.94	7.06	21.17	28.26
113	5/16/2013	14	37	0.00	0.00	0.00	1.37	7.55	16.46	7.55	0.69	2.74	6.17	19.21	38.27
114	5/16/2013	14	46	0.89	0.00	0.00	0.00	2.67	3.56	1.78	0.00	2.67	4.45	19.59	64.38
115	5/16/2013	14	53	0.00	0.00	0.00	0.00	6.29	43.50	31.44	2.10	1.05	1.57	5.24	8.81
116	5/16/2013	15	4	0.00	0.00	0.00	1.07	6.97	26.80	36.44	9.65	4.29	1.61	3.22	9.97
117	5/16/2013	15	12	0.00	0.00	2.38	12.40	40.52	34.80	8.58	0.00	0.00	0.00	0.00	1.32
118	5/16/2013	15	19	0.00	0.00	0.00	0.00	1.96	5.23	11.12	10.46	10.46	6.54	18.96	35.26
119	5/16/2013	15	29	0.00	0.58	1.73	4.62	12.70	23.67	24.25	8.08	4.62	1.15	2.31	16.29
120	5/16/2013	15	39	0.00	0.00	0.00	0.00	0.00	0.00	0.00	0.00	0.00	0.00	6.90	93.10
121	5/16/2013	16	0	0.50	2.52	7.56	18.65	34.27	21.67	5.54	1.51	0.50	0.00	0.00	7.27
122	5/16/2013	16	7	3.22	2.69	3.22	5.91	16.65	18.26	13.43	8.06	7.52	3.22	4.30	13.51
123	5/16/2013	16	13	0.00	0.00	1.11	2.78	10.56	22.79	26.13	11.67	8.34	2.22	2.22	12.17
124	5/16/2013	16	22	3.18	1.06	1.06	2.12	6.88	14.83	27.54	22.24	10.06	1.06	0.53	9.45
125	5/16/2013	16	29	0.00	0.00	0.56	1.12	6.18	29.20	45.49	14.04	1.12	0.00	0.00	2.28
126	5/16/2013	16	50	0.00	0.00	0.00	0.00	0.00	0.00	0.00	2.50	14.35	30.57	31.81	20.78
127	5/16/2013	16	54	0.00	0.00	1.46	11.17	31.56	28.64	20.88	4.37	0.00	0.00	0.00	1.93
128	5/16/2013	16	58	0.53	2.11	5.81	10.03	15.84	16.37	16.37	19.01	11.09	1.06	0.00	1.80
129	5/16/2013	17	3	0.00	0.00	2.06	5.68	16.00	28.90	32.52	11.36	2.06	0.00	0.00	1.41
130	5/16/2013	17	8	0.00	0.00	0.00	0.00	9.10	29.83	39.43	16.68	3.03	0.00	0.00	1.93
131	5/16/2013	17	17	0.00	0.00	0.55	4.40	24.74	31.88	14.84	4.40	3.85	2.75	3.85	8.75
132	5/16/2013	17	21	0.00	0.53	2.63	8.43	22.65	32.13	20.54	6.85	3.16	0.53	0.00	2.55
133	5/16/2013	17	26	1.51	1.51	3.52	8.54	24.62	28.64	13.57	9.55	4.02	1.00	1.00	2.53
134	5/16/2013	17	32	0.00	0.51	1.02	4.08	18.34	40.75	27.51	5.60	1.02	0.00	0.00	1.17
135	5/16/2013	17	37	0.00	0.00	0.00	0.93	11.57	43.03	37.48	5.09	0.46	0.00	0.00	1.44
136	11/4/2013	8	7	0.00	0.00	0.00	0.00	0.00	0.00	0.00	0.00	0.00	0.00	6.74	93.26
137	11/4/2013	8	26	2.80	2.80	7.92	18.17	27.49	11.65	3.26	2.33	3.73	4.19	6.99	8.69
138	11/4/2013	8	35	0.00	0.00	0.00	2.64	1.76	2.64	14.97	14.97	19.37	8.81	3.52	31.31
139	11/4/2013	8	42	0.00	0.00	0.00	0.00	0.60	4.19	29.36	24.57	22.17	4.19	0.00	14.90
140	11/4/2013	8	49	0.00	0.00	0.00	0.00	1.69	6.18	17.98	20.23	30.90	8.99	2.25	11.78
141	11/4/2013	8	53	0.00	0.00	0.00	0.70	3.49	15.35	24.42	20.94	16.05	6.98	3.49	8.58
142	11/4/2013	9	3	0.00	0.00	0.00	1.72	10.33	26.41	31.00	21.81	4.59	0.57	0.00	3.56
143	11/4/2013	9	8	0.00	0.00	0.00	0.69	3.43	12.34	15.08	4.11	6.85	6.85	8.22	42.43
144	11/4/2013	9	12	0.49	1.47	4.90	13.22	31.83	19.59	6.37	1.47	3.43	2.45	1.96	12.84
145	11/4/2013	9	18	0.00	0.00	1.38	8.28	34.03	40.92	10.58	0.92	0.00	0.46	0.00	3.44
146	11/4/2013	9	26	0.91	3.19	13.65	27.76	27.30	10.92	3.19	1.82	1.82	1.37	3.19	4.90
147	11/4/2013	9	31	0.00	0.00	0.00	0.00	0.00	0.00	0.00	0.00	0.00	4.05	28.37	67.57
148	11/4/2013	9	39	0.00	0.00	0.00	0.00	0.00	0.00	0.00	0.00	0.00	2.70	21.59	75.72
149	11/4/2013	9	58	0.00	0.00	3.46	9.68	21.44	13.14	4.84	2.07	1.38	4.15	14.52	25.31
150	11/4/2013	10	5	1.08	0.00	1.63	8.68	24.95	21.15	9.22	3.25	3.25	3.25	6.51	17.01
151	11/4/2013	10	13	0.00	0.00	1.11	2.76	8.29	25.43	33.72	10.50	4.42	2.76	1.11	9.89
152	11/4/2013	10	18	0.00	0.00	0.00	1.35	10.15	29.78	33.84	12.18	6.09	1.35	0.00	5.24
153	11/4/2013	10	27	0.00	0.00	0.00	0.00	0.00	1.97	5.25	30.21	36.12	11.16	3.28	12.00
154	11/4/2013	10	32	0.00	0.00	0.63	1.90	7.62	18.41	19.68	6.35	4.44	5.08	10.79	25.08
155	11/4/2013	10	37	5.17	1.15	4.02	6.89	16.65	15.50	8.61	6.31	4.59	5.74	9.76	15.61
156	11/4/2013	10	42	0.00	0.71	4.23	10.58	21.17	11.29	4.23	1.41	0.00	3.53	13.40	29.45
157	11/4/2013	10	46	0.75	0.75	0.00	0.75	1.50	1.50	1.50	2.26	6.77	10.53	25.58	48.09
158	11/4/2013	10	51	0.00	0.00	0.80	0.00	2.41	3.21	8.04	5.63	7.23	5.63	18.48	48.57
159	11/4/2013	10	59	0.00	0.00	0.00	0.00	0.00	0.00	0.00	0.00	1.49	6.69	23.77	68.06
160	11/4/2013	11	8	17.89	2.18	5.24	9.16	12.65	6.55	2.62	3.49	3.49	2.18	10.47	24.07
161	11/4/2013	11	13	0.00	0.00	2.32	7.55	23.82	24.40	9.29	1.74	0.58	2.90	6.97	20.42
162	11/4/2013	11	22	0.00	0.00	0.00	1.99	10.59	25.82	20.53	8.61	1.99	1.32	3.97	25.18
163	11/4/2013	11	30	36.37	1.04	1.04	1.56	3.12	4.68	6.75	6.23	9.87	11.43	9.35	8.56
164	11/4/2013	12	22	0.00	0.00	0.00	0.00	4.43	25.33	34.19	5.07	3.17	4.43	8.23	15.16
165	11/4/2013	12	27	0.81	0.00	0.00	0.00	0.00	3.23	2.42	0.00	4.04	8.89	20.21	60.39
166	11/4/2013	12	32	0.00	1.06	0.00	1.06	7.91	24.80	15.30	3.17	3.17	6.86	18.47	18.21
167	11/4/2013	12	40	0.00	0.00	1.03	2.57	8.74	19.02	24.68	5.66	2.57	5.14	18.51	12.09
168	11/4/2013	12	52	4.02	3.44	4.02	4.59	6.89	8.61	17.79	17.79	5.74	1.72	12.63	12.77
169	11/4/2013	13	1	0.45	0.90	2.25	2.70	4.94	8.54	18.43	18.88	11.24	3.15	10.79	17.76

170	11/4/2013	13	7	1.60	0.80	1.20	2.79	9.98	17.56	25.95	7.58	3.19	3.59	14.77	10.99
171	11/4/2013	13	15	0.00	0.54	1.63	2.17	7.60	19.54	13.03	4.34	6.51	10.31	17.37	16.94
172	11/4/2013	13	21	0.00	0.00	0.00	0.00	3.20	5.60	4.80	2.40	6.40	14.40	26.40	36.79
173	11/4/2013	13	26	0.00	0.55	1.09	2.19	5.46	13.66	25.68	5.46	4.37	7.10	12.57	21.87
174	11/4/2013	13	31	0.00	0.00	0.00	0.00	0.69	0.69	6.88	7.57	6.19	17.88	33.01	27.09
175	11/4/2013	13	37	0.00	0.00	0.00	0.00	0.00	1.58	14.20	9.99	8.94	13.15	25.77	26.39
176	11/4/2013	13	44	0.93	0.00	0.00	0.00	0.00	0.00	0.00	0.00	0.00	1.86	17.63	79.59
177	11/4/2013	13	51	0.00	0.00	0.00	1.32	1.98	3.95	5.93	1.98	1.98	3.29	17.12	62.46
178	11/4/2013	14	0	0.00	0.00	1.11	2.76	6.63	22.66	35.36	12.16	3.32	2.21	4.42	9.38
179	11/4/2013	14	4	0.00	0.00	0.00	1.16	4.07	13.36	26.72	8.71	6.97	8.13	18.01	12.88
180	11/4/2013	14	8	1.30	0.86	2.59	4.32	10.37	14.26	18.14	19.01	4.32	0.86	8.64	15.33
181	11/4/2013	14	20	0.00	0.00	0.00	0.00	3.35	5.03	1.68	0.00	1.68	8.39	25.16	54.72
182	11/4/2013	14	24	0.00	1.49	5.97	14.92	26.36	19.40	11.44	3.98	2.49	2.98	3.98	6.98
183	11/4/2013	14	33	0.00	0.00	1.12	1.12	3.93	10.67	24.72	23.60	10.11	3.37	6.74	14.60
184	11/4/2013	14	39	0.00	0.00	0.00	0.60	2.40	8.99	17.39	22.18	9.59	4.80	10.79	23.26
185	11/4/2013	14	42	0.00	0.50	2.01	5.52	15.56	28.12	27.11	10.54	6.03	1.00	0.50	3.10
186	11/4/2013	15	28	0.00	0.00	0.86	4.28	13.68	31.64	36.34	8.98	2.14	0.00	0.00	2.10
187	11/4/2013	15	32	0.00	0.00	4.09	11.26	21.49	22.51	11.77	2.05	1.02	1.53	7.67	16.61
188	11/4/2013	15	37	1.00	0.50	1.00	2.50	8.99	20.47	20.97	11.98	3.99	1.50	8.99	18.12
189	11/4/2013	15	41	1.41	5.18	8.94	11.30	16.95	14.12	20.71	10.36	3.30	0.00	1.88	5.85
190	11/4/2013	15	47	0.00	1.05	5.23	12.02	25.62	23.53	22.48	6.27	1.57	0.00	0.00	2.24
191	11/4/2013	15	54	0.00	0.00	0.00	0.00	0.00	4.21	12.04	15.05	13.24	6.02	18.66	30.79
192	11/8/2013	14	6	0.00	0.00	0.00	2.72	17.69	29.94	19.73	4.76	5.44	4.76	2.72	12.23
193	11/8/2013	14	15	0.00	2.72	4.54	9.99	23.61	28.60	19.97	6.81	1.82	0.00	0.00	1.95
194	11/8/2013	14	29	16.54	1.18	1.97	5.12	16.15	22.84	17.33	8.27	5.51	1.58	0.79	2.72
195	11/8/2013	14	34	0.86	0.43	1.28	3.85	19.27	36.39	28.26	6.85	1.28	0.00	0.00	1.53
196	11/8/2013	14	37	0.00	0.00	0.00	3.08	25.13	43.09	20.52	5.13	1.03	0.00	0.00	2.03
197	11/8/2013	14	51	0.00	0.00	0.00	0.00	1.76	18.05	34.34	15.85	9.25	5.28	3.96	11.50
198	11/8/2013	14	57	0.00	0.00	0.00	0.00	8.73	30.55	35.78	15.71	3.49	0.87	1.75	3.12
199	11/8/2013	15	6	0.00	2.38	6.66	17.12	32.81	29.00	8.08	1.43	0.95	0.00	0.00	1.58
200	11/8/2013	15	12	0.00	0.00	2.50	8.00	26.50	29.00	22.50	7.00	2.00	0.00	0.00	2.50
201	11/8/2013	15	18	0.00	0.00	0.50	8.97	33.39	36.39	11.96	2.49	1.00	0.50	0.00	4.80
202	11/8/2013	15	33	0.00	0.00	0.00	0.00	3.48	16.90	41.24	23.36	9.44	2.48	0.50	2.60
203	11/8/2013	15	40	0.53	0.00	0.00	3.73	13.33	25.05	30.38	19.19	3.73	1.60	0.00	2.46
204	11/8/2013	15	46	0.60	0.00	1.79	7.76	20.89	27.45	18.50	8.95	5.37	1.19	0.00	7.50
205	11/8/2013	15	51	0.00	0.00	0.63	5.69	24.64	29.70	22.11	9.48	3.16	0.63	0.00	3.96
206	11/8/2013	16	4	0.00	0.00	0.00	0.00	0.00	0.00	0.00	0.00	1.79	8.03	28.57	61.61
207	11/8/2013	16	13	0.00	0.58	0.00	1.16	8.69	26.06	41.11	11.00	2.32	0.00	0.00	9.09
208	11/8/2013	16	19	0.00	0.00	0.00	0.00	4.80	14.39	25.35	21.24	13.02	3.43	1.37	16.43
209	11/8/2013	16	25	0.00	0.00	0.94	6.56	27.17	39.82	14.06	4.69	1.41	0.00	0.47	4.89
210	11/9/2013	7	51	1.61	1.61	4.29	10.19	25.20	28.42	14.48	5.90	3.22	0.00	0.00	5.09
211	11/9/2013	7	58	0.76	0.00	0.00	0.00	2.28	3.04	5.33	9.13	17.50	13.70	12.18	36.07
212	11/9/2013	8	19	0.00	0.00	0.00	2.23	11.15	34.34	39.69	9.81	1.34	0.00	0.00	1.44
213	11/9/2013	8	27	0.00	0.00	0.00	0.49	9.38	40.98	38.51	7.41	1.48	0.00	0.00	1.75
214	11/9/2013	8	34	3.16	1.05	1.05	5.26	14.74	23.68	17.37	10.00	4.74	1.58	2.63	14.74
215	11/9/2013	8	43	0.00	0.00	0.64	0.64	1.91	7.63	15.26	17.80	29.25	6.99	2.54	17.35
216	11/9/2013	8	48	0.00	0.00	0.00	2.00	7.02	24.56	41.60	18.54	3.51	0.50	0.00	2.28
217	11/9/2013	8	54	0.00	0.00	2.55	6.63	20.91	29.58	25.50	8.16	3.57	0.00	0.00	3.10
218	11/9/2013	8	59	4.40	2.75	6.60	9.91	20.36	17.06	11.01	3.30	2.75	2.75	6.05	13.04
219	11/9/2013	9	6	0.00	3.45	9.19	19.91	32.16	22.59	9.19	2.30	0.00	0.00	0.00	1.21
220	11/9/2013	9	15	0.00	0.00	0.00	5.05	33.26	40.42	15.16	2.11	0.00	0.00	0.00	4.01
221	11/9/2013	9	25	0.00	0.00	4.24	12.18	34.41	38.12	8.47	0.00	0.00	0.00	0.00	2.59
222	11/9/2013	9	30	0.89	0.89	1.79	6.25	25.02	42.89	17.87	1.34	0.00	0.00	0.00	3.06
223	11/9/2013	9	34	0.00	0.00	1.16	1.75	5.24	19.79	46.55	16.29	4.07	0.58	0.00	4.56
224	11/9/2013	9	37	0.00	0.00	0.00	0.00	3.17	10.79	10.79	3.81	7.62	8.89	12.70	42.22
225	11/9/2013	9	51	0.00	0.00	0.00	0.00	0.00	0.00	0.00	3.57	10.72	9.29	16.44	59.97
226	11/9/2013	10	0	0.00	0.00	0.00	0.00	0.64	7.73	33.50	20.62	9.66	2.58	0.00	25.27
227	11/9/2013	10	6	0.00	1.79	5.36	10.12	18.45	25.59	25.59	7.74	1.19	0.00	0.00	4.18
228	11/9/2013	10	13	0.00	1.70	5.95	16.16	31.46	28.48	10.63	1.70	0.00	0.00	0.00	3.92
229	11/9/2013	10	18	0.00	0.84	5.02	17.16	30.97	23.86	9.63	2.09	1.26	0.84	1.67	6.67
230	11/9/2013	10	24	0.00	0.00	0.50	6.44	27.74	46.07	15.36	1.49	0.00	0.00	0.00	2.42
231	11/9/2013	10	33	0.90	0.90	4.51	9.02	22.10	27.96	20.75	4.51	0.90	0.00	1.35	7.09
232	11/9/2013	10	39	0.00	0.00	0.00	0.00	0.65	10.33	39.38	28.40	11.62	1.94	1.29	6.40
233	11/9/2013	10	43	0.00	0.00	0.00	2.03	15.84	42.24	33.30	4.47	0.41	0.00	0.00	1.71
234	11/9/2013	10	50	1.43	3.34	6.20	12.41	25.77	30.55	14.80	2.86	0.00	0.00	0.00	2.63
235	11/9/2013	11	13	0.00	0.00	1.52	7.11	22.33	28.93	21.83	8.12	2.54	0.00	1.02	6.60
236	11/9/2013	11	16	0.00	0.00	0.00	3.43	7.71	11.99	4.28	0.00	0.00	6.00	24.84	41.75
237	11/9/2013	11	21	0.00	0.00	0.00	1.40	5.61	8.41	20.32	33.63	16.12	4.20	2.80	7.51
238	11/9/2013	11	27	0.62	0.94	2.81	6.55	17.47	24.02	28.07	11.23	4.05	0.94	0.00	3.32
239	11/9/2013	11	31	0.00	0.00	0.00	0.00	3.19	16.60	26.81	11.49	3.19	0.64	10.85	27.22
240	11/9/2013	11	42	2.85	0.00	0.00	0.00	3.99	14.23	18.79	7.40	9.11	7.40	14.80	21.43
241	11/9/2013	11	50	0.00	0.00	0.47	7.92	27.47	27.01	13.50	3.26	1.40	1.86	6.52	10.60
242	11/9/2013	11	54	0.00	0.00	0.00	0.00	0.56	4.48	10.63	9.52	6.72	6.16	31.90	30.03
243	11/9/2013	11	59	0.62	0.00	0.00	0.00	3.10	9.91	16.73	8.67	6.20	3.72	17.35	33.71
244	11/9/2013	12	2	0.00	0.00	0.00	0.00	0.00	0.90	0.00	0.00	0.00	1.79	24.22	73.08
245	11/9/2013	12	14	0.00	0.00	0.00	0.00	0.00	3.53	8.48	4.24	3.53	3.53	17.66	59.03
246	11/9/2013	12	18	0.00	0.00	0.00	1.45	1.45	2.18	3.64	3.64	2.18	4.36	32.72	48.38
247	11/9/2013	12	24	0.00	0.00	0.95	6.16	31.29	42.67	12.80	0.95	0.00	0.00	0.95	4.24
248	11/9/2013	12	30	0.00	0.00	0.00	0.00	3.23	14.75	23.05	5.99	4.61	9.22	18.90	20.23
249	11/9/2013	12	36	3.53	0.50	0.50	0.00	1.51	15.12	39.82	13.61	7.56	5.04	4.03	8.76
250	11/9/2013	12	55	1.66	0.00	1.11	4.44	13.31	26.06	31.60	14.97	2.77	0.00	0.55	3.53
251	5/13/2014	9	45	8.20	0.00	0.00	0.00	5.47	5.47	4.10	2.73	1.37	0.00	9.57	63.08
252	5/13/2014	10	9	2.54	2.96	8.47	18.20	26.24	17.78	12.70	4.23	0.85	0.85	2.54	2.65
253	5/13/2014	10	17	1.33	0.00	0.00	0.00	0.00	0.00	0.00	0.00	0.00	3.98	26.53	68.17
254	5/13/2014	10	32	0.00	0.00	0.00	0.00	2.49	7.96	15.42	16.91	15.91	6.96	14.92	19.44
255	5/13/2014	10	40	0.00	0.00	0.46	4.64	14.39	35.27	30.63	10.21	2.32	0.00	0.00	2.08
256	5/13/2014	10	48	0.00	0.00	0.00	2.35	15.48	36.11	33.77	9.38	0.94	0.00	0.00	1.97

257	5/13/2014	10	55	0.00	0.00	0.00	0.00	0.00	3.18	10.33	12.71	10.33	2.38	8.74	52.34
258	5/13/2014	11	7	0.00	0.00	0.00	0.00	0.89	4.47	17.44	28.62	13.86	5.81	8.50	20.41
259	5/13/2014	11	17	0.00	0.00	2.36	8.48	21.20	23.08	16.02	3.30	0.00	0.94	8.95	15.69
260	5/13/2014	11	29	0.00	0.00	0.00	0.00	0.00	0.00	0.00	0.00	0.00	0.00	8.25	91.75
261	5/13/2014	11	40	0.00	0.00	0.00	0.00	0.00	0.00	0.00	0.00	0.00	0.00	11.58	88.42
262	5/13/2014	11	45	0.00	0.00	0.00	1.07	4.28	12.83	19.24	5.34	2.67	3.21	15.50	35.87
263	5/13/2014	11	58	0.00	0.00	0.00	0.00	1.29	4.50	7.07	3.21	3.86	4.50	29.56	46.02
264	5/13/2014	12	4	0.00	0.00	0.00	0.86	5.61	16.82	24.59	11.65	7.33	5.18	14.67	13.29
265	5/13/2014	12	14	0.00	0.00	1.17	2.93	8.20	17.58	26.37	12.89	3.52	1.76	7.62	17.96
266	5/13/2014	12	28	0.00	0.00	0.64	0.64	3.19	11.48	21.06	10.21	3.83	1.91	16.59	30.45
267	5/13/2014	12	38	0.00	0.00	0.00	1.11	4.82	21.11	23.34	9.26	7.04	3.70	15.56	14.06
268	5/13/2014	12	48	0.00	0.00	0.00	3.22	12.24	25.77	15.46	1.93	0.00	1.93	12.89	26.55
269	5/13/2014	12	58	0.00	0.00	0.00	1.07	4.79	22.90	33.56	7.99	4.79	2.13	7.46	15.31
270	5/13/2014	13	6	0.00	0.00	0.00	0.00	0.00	0.00	0.00	0.00	0.00	0.00	15.05	84.95
271	5/13/2014	13	17	0.00	0.00	0.00	0.00	2.67	20.28	22.42	6.94	5.34	4.27	14.41	23.67
272	5/13/2014	13	29	0.00	0.00	0.00	3.05	18.91	29.89	15.86	2.44	1.22	1.83	7.32	19.49
273	5/13/2014	13	39	0.00	0.00	0.00	1.84	12.27	27.62	15.34	2.45	2.45	3.07	12.89	22.06
274	5/13/2014	13	45	45.30	4.15	3.02	4.15	6.42	11.33	12.08	4.53	1.51	0.76	2.27	4.49
275	5/13/2014	14	1	0.00	0.00	0.00	0.00	0.00	5.49	17.83	21.94	8.91	2.74	11.66	31.43
276	5/13/2014	14	12	0.00	0.00	0.00	0.00	1.75	15.18	51.96	18.68	3.50	0.00	0.00	8.93
277	5/13/2014	14	22	0.00	0.00	0.00	0.00	0.00	3.23	11.31	18.86	9.16	5.93	19.93	31.58
278	5/13/2014	14	30	0.00	0.00	0.00	2.20	19.23	41.22	22.53	3.85	2.20	0.00	1.65	7.13
279	5/13/2014	14	40	0.00	0.00	0.55	3.32	17.15	39.83	25.45	5.53	1.11	0.00	0.55	6.50
280	5/13/2014	14	54	1.97	0.00	0.00	0.00	6.39	31.46	37.85	10.32	2.46	0.00	2.46	7.08
281	5/13/2014	15	4	0.00	0.00	0.00	2.51	13.39	42.28	36.00	4.19	0.00	0.00	0.00	1.63
282	5/13/2014	15	10	0.86	0.00	1.73	4.32	15.98	23.76	22.03	10.80	5.18	2.59	5.18	7.56
283	5/13/2014	15	18	0.00	0.00	0.00	0.93	3.24	5.56	21.76	22.22	14.35	6.48	11.57	13.90
284	5/13/2014	15	24	0.00	0.00	0.00	0.00	1.88	7.06	28.26	36.74	12.72	4.24	2.83	6.28
285	5/13/2014	15	32	4.37	5.57	6.36	9.94	17.50	30.22	18.29	4.37	1.59	0.00	0.00	1.79
286	5/13/2014	15	42	2.03	0.00	1.53	2.03	9.66	24.91	43.22	11.19	2.03	0.00	0.00	3.39
287	5/13/2014	15	48	0.00	1.23	3.68	6.54	12.67	18.39	33.10	17.16	4.49	1.23	0.00	1.52
288	5/13/2014	15	54	0.00	0.00	2.80	7.47	18.21	32.21	23.81	9.34	3.27	0.00	0.00	2.89
289	5/13/2014	16	0	0.00	1.34	5.37	13.42	25.05	30.42	16.10	3.58	1.34	0.00	0.45	2.93
290	5/13/2014	16	5	0.00	0.00	1.11	5.55	23.30	43.28	18.86	1.11	0.00	0.00	0.00	6.79
291	5/13/2014	16	13	12.37	0.00	2.06	4.95	17.31	29.27	18.96	4.95	2.47	1.24	1.24	5.20
292	5/13/2014	16	18	0.00	0.00	0.00	2.64	15.42	36.56	26.87	5.73	2.20	1.32	1.76	7.51
293	5/13/2014	16	24	0.00	0.00	2.09	7.09	20.44	30.04	24.61	10.01	2.50	0.42	0.00	2.80
294	5/13/2014	16	36	0.00	0.00	0.00	3.30	12.64	27.49	38.48	11.54	4.40	0.00	0.00	2.14
295	5/13/2014	16	40	0.00	0.00	0.00	0.00	3.01	15.06	37.14	21.58	9.04	3.51	1.51	9.15
296	5/13/2014	16	46	0.00	0.00	1.43	3.34	11.46	30.55	33.89	10.98	4.77	0.95	0.00	2.62
297	5/13/2014	16	50	0.00	0.00	0.46	1.84	7.84	21.21	43.81	17.06	4.15	1.38	0.00	2.23
298	5/13/2014	16	55	1.61	3.75	4.82	8.03	15.00	25.17	26.24	9.11	3.21	0.00	0.00	3.06
299	5/13/2014	17	1	0.00	3.57	8.48	15.17	25.43	24.98	16.06	3.57	0.89	0.00	0.00	1.86
300	5/13/2014	17	5	0.00	0.00	0.00	2.42	11.48	17.52	11.48	6.64	7.25	3.62	4.23	35.37
301	5/13/2014	17	11	0.00	0.44	2.20	8.80	25.08	32.12	22.44	5.72	1.32	0.00	0.00	1.89
302	5/13/2014	17	30	0.00	1.53	3.56	7.63	15.26	32.04	28.48	7.63	2.03	0.00	0.00	1.85
303	5/13/2014	17	35	0.00	0.00	0.00	0.00	0.00	5.34	25.34	31.12	25.79	4.89	2.22	5.29
304	5/13/2014	17	44	0.00	0.00	0.00	0.00	0.00	0.00	0.00	2.07	3.10	7.24	15.51	72.08
305	5/13/2014	17	53	0.00	0.00	2.08	5.71	15.57	25.96	26.99	14.54	5.71	0.52	0.00	2.92
306	5/14/2014	17	0	2.33	1.95	3.50	5.84	16.73	28.79	29.96	8.17	1.56	0.00	0.00	1.17
307	5/14/2014	17	11	0.00	0.00	0.00	3.01	22.18	46.99	24.44	2.26	0.00	0.00	0.00	1.13
308	5/14/2014	17	17	0.00	1.12	5.98	17.18	32.12	32.87	8.22	1.12	0.00	0.00	0.00	1.40
309	5/14/2014	17	20	0.00	0.00	5.79	21.72	38.13	26.07	5.79	0.97	0.00	0.00	0.00	1.53
310	5/14/2014	17	24	0.00	1.01	1.01	1.51	6.05	22.18	43.86	18.15	4.03	0.00	0.00	2.20
311	5/16/2014	7	58	0.00	0.50	1.49	9.90	34.65	32.67	12.38	3.47	1.98	0.50	0.00	2.48
312	5/16/2014	8	7	3.59	6.72	9.86	12.55	14.79	18.83	16.14	6.28	4.48	1.79	1.34	3.61
313	5/16/2014	8	14	14.85	0.80	0.80	3.21	10.44	25.69	25.29	10.04	3.61	2.01	1.20	2.05
314	5/16/2014	8	23	1.53	1.91	2.67	5.35	16.81	25.98	25.60	11.46	5.35	0.76	0.76	1.80
315	5/16/2014	8	37	1.46	0.73	1.10	2.92	10.60	38.73	37.27	4.38	0.73	0.00	0.00	2.07
316	5/16/2014	8	46	0.00	0.00	0.88	0.88	4.41	18.52	50.70	19.40	3.53	0.00	0.00	1.68
317	5/16/2014	8	53	9.97	1.81	4.08	6.34	14.49	27.63	23.55	7.25	2.26	0.91	0.00	1.71
318	5/16/2014	9	0	21.98	5.37	6.35	7.82	17.10	20.03	12.21	4.40	2.93	0.00	0.00	1.81
319	5/16/2014	9	6	0.00	0.00	2.97	14.38	41.15	31.73	6.94	0.99	0.00	0.00	0.00	1.83
320	5/16/2014	9	17	0.92	2.76	9.19	14.24	24.35	22.05	11.02	5.97	4.59	0.92	0.92	3.07
321	5/16/2014	9	27	1.07	1.43	2.85	7.84	21.39	31.01	23.17	6.06	2.14	1.07	0.00	1.98
322	5/16/2014	9	33	0.00	0.00	0.98	2.94	11.76	29.88	37.23	11.27	3.92	0.00	0.00	2.03
323	5/16/2014	9	38	2.46	1.23	2.05	3.29	10.27	25.46	36.96	12.73	3.29	0.41	0.41	1.45
324	5/16/2014	9	44	0.00	0.00	0.00	1.39	13.39	39.72	35.10	6.93	1.85	0.00	0.00	1.63
325	5/16/2014	9	50	0.00	1.77	3.09	7.06	16.77	36.64	29.13	3.53	0.00	0.00	0.00	2.01
326	5/16/2014	9	58	0.00	1.45	6.26	20.71	33.24	20.23	5.30	2.89	3.37	1.93	0.96	3.67
327	5/16/2014	10	9	0.49	1.98	4.95	11.88	25.73	23.75	14.35	7.42	3.96	0.99	0.99	3.50
328	5/16/2014	10	15	0.00	0.00	0.00	0.00	8.52	35.08	41.09	10.02	3.01	0.00	0.00	2.28
329	5/16/2014	10	21	0.00	0.00	0.43	1.71	6.83	23.50	41.44	20.50	3.42	0.00	0.00	2.17
330	5/16/2014	10	28	0.00	0.00	0.96	2.41	11.06	23.57	29.82	20.69	9.14	0.00	0.00	2.35
331	5/16/2014	10	35	0.00	0.00	0.00	1.83	12.81	37.50	36.13	8.69	1.37	0.00	0.00	1.67
332	5/16/2014	10	41	1.33	1.33	1.33	3.10	18.15	35.85	24.34	8.41	3.10	0.89	0.00	2.18
333	5/16/2014	10	47	0.00	1.16	6.95	21.62	40.16	22.78	4.63	1.16	0.00	0.00	0.00	1.54
334	5/16/2014	10	52	2.12	2.55	9.76	25.88	38.18	15.70	4.24	0.00	0.00	0.00	0.00	1.58
335	5/16/2014	11	3	0.88	0.88	3.97	13.22	27.76	24.68	13.66	7.93	2.20	0.88	0.88	3.05
336	5/16/2014	11	9	1.30	4.34	13.01	30.35	31.65	10.84	3.90	2.17	0.87	0.00	0.00	1.60
337	5/16/2014	11	14	3.79	3.37	7.15	13.88	27.76	23.98	9.68	4.21	2.10	1.26	0.84	1.98
338	5/16/2014	11	21	0.00	0.85	2.56	6.82	21.30	34.51	24.71	5.96	1.70	0.00	0.00	1.58
339	5/16/2014	11	40	0.00	0.00	0.00	0.00	4.04	14.37	31.45	27.40	14.82	3.59	0.90	3.42
340	5/16/2014	11	45	0.00	0.00	0.00	1.39	11.48	39.31	34.79	9.39	2.09	0.00	0.00	1.55
341	5/16/2014	11	51	0.00	1.97	5.11	13.76	31.45	30.27	13.37	2.75	0.00	0.00	0.00	1.32
342	5/16/2014	11	57	1.27	1.70	6.79	19.09	33.52	19.94	7.64	3.39	2.12	1.27	1.27	1.99
343	5/16/2014	12	3	0.00	0.00	0.00	0.00	0.00	0.00	0.00	0.00	0.00	2.07	5.18	92.74

344	5/16/2014	12	30	8.80	0.00	0.00	0.00	0.00	0.00	1.26	5.66	15.09	15.72	23.90	29.56
345	5/16/2014	12	39	0.82	3.27	10.62	23.28	35.12	14.70	4.49	2.04	1.23	0.82	0.00	3.63
346	5/16/2014	12	44	0.00	0.00	0.00	4.25	21.25	44.09	22.84	3.72	1.59	0.00	0.00	2.25
347	5/16/2014	12	51	0.00	0.00	0.84	2.11	9.28	18.98	31.21	22.36	8.44	1.69	1.27	3.83
348	5/16/2014	12	56	0.00	0.00	0.00	0.00	2.74	8.23	15.08	32.45	31.53	5.03	1.37	3.58
349	5/16/2014	13	6	0.00	0.00	0.00	0.00	1.26	5.89	17.66	39.52	23.97	5.89	1.68	4.13
350	5/16/2014	13	18	0.00	0.00	1.32	4.42	24.73	41.96	23.41	2.65	0.00	0.00	0.00	1.51
351	5/16/2014	13	24	0.00	1.13	4.14	14.69	35.79	30.14	10.17	1.51	0.00	0.00	0.75	1.68
352	5/16/2014	13	37	1.76	5.28	10.99	21.99	29.02	16.27	6.16	1.76	1.76	0.88	1.32	2.81
353	5/16/2014	13	55	19.20	0.00	0.00	0.00	0.00	0.00	2.62	2.62	2.62	1.75	6.11	65.09
354	5/16/2014	14	3	14.29	2.04	5.31	14.69	32.65	24.90	4.49	0.00	0.00	0.00	0.00	1.64
355	5/16/2014	14	11	0.00	0.00	0.00	0.00	5.93	34.42	51.04	5.93	0.79	0.00	0.00	1.88
356	5/16/2014	14	17	0.00	0.00	0.00	0.00	0.00	1.21	32.70	54.50	8.07	0.00	0.40	3.11
357	5/16/2014	14	25	0.00	0.00	0.00	0.00	2.78	17.12	34.71	20.83	16.20	3.24	1.39	3.74
358	5/16/2014	14	32	0.00	0.00	0.00	0.00	3.27	15.88	32.24	19.62	14.95	5.14	2.80	6.10
359	5/16/2014	14	44	0.00	0.00	0.00	1.82	14.58	40.55	34.17	5.47	1.37	0.00	0.00	2.05
360	5/16/2014	14	53	31.42	0.00	0.00	0.00	0.00	0.65	0.00	1.96	2.62	1.96	3.93	57.45
361	5/16/2014	15	6	0.00	0.00	2.69	11.64	39.84	36.26	7.16	0.45	0.45	0.00	0.00	1.51
362	5/16/2014	15	12	0.00	1.15	1.92	8.43	22.61	29.89	25.67	6.90	1.53	0.00	0.00	1.92
363	5/16/2014	15	19	0.00	0.00	0.00	1.29	5.60	19.39	37.05	24.56	9.05	1.29	0.00	1.77
364	5/16/2014	15	20	0.00	0.00	0.00	0.86	5.19	16.42	35.44	30.25	8.21	1.73	0.00	1.89
365	5/16/2014	15	45	0.00	0.00	0.00	0.56	6.18	17.96	35.37	25.82	10.67	1.12	0.00	2.32
366	5/16/2014	15	56	0.00	0.00	0.41	7.71	26.37	34.49	19.88	8.12	1.62	0.00	0.00	1.40
367	5/16/2014	16	7	0.00	0.00	0.00	0.86	6.88	18.91	38.67	21.92	8.16	1.72	0.86	2.02
368	5/16/2014	16	12	0.00	0.00	0.44	4.40	16.28	32.99	33.87	9.24	1.32	0.00	0.00	1.46
369	5/16/2014	16	18	7.62	4.57	7.24	11.82	19.44	16.39	12.20	9.91	6.48	1.52	0.76	2.04
370	5/16/2014	16	27	0.00	0.00	0.00	1.48	5.91	16.75	35.46	20.69	6.90	2.46	1.97	8.38
371	5/16/2014	16	39	0.00	0.00	0.00	0.00	0.00	0.00	2.10	7.88	14.71	8.40	13.13	53.78
372	5/16/2014	16	46	0.00	1.06	2.48	8.50	25.87	34.02	20.20	5.67	1.06	0.00	0.00	1.13
373	5/16/2014	16	57	20.59	4.72	3.00	6.43	14.15	18.01	14.58	8.58	5.58	1.72	0.86	1.78
374	5/16/2014	17	4	0.00	0.00	0.00	3.11	15.18	36.97	31.52	10.12	1.95	0.00	0.00	1.16
375	5/16/2014	17	8	0.00	0.00	0.00	0.44	11.42	36.46	34.71	10.10	3.08	1.32	0.88	1.59
376	5/16/2014	17	14	0.00	0.00	1.28	5.98	24.34	41.84	22.63	2.56	0.00	0.00	0.00	1.38
377	5/16/2014	17	23	0.00	0.00	0.94	4.72	21.70	36.33	30.20	4.72	0.00	0.00	0.00	1.39
378	5/16/2014	17	28	2.32	0.46	1.86	7.43	22.30	30.20	20.91	10.22	2.79	0.00	0.00	1.50
379	5/16/2014	17	34	0.00	0.85	4.69	11.09	26.01	29.00	16.21	5.97	2.99	1.28	0.00	1.91
380	5/16/2014	17	40	0.00	0.00	0.00	0.46	7.35	13.78	8.27	3.22	3.68	10.11	26.19	26.94
381	5/17/2014	8	1	0.00	0.00	0.00	2.86	21.65	35.55	22.88	6.54	4.90	1.63	1.23	2.76
382	5/17/2014	10	33	0.00	0.00	0.00	3.16	15.32	36.96	25.24	7.21	3.16	2.25	1.80	4.89
383	5/17/2014	14	12	0.00	0.00	0.00	0.00	3.28	9.02	14.34	14.34	13.12	8.61	17.62	19.67

A.3 Sediment Characteristics

Core ID	Date	Hr.	Min.	Water content	Porosity	Bulk Sediment Density (g/cm3)	LOI (%)	D50 coarse (Φ)	D50 all	D10 c	D10 all	D90 c	D90 all
1	11/12/2012	10	19	0.46	0.70	0.82	4.83	3.71		3.93		3.48	3.57
2	11/12/2012	10	45	0.37	0.62	1.06	3.50	1.91	3.35	3.69		0.98	1.15
3	11/12/2012	10	56	0.23	0.45	1.50	1.53	1.85	1.99	3.65		1.03	1.08
4	11/12/2012	11	4	0.23	0.45	1.52	1.58	1.75	1.83	3.49		0.87	0.97
5	11/12/2012	11	24	0.21	0.42	1.60	1.29	1.65	1.73	3.16	3.93	0.38	0.49
6	11/12/2012	11	36	0.24	0.47	1.47	3.53	1.61	1.69	3.07	3.91	0.41	0.50
7	11/13/2012	6	54	0.54	0.77	0.64	6.77	3.49		3.89		2.51	3.43
8	11/13/2012	7	10	0.13	0.28	1.97	0.84	0.76	0.78	1.70	1.88	-0.37	-0.35
9	11/13/2012	7	27	0.18	0.38	1.70	0.69	1.43	1.44	1.99	2.10	0.84	0.85
10	11/13/2012	7	43	0.34	0.58	1.14	2.84	2.54	2.74	3.16		1.89	2.01
11	11/13/2012	7	58	0.21	0.43	1.57	0.93	2.00	2.03	2.79	2.88	1.27	1.28
12	11/13/2012	8	10	0.24	0.47	1.45	0.99	2.45	2.48	3.31	3.42	1.53	1.54
13	11/13/2012	8	23	0.56	0.78	0.60	8.45	3.55		3.90		2.85	3.33
14	11/13/2012	8	29	0.24	0.47	1.45	1.95	0.99	1.27	3.48		0.09	0.15
15	11/13/2012	8	33	0.28	0.51	1.34	2.10	1.15	1.30	2.56		0.33	0.43
16	11/13/2012	8	40	0.21	0.43	1.57	0.83	1.41	1.45	2.01	2.34	0.72	0.74
17	11/13/2012	9	28	0.23	0.45	1.50	1.16	1.77	1.87	2.77	3.98	1.03	1.05
18	11/13/2012	9	43	0.23	0.46	1.50	0.97	1.67	1.75	2.80	3.37	0.98	1.01
19	11/13/2012	9	50	0.52	0.75	0.68	5.97	2.18		3.74		1.19	1.50
20	11/13/2012	9	58	0.15	0.32	1.87	0.77	0.84	0.86	1.50	1.68	-0.01	0.01
21	11/13/2012	10	6	0.22	0.44	1.54	1.63	1.12	1.67	3.32		0.18	0.25
22	11/13/2012	16	57	0.16	0.34	1.81	0.43	1.03	1.04	1.65	1.76	0.31	0.32
23	11/13/2012	17	1	0.20	0.40	1.64	0.43	1.04	1.05	1.71	1.77	0.36	0.37
24	11/13/2012	17	4	0.15	0.33	1.84	0.50	1.52	1.55	2.34	2.47	0.52	0.54
25	11/13/2012	17	9	0.21	0.43	1.58	0.65	1.85	1.86	2.43	2.52	1.30	1.31
26	11/13/2012	17	16	0.32	0.57	1.19	2.93	2.82	3.26	3.72		1.60	1.82
27	11/14/2012	6	58	0.51	0.75	0.69	5.59	3.09		3.83		1.54	2.37
28	11/14/2012	7	1	0.21	0.43	1.58	1.53	0.73	0.82	1.90		0.00	0.03
29	11/14/2012	7	6	0.25	0.48	1.43	1.04	1.16	1.32	2.54		0.34	0.50
30	11/14/2012	7	14	0.16	0.35	1.79	0.62	1.29	1.32	2.08	2.32	0.55	0.56
31	11/14/2012	7	23	0.20	0.41	1.61	0.62	1.97	2.01	2.93	3.18	0.73	0.78
32	11/14/2012	7	52	0.70	0.87	0.35	10.66	1.37		1.85		1.07	
33	11/14/2012	7	59	0.21	0.42	1.60	0.97	1.22	1.25	1.99	2.44	0.26	0.29
34	11/14/2012	8	4	0.16	0.35	1.80	1.04	1.37	1.40	2.35	2.53	0.31	0.33
35	11/14/2012	8	7	0.18	0.38	1.70	0.73	1.35	1.36	2.10	2.21	0.48	0.50
36	11/14/2012	8	57	0.23	0.46	1.50	0.91	1.48	1.51	1.96	2.06	1.05	1.06
37	11/14/2012	9	0	0.21	0.43	1.58	0.93	1.38	1.40	1.93	1.98	0.86	0.87
38	11/14/2012	9	3	0.24	0.47	1.46	1.40	1.37	1.44	2.99		0.69	0.73
39	11/14/2012	9	6	0.18	0.37	1.73	1.23	1.33	1.37	2.02	2.37	0.47	0.50
40	11/14/2012	9	11	0.35	0.60	1.09	2.69	2.03	2.80	2.99		1.14	1.51
41	11/14/2012	9	19	0.34	0.59	1.13	3.34	3.65	3.89	3.92		3.02	3.24

42	11/14/2012	9	23	0.25	0.48	1.43	1.27	1.75	1.88	3.66		0.94	1.02
43	11/14/2012	9	33	0.30	0.54	1.25	2.10	1.84	2.68	3.80		0.80	0.99
44	11/14/2012	9	37	0.23	0.45	1.52	1.43	1.61	1.65	2.30	2.46	0.68	0.71
45	11/14/2012	9	44	0.44	0.69	0.86	4.45	3.71		3.93		3.49	3.60
46	11/14/2012	9	47	0.18	0.38	1.70	0.93	1.58	1.64	2.81	3.66	0.58	0.62
47	11/14/2012	10	15	0.45	0.70	0.84	5.07	3.69		3.93		3.38	3.58
48	11/14/2012	10	26	0.31	0.56	1.21	3.11	1.91	3.22	3.72		0.79	1.05
49	11/14/2012	10	30	0.22	0.44	1.55	1.54	1.65	1.71	3.09	3.60	0.76	0.80
50	11/14/2012	10	44	0.25	0.48	1.44	1.28	1.81	2.08	3.74		0.89	1.03
51	11/14/2012	10	48	0.31	0.55	1.24	5.76	2.13	3.61	3.83		1.11	1.28
52	11/14/2012	11	9	0.20	0.40	1.64	1.38	1.44	1.51	2.67	3.36	0.50	0.52
53	11/14/2012	11	17	0.40	0.65	0.97	5.79	1.48	3.89	3.68		0.57	0.86
54	11/14/2012	11	22	0.20	0.41	1.61	1.08	1.06	1.09	1.95	2.10	0.02	0.04
55	11/14/2012	11	28	0.19	0.40	1.65	0.92	1.17	1.23	2.21	2.46	-0.37	-0.34
56	11/14/2012	11	34	0.25	0.47	1.44	1.27	1.43	1.50	2.17	2.80	0.60	0.64
57	11/15/2012	12	57	0.19	0.40	1.65	1.39	1.10	1.13	2.25	2.54	-0.05	0.00
58	11/15/2012	13	51	0.23	0.45	1.50	0.53	1.28	1.30	1.99	2.09	0.57	0.58
59	11/15/2012	13	57	0.21	0.43	1.57	0.74	1.41	1.42	1.96	1.98	0.83	0.83
60	11/15/2012	14	4	0.24	0.47	1.47	0.94	0.93	0.97	1.94	2.25	0.12	0.14
61	11/15/2012	14	19	0.23	0.45	1.52	1.11	1.48	1.53	2.36	3.02	0.68	0.70
62	11/15/2012	14	45	0.23	0.46	1.50	0.66	1.09	1.10	1.75	1.81	0.48	0.49
63	11/15/2012	14	51	0.11	0.26	2.03	0.58	1.07	1.09	1.89	1.94	-0.33	-0.31
64	5/14/2013	10	6	0.58	0.80	0.56	5.94	3.70		3.93		3.48	3.74
65	5/14/2013	10	15	0.56	0.78	0.59	5.87	3.73		3.94		3.53	3.83
66	5/14/2013	10	26	0.52	0.75	0.68	5.03	3.70		3.93		3.45	3.62
67	5/14/2013	10	35	0.46	0.71	0.81	4.12	3.59		3.91		1.02	2.96
68	5/14/2013	11	9	0.23	0.46	1.50	1.23	1.99	2.38	3.77		1.22	1.30
69	5/14/2013	11	16	0.29	0.53	1.28	1.81	1.61	1.80	3.50		0.02	0.16
70	5/14/2013	15	42	0.24	0.47	1.45	0.60	1.69	1.73	2.44	2.75	0.89	0.91
71	5/14/2013	15	58	0.21	0.43	1.58	0.98	1.96	2.03	3.05	3.53	0.61	0.69
72	5/14/2013	16	4	0.19	0.39	1.69	1.08	1.31	1.40	2.83	3.83		
73	5/14/2013	16	14	0.21	0.42	1.59	1.31	0.99	1.08	1.77		0.26	0.33
74	5/14/2013	16	21	0.35	0.60	1.10	3.24	0.96	1.29	3.17		0.06	0.14
75	5/14/2013	16	37	0.56	0.78	0.61	6.94	3.36		3.88		1.71	2.79
76	5/14/2013	16	41	0.31	0.55	1.23	1.46	2.73	2.87	3.67		2.04	2.07
77	5/14/2013	17	25	0.24	0.46	1.48	1.10	1.76	1.83	2.71	3.46	0.92	0.97
78	5/14/2013	17	33	0.15	0.33	1.85	1.49	0.82	0.86	1.62	1.93	0.03	0.04
79	5/14/2013	17	39	0.36	0.61	1.08	2.55	1.23	2.41	3.66		0.05	0.19
80	5/14/2013	17	49	0.48	0.72	0.77	3.69	3.52		3.90		2.77	3.14
81	5/15/2013	9	21	0.26	0.50	1.39	1.91	1.61	1.77	2.53		0.45	0.55
82	5/15/2013	9	33	0.14	0.31	1.89	0.91	1.24	1.28	1.97	2.20	0.18	0.21
83	5/15/2013	9	41	0.29	0.54	1.28	2.15	1.82	1.99	2.73		1.15	1.23
84	5/15/2013	13	58	0.50	0.74	0.73	4.11	1.65	3.88	3.67		0.79	1.06
85	5/15/2013	14	7	0.20	0.41	1.61	1.29	0.91	1.02	1.68		0.10	0.14
86	5/15/2013	14	20	0.70	0.87	0.36	4.63	1.58		3.68		0.80	1.54
87	5/15/2013	14	32	0.14	0.31	1.91	0.64	1.17	1.18	1.88	1.92	0.24	0.26
88	5/15/2013	14	40	0.19	0.40	1.66	0.75	1.00	1.02	1.79	1.87	0.20	0.21
89	5/15/2013	14	45	0.24	0.47	1.45	1.66	1.45	1.55	2.27		0.52	0.56
90	5/15/2013	14	52	0.63	0.83	0.48	6.76	3.24		3.87		2.02	3.22
91	5/15/2013	15	1	0.21	0.43	1.58	0.68	1.69	1.70	2.22	2.28	1.13	1.14
92	5/15/2013	15	8	0.08	0.20	2.19	0.86	0.09	0.12	1.87	1.97	-0.96	-0.95
93	5/15/2013	15	15	0.65	0.84	0.44	8.68	1.11		2.09		-0.39	0.43
94	5/15/2013	15	24	0.15	0.32	1.86	1.17	0.78	0.83	1.68	1.94	-0.06	-0.03
95	5/15/2013	15	59	0.27	0.51	1.36	1.21	2.59	2.65	3.30	3.91	2.06	2.07
96	5/15/2013	16	8	0.19	0.39	1.67	0.69	1.20	1.22	1.85	1.91	0.52	0.52
97	5/15/2013	16	15	0.14	0.31	1.89	0.76	1.02	1.04	1.78	1.91	0.15	0.16
98	5/15/2013	16	21	0.15	0.33	1.84	0.92	0.82	0.85	1.53	1.84	-0.22	-0.18
99	5/15/2013	16	28	0.28	0.52	1.31	1.32	0.53	0.81	2.47		-0.46	-0.39
100	5/15/2013	16	40	0.22	0.44	1.55	0.89	1.31	1.34	2.08	2.34	0.67	0.68
101	5/15/2013	16	48	0.21	0.42	1.61	0.73	2.07	2.12	2.92	3.08	0.69	0.71
102	5/15/2013	16	54	0.25	0.48	1.43	1.24	1.79	1.88	2.83		1.10	1.12
103	5/16/2013	13	3	0.49	0.73	0.75	4.29	2.24		3.82		1.45	1.69
104	5/16/2013	13	16	0.20	0.41	1.62	0.61	1.37	1.39	2.00	2.10	0.57	0.58
105	5/16/2013	13	22	0.35	0.60	1.11	4.41	1.12	1.62	3.75		0.07	0.19
106	5/16/2013	13	43	0.50	0.74	0.71	5.68	3.72		3.94		3.51	3.68
107	5/16/2013	13	54	0.47	0.71	0.80	5.53	3.56		3.90		1.73	3.51
108	5/16/2013	14	2	0.51	0.75	0.70	5.45	3.66	3.73	3.92		3.18	3.23
109	5/16/2013	14	9	0.31	0.55	1.23	2.25	1.70	2.24	3.76		0.58	0.75
110	5/16/2013	14	15	0.23	0.45	1.51	1.35	1.96	2.25	3.68		0.74	0.87
111	5/16/2013	14	23	0.38	0.64	1.01	5.22	2.13	3.96	3.77		1.05	1.50
112	5/16/2013	14	30	0.30	0.55	1.25	2.64	1.88	3.44	3.81		0.68	0.86
113	5/16/2013	14	37	0.40	0.65	0.97	3.95	1.86	3.67	3.82		0.82	1.03
114	5/16/2013	14	46	0.52	0.75	0.68	5.85	3.52		3.89		1.00	2.69
115	5/16/2013	14	53	0.22	0.44	1.55	1.40	1.45	1.50	2.19	3.87	1.03	1.04
116	5/16/2013	15	4	0.24	0.47	1.46	1.23	1.64	1.70	2.49	3.98	1.02	1.04
117	5/16/2013	15	12	0.10	0.23	2.12	0.58	0.93	0.93	1.48	1.49	0.30	0.30
118	5/16/2013	15	19	0.36	0.61	1.06	2.74	2.66	3.59	3.81		1.43	1.62
119	5/16/2013	15	29	0.24	0.47	1.47	1.69	1.46	1.63	2.46		0.55	0.62
120	5/16/2013	15	39	0.68	0.86	0.39	8.38	3.73		3.94		3.53	
121	5/16/2013	16	0	0.18	0.38	1.70	1.35	0.75	0.80	1.46	1.93	-0.08	-0.04
122	5/16/2013	16	7	0.23	0.46	1.49	1.32	1.31	1.50	2.92		-0.07	0.07
123	5/16/2013	16	13	0.25	0.47	1.45	1.54	1.62	1.74	2.73		0.73	0.79
124	5/16/2013	16	22	0.23	0.45	1.51	1.13	1.79	1.88	2.61	3.46	0.61	0.68
125	5/16/2013	16	29	0.20	0.41	1.64	0.70	1.63	1.64	2.18	2.25	1.03	1.04
126	5/16/2013	16	50	0.36	0.61	1.08	1.79	3.35	3.52	3.86		2.67	2.75
127	5/16/2013	16	54	0.13	0.30	1.93	0.66	1.08	1.10	1.87	1.91	0.37	0.38
128	5/16/2013	16	58	0.16	0.35	1.79	0.45	1.45	1.47	2.58	2.66	0.07	0.08
129	5/16/2013	17	3	0.17	0.37	1.74	0.50	1.44	1.45	2.15	2.20	0.56	0.57
130	5/16/2013	17	8	0.19	0.39	1.69	0.49	1.62	1.64	2.28	2.33	1.01	1.01
131	5/16/2013	17	17	0.21	0.42	1.58	0.88	1.25	1.31	2.65	3.82	0.58	0.60
132	5/16/2013	17	21	0.21	0.42	1.59	0.55	1.22	1.24	2.05	2.21	0.39	0.40
133	5/16/2013	17	26	0.15	0.33	1.84	1.82	1.16	1.18	2.29	2.40	0.19	0.20
134	5/16/2013	17	32	0.14	0.30	1.91	0.41	1.31	1.32	1.94	1.96	0.61	0.62
135	5/16/2013	17	37	0.14	0.31	1.90	0.35	1.42	1.43	1.94	1.96	0.88	0.89

136	11/4/2013	8	7	0.66	0.85	0.42	8.86	3.73		3.94		3.53	4.20
137	11/4/2013	8	26	0.16	0.35	1.78	0.89	0.75	0.83	3.23	3.89	-0.27	-0.22
138	11/4/2013	8	35	0.38	0.63	1.02	4.10	2.39	2.83	3.29		1.46	1.59
139	11/4/2013	8	42	0.28	0.52	1.32	1.89	2.16	2.31	2.90		1.56	1.58
140	11/4/2013	8	49	0.30	0.54	1.27	1.87	2.43	2.54	3.13		1.52	1.55
141	11/4/2013	8	53	0.30	0.55	1.25	1.18	2.04	2.14	3.09	3.78	1.16	1.19
142	11/4/2013	9	3	0.22	0.44	1.53	0.74	1.65	1.68	2.38	2.45	0.88	0.90
143	11/4/2013	9	8	0.38	0.63	1.00	4.42	1.91	3.51	3.63		1.07	1.24
144	11/4/2013	9	12	0.25	0.48	1.43	1.67	0.87	0.97	2.19		0.07	0.12
145	11/4/2013	9	18	0.22	0.44	1.54	0.75	1.06	1.08	1.60	1.75	0.49	0.50
146	11/4/2013	9	26	0.10	0.23	2.10	1.06	0.53	0.58	1.79	2.84	-0.29	-0.28
147	11/4/2013	9	31	0.55	0.77	0.62	6.43	3.69		3.93		3.38	3.58
148	11/4/2013	9	39	0.52	0.75	0.68	6.63	3.70		3.93		3.43	3.65
149	11/4/2013	9	58	0.26	0.50	1.38	2.42	1.10	1.73	3.72		0.20	0.33
150	11/4/2013	10	5	0.23	0.46	1.50	2.15	1.12	1.32	3.21		0.32	0.41
151	11/4/2013	10	13	0.24	0.47	1.45	1.39	1.61	1.68	2.44	3.94	0.81	0.87
152	11/4/2013	10	18	0.23	0.45	1.50	1.17	1.59	1.62	2.39	2.71	0.90	0.92
153	11/4/2013	10	27	0.28	0.52	1.31	1.41	2.57	2.66	3.24		2.02	2.04
154	11/4/2013	10	32	0.27	0.50	1.36	2.04	1.72	2.13	3.63		0.82	0.99
155	11/4/2013	10	37	0.23	0.45	1.51	1.23	1.27	1.53	3.54		-0.23	-0.04
156	11/4/2013	10	42	0.30	0.54	1.26	2.12	0.97	1.74	3.72		0.10	0.24
157	11/4/2013	10	46	0.37	0.63	1.03	2.79	3.46	3.95	3.88		1.47	2.55
158	11/4/2013	10	51	0.41	0.66	0.94	3.10	2.88	3.95	3.85		1.30	1.72
159	11/4/2013	10	59	0.37	0.62	1.06	3.25	3.64		3.92		3.12	3.51
160	11/4/2013	11	8	0.28	0.52	1.32	2.27	0.63	1.22	3.62			
161	11/4/2013	11	13	0.25	0.48	1.42	1.75	1.12	1.33	3.31		0.37	0.50
162	11/4/2013	11	22	0.30	0.55	1.24	2.07	1.48	1.78	2.46		0.76	0.88
163	11/4/2013	11	30	0.18	0.37	1.73	1.17	1.28	1.66	3.49	3.91		
164	11/4/2013	12	22	0.22	0.44	1.54	1.24	1.68	1.79	3.45		1.08	1.11
165	11/4/2013	12	27	0.39	0.65	0.98	4.76	3.48		3.89		1.48	2.93
166	11/4/2013	12	32	0.26	0.50	1.38	1.38	1.70	2.00	3.76		0.88	1.00
167	11/4/2013	12	40	0.20	0.41	1.63	1.30	1.75	1.88	3.74		0.79	0.86
168	11/4/2013	12	52	0.20	0.40	1.64	1.11	1.84	2.02	3.63		-0.33	-0.18
169	11/4/2013	13	1	0.23	0.45	1.51	1.51	2.07	2.30	3.60		0.69	0.87
170	11/4/2013	13	7	0.22	0.44	1.54	1.31	1.70	1.81	3.68		0.62	0.68
171	11/4/2013	13	15	0.27	0.50	1.37	2.10	1.88	2.57	3.74		0.76	0.87
172	11/4/2013	13	21	0.35	0.60	1.11	2.85	3.30	3.73	3.87		1.28	1.62
173	11/4/2013	13	26	0.33	0.58	1.15	1.94	1.81	2.12	3.67		0.86	1.03
174	11/4/2013	13	31	0.39	0.64	0.99	2.89	3.38	3.63	3.87		1.93	2.11
175	11/4/2013	13	37	0.33	0.58	1.17	2.10	3.08	3.52	3.84		1.70	1.79
176	11/4/2013	13	44	0.56	0.78	0.61	5.43	3.69		3.93		3.28	3.68
177	11/4/2013	13	51	0.43	0.68	0.87	4.65	3.24		3.88		1.06	1.73
178	11/4/2013	14	0	0.24	0.46	1.49	1.11	1.67	1.74	2.61	3.92	0.89	0.96
179	11/4/2013	14	4	0.24	0.46	1.48	0.82	1.97	2.26	3.74		1.13	1.18
180	11/4/2013	14	8	0.24	0.47	1.46	1.55	1.74	1.95	3.48		0.42	0.54
181	11/4/2013	14	20	0.50	0.74	0.72	3.86	3.53		3.90		1.12	1.98
182	11/4/2013	14	24	0.20	0.41	1.62	1.17	0.96	1.03	2.51	3.60	0.06	0.08
183	11/4/2013	14	33	0.31	0.55	1.23	1.49	2.02	2.17	3.22		1.11	1.18
184	11/4/2013	14	39	0.30	0.55	1.25	2.49	2.19	2.44	3.62		1.26	1.38
185	11/4/2013	14	42	0.22	0.44	1.55	0.92	1.44	1.46	2.38	2.53	0.55	0.56
186	11/4/2013	15	28	0.20	0.41	1.63	0.49	1.47	1.49	2.07	2.17	0.67	0.67
187	11/4/2013	15	32	0.27	0.51	1.35	2.41	1.11	1.29	3.27		0.19	0.26
188	11/4/2013	15	37	0.30	0.54	1.26	1.87	1.65	1.87	3.52		0.67	0.78
189	11/4/2013	15	41	0.21	0.42	1.60	0.99	1.12	1.22	2.28	2.64	-0.33	-0.30
190	11/4/2013	15	47	0.20	0.41	1.62	0.67	1.10	1.13	1.96	2.01	0.14	0.15
191	11/4/2013	15	54	0.37	0.62	1.06	2.39	2.61	3.43	3.80		1.61	1.74
192	11/8/2013	14	6	0.26	0.50	1.38	0.98	1.39	1.49	2.88		0.67	0.70
193	11/8/2013	14	15	0.20	0.41	1.64	0.59	1.14	1.16	1.97	2.04	0.13	0.14
194	11/8/2013	14	29	0.17	0.37	1.74	0.65	1.17	1.20	2.37	2.53		
195	11/8/2013	14	34	0.17	0.37	1.74	0.62	1.32	1.33	1.97	1.99	0.58	0.59
196	11/8/2013	14	37	0.11	0.25	2.07	0.61	1.24	1.25	1.91	1.96	0.63	0.63
197	11/8/2013	14	51	0.27	0.50	1.38	1.39	1.85	1.94	3.04		1.19	1.23
198	11/8/2013	14	57	0.18	0.38	1.71	0.80	1.62	1.65	2.37	2.45	1.02	1.02
199	11/8/2013	15	6	0.16	0.35	1.80	0.68	0.85	0.86	1.53	1.62	0.02	0.03
200	11/8/2013	15	12	0.20	0.41	1.62	0.85	1.20	1.22	1.98	2.10	0.45	0.46
201	11/8/2013	15	18	0.21	0.42	1.60	0.96	1.06	1.10	1.77	1.95	0.49	0.50
202	11/8/2013	15	33	0.22	0.44	1.55	0.79	1.84	1.86	2.62	2.75	1.18	1.19
203	11/8/2013	15	40	0.21	0.43	1.57	0.93	1.60	1.62	2.36	2.42	0.70	0.71
204	11/8/2013	15	46	0.23	0.46	1.49	1.49	1.27	1.34	2.33	2.87	0.44	0.48
205	11/8/2013	15	51	0.23	0.45	1.52	0.96	1.28	1.32	2.18	2.36	0.56	0.57
206	11/8/2013	16	4	0.51	0.74	0.71	5.85	3.64		3.92		3.12	3.48
207	11/8/2013	16	13	0.27	0.51	1.35	4.02	1.61	1.66	2.18	2.79	0.92	0.98
208	11/8/2013	16	19	0.39	0.64	0.99	4.76	1.95	2.12	2.86		1.12	1.18
209	11/8/2013	16	25	0.20	0.41	1.62	1.21	1.16	1.19	1.89	2.15	0.53	0.54
210	11/9/2013	7	51	0.21	0.42	1.59	1.31	1.08	1.12	1.99	2.34	0.10	0.12
211	11/9/2013	7	58	0.42	0.67	0.92	3.63	2.82	3.41	3.72		1.52	1.87
212	11/9/2013	8	19	0.21	0.42	1.58	0.57	1.51	1.52	2.06	2.13	0.84	0.85
213	11/9/2013	8	27	0.20	0.41	1.62	0.60	1.47	1.48	1.99	2.04	1.00	1.00
214	11/9/2013	8	34	0.26	0.49	1.40	1.54	1.36	1.52	2.52		0.31	0.44
215	11/9/2013	8	43	0.31	0.55	1.23	2.29	2.41	2.58	3.09		1.33	1.44
216	11/9/2013	8	48	0.20	0.41	1.63	0.66	1.68	1.69	2.33	2.38	1.02	1.02
217	11/9/2013	8	54	0.20	0.42	1.61	0.71	1.31	1.33	2.12	2.28	0.51	0.51
218	11/9/2013	8	59	0.23	0.45	1.52	1.57	0.99	1.17	3.02		-0.37	-0.28
219	11/9/2013	9	6	0.11	0.26	2.04	0.57	0.76	0.77	1.58	1.64	-0.15	-0.14
220	11/9/2013	9	15	0.23	0.45	1.51	0.84	1.12	1.14	1.75	1.87	0.56	0.57
221	11/9/2013	9	25	0.14	0.31	1.89	0.83	0.97	0.99	1.48	1.56	0.22	0.23
222	11/9/2013	9	30	0.22	0.44	1.53	0.91	1.16	1.17	1.76	1.84	0.48	0.50
223	11/9/2013	9	34	0.23	0.45	1.51	0.85	1.71	1.73	2.33	2.45	1.03	1.05
224	11/9/2013	9	37	0.47	0.71	0.80	4.38	2.50	3.67	3.75		1.12	1.31
225	11/9/2013	9	51	0.51	0.74	0.71	4.87	3.29		3.86		2.49	2.79
226	11/9/2013	10	0	0.35	0.60	1.09	2.08	1.93	2.19	2.73		1.44	1.52
227	11/9/2013	10	6	0.19	0.39	1.66	1.57	1.24	1.28	1.99	2.19	0.12	0.14
228	11/9/2013	10	13	0.16	0.34	1.81	0.73	0.88	0.92	1.62	1.79	0.06	0.07
229	11/9/2013	10	18	0.19	0.40	1.66	0.82	0.88	0.93	1.82	2.66	0.10	0.12

230	11/9/2013	10	24	0.15	0.33	1.85	0.70	1.15	1.16	1.73	1.80	0.55	0.55
231	11/9/2013	10	33	0.22	0.44	1.53	1.11	1.16	1.22	1.94	2.40	0.16	0.20
232	11/9/2013	10	39	0.24	0.46	1.49	1.33	1.95	2.00	2.72	2.98	1.42	1.45
233	11/9/2013	10	43	0.24	0.47	1.45	0.63	1.37	1.38	1.92	1.95	0.74	0.75
234	11/9/2013	10	50	0.17	0.36	1.76	0.50	0.99	1.01	1.77	1.85	-0.10	-0.08
235	11/9/2013	11	13	0.23	0.45	1.52	0.93	1.27	1.33	2.14	2.51	0.51	0.53
236	11/9/2013	11	16	0.42	0.67	0.92	2.66	3.14	3.82	3.87		0.65	0.93
237	11/9/2013	11	21	0.26	0.49	1.40	0.91	2.15	2.20	2.93	3.53	1.13	1.18
238	11/9/2013	11	27	0.23	0.45	1.52	0.75	1.41	1.44	2.28	2.40	0.40	0.43
239	11/9/2013	11	31	0.27	0.50	1.36	2.03	1.81	2.14	3.64		1.12	1.20
240	11/9/2013	11	42	0.24	0.47	1.46	3.94	1.99	2.63	3.72		1.04	1.11
241	11/9/2013	11	50	0.21	0.42	1.60	1.08	1.16	1.26	2.79		0.50	0.52
242	11/9/2013	11	54	0.28	0.51	1.34	1.75	3.24	3.67	3.88		1.59	1.73
243	11/9/2013	11	59	0.32	0.56	1.20	5.36	2.15	3.51	3.79		1.15	1.31
244	11/9/2013	12	2	0.52	0.76	0.67	3.71	3.70		3.93		3.47	3.63
245	11/9/2013	12	14	0.39	0.64	0.99	3.35	3.10		3.87		1.53	1.88
246	11/9/2013	12	18	0.39	0.64	0.98	2.49	3.58	3.96	3.91		1.50	2.17
247	11/9/2013	12	24	0.13	0.29	1.95	0.62	1.11	1.13	1.70	1.85	0.53	0.54
248	11/9/2013	12	30	0.28	0.52	1.32	1.62	1.98	2.81	3.77		1.16	1.23
249	11/9/2013	12	36	0.27	0.51	1.35	1.10	1.81	1.86	3.00	3.83	1.10	1.13
250	11/9/2013	12	55	0.17	0.36	1.76	0.65	1.52	1.55	2.27	2.37	0.59	0.60
251	5/13/2014	9	45	0.56	0.78	0.59	7.85	1.43		3.79			0.66
252	5/13/2014	10	9	0.18	0.38	1.69	0.76	0.81	0.84	1.95	2.12	-0.24	-0.23
253	5/13/2014	10	17	0.65	0.84	0.44	13.13	3.68		3.93		3.22	3.56
254	5/13/2014	10	32	0.26	0.49	1.41	1.92	2.40	2.71	3.71		1.35	1.47
255	5/13/2014	10	40	0.18	0.37	1.73	0.67	1.41	1.43	2.13	2.21	0.66	0.67
256	5/13/2014	10	48	0.20	0.40	1.64	0.56	1.43	1.44	2.03	2.12	0.74	0.74
257	5/13/2014	10	55	0.52	0.75	0.68	5.84	2.39		3.71		1.57	1.83
258	5/13/2014	11	7	0.29	0.54	1.28	3.01	2.28	2.45	3.51		1.57	1.63
259	5/13/2014	11	17	0.27	0.50	1.37	1.76	1.22	1.38	3.50		0.35	0.45
260	5/13/2014	11	29	0.66	0.85	0.42	10.29	3.73		3.94		3.53	
261	5/13/2014	11	40	0.63	0.83	0.46	8.91	3.73		3.94		3.53	3.92
262	5/13/2014	11	45	0.35	0.60	1.10	2.16	1.86	3.52	3.78		1.04	1.18
263	5/13/2014	11	58	0.43	0.68	0.89	3.60	3.52	3.92	3.89		1.45	1.80
264	5/13/2014	12	4	0.24	0.47	1.45	1.40	1.91	2.09	3.68		1.06	1.10
265	5/13/2014	12	14	0.27	0.50	1.37	1.77	1.71	1.88	3.32		0.75	0.86
266	5/13/2014	12	28	0.31	0.56	1.21	3.05	1.95	2.86	3.77		1.11	1.24
267	5/13/2014	12	38	0.22	0.44	1.54	1.23	1.84	1.99	3.70		1.06	1.10
268	5/13/2014	12	48	0.30	0.55	1.25	2.14	1.41	1.78	3.70		0.66	0.77
269	5/13/2014	12	58	0.24	0.47	1.46	1.91	1.70	1.81	3.25		1.06	1.09
270	5/13/2014	13	6	0.53	0.76	0.67	7.54	3.73		3.94		3.53	3.82
271	5/13/2014	13	17	0.32	0.57	1.18	2.33	1.84	2.32	3.72		1.12	1.18
272	5/13/2014	13	29	0.28	0.52	1.32	3.10	1.30	1.46	3.28		0.63	0.68
273	5/13/2014	13	39	0.30	0.54	1.27	2.77	1.44	1.77	3.68		0.74	0.83
274	5/13/2014	13	45	0.13	0.29	1.95	1.29	-0.70	-0.40	1.98	2.37		
275	5/13/2014	14	1	0.34	0.59	1.14	2.85	2.24	2.75	3.69		1.53	1.62
276	5/13/2014	14	12	0.26	0.50	1.38	1.74	1.77	1.82	2.33	2.84	1.24	1.27
277	5/13/2014	14	22	0.29	0.53	1.29	2.31	2.52	3.51	3.81		1.66	1.80
278	5/13/2014	14	30	0.24	0.46	1.48	0.91	1.30	1.34	1.96	2.71	0.68	0.70
279	5/13/2014	14	40	0.24	0.47	1.46	0.84	1.32	1.36	1.96	2.32	0.66	0.67
280	5/13/2014	14	54	0.21	0.42	1.60	0.76	1.58	1.63	2.27	2.90	1.01	1.03
281	5/13/2014	15	4	0.20	0.41	1.62	0.61	1.39	1.40	1.92	1.94	0.77	0.78
282	5/13/2014	15	10	0.20	0.41	1.63	1.02	1.49	1.57	2.85	3.75	0.57	0.59
283	5/13/2014	15	18	0.27	0.50	1.37	1.44	2.25	2.40	3.61		1.40	1.50
284	5/13/2014	15	24	0.22	0.43	1.55	1.46	2.12	2.17	2.90	3.37	1.50	1.51
285	5/13/2014	15	32	0.18	0.38	1.69	0.58	1.09	1.10	1.89	1.94	-0.50	-0.48
286	5/13/2014	15	42	0.21	0.42	1.59	0.75	1.59	1.61	2.15	2.28	0.71	0.72
287	5/13/2014	15	48	0.18	0.38	1.71	0.66	1.60	1.61	2.36	2.40	0.37	0.39
288	5/13/2014	15	54	0.14	0.30	1.92	1.28	1.31	1.33	2.15	2.28	0.46	0.48
289	5/13/2014	16	0	0.22	0.44	1.54	0.89	1.05	1.08	1.86	1.95	0.11	0.12
290	5/13/2014	16	5	0.21	0.42	1.59	1.25	1.19	1.23	1.78	1.94	0.55	0.57
291	5/13/2014	16	13	0.20	0.41	1.62	1.04	1.18	1.22	2.04	2.50		
292	5/13/2014	16	18	0.21	0.42	1.60	1.24	1.38	1.43	2.15	3.21	0.71	0.74
293	5/13/2014	16	24	0.22	0.44	1.54	0.63	1.31	1.34	2.15	2.27	0.51	0.51
294	5/13/2014	16	36	0.21	0.43	1.57	0.51	1.57	1.58	2.25	2.33	0.75	0.76
295	5/13/2014	16	40	0.25	0.48	1.42	1.70	1.87	1.93	2.76	3.70	1.20	1.23
296	5/13/2014	16	46	0.23	0.45	1.52	0.70	1.52	1.54	2.30	2.40	0.71	0.72
297	5/13/2014	16	50	0.21	0.43	1.58	0.68	1.70	1.71	2.36	2.41	0.98	0.99
298	5/13/2014	16	55	0.21	0.42	1.58	2.07	1.30	1.33	2.14	2.28	-0.05	-0.02
299	5/13/2014	17	1	0.13	0.29	1.96	0.63	0.93	0.95	1.83	1.88	-0.13	-0.12
300	5/13/2014	17	5	0.41	0.66	0.94	4.18	1.53	2.51	3.18		0.67	0.83
301	5/13/2014	17	11	0.13	0.30	1.93	0.66	1.19	1.21	1.94	1.98	0.40	0.41
302	5/13/2014	17	30	0.15	0.34	1.83	0.75	1.33	1.34	2.00	2.09	0.31	0.32
303	5/13/2014	17	35	0.24	0.47	1.46	1.36	2.25	2.29	2.95	3.23	1.58	1.59
304	5/13/2014	17	44	0.59	0.81	0.53	14.94	3.53	5.22	3.90	7.44	2.60	3.32
305	5/13/2014	17	53	0.25	0.48	1.42	3.48	1.48	1.51	2.36	2.45	0.56	0.57
306	5/14/2014	17	0	0.17	0.37	1.74	0.39	1.33	1.34	2.00	2.05	0.18	0.19
307	5/14/2014	17	11	0.09	0.21	2.18	0.29	1.25	1.26	1.84	1.86	0.65	0.65
308	5/14/2014	17	17	0.12	0.27	2.01	0.48	0.89	0.90	1.49	1.54	0.08	0.08
309	5/14/2014	17	20	0.18	0.38	1.70	0.58	0.78	0.79	1.44	1.46	0.09	0.10
310	5/14/2014	17	24	0.22	0.43	1.56	0.63	1.69	1.70	2.32	2.38	1.00	1.01
311	5/16/2014	7	58	0.15	0.34	1.83	0.56	1.03	1.05	1.84	1.94	0.39	0.40
312	5/16/2014	8	7	0.20	0.41	1.62	2.28	1.02	1.06	2.32	2.62	-0.54	-0.51
313	5/16/2014	8	14	0.18	0.37	1.72	0.51	1.36	1.38	2.33	2.42		
314	5/16/2014	8	23	0.14	0.31	1.89	0.39	1.40	1.41	2.35	2.42	0.34	0.36
315	5/16/2014	8	37	0.14	0.31	1.90	0.57	1.41	1.42	1.94	1.96	0.67	0.67
316	5/16/2014	8	46	0.18	0.38	1.71	0.49	1.74	1.75	2.32	2.36	1.10	1.10
317	5/16/2014	8	53	0.11	0.25	2.07	0.41	1.22	1.24	2.04	2.14		-0.99
318	5/16/2014	9	0	0.10	0.24	2.09	0.45	0.72	0.74	1.90	1.96		
319	5/16/2014	9	6	0.07	0.18	2.26	0.34	0.88	0.90	1.46	1.49	0.24	0.24
320	5/16/2014	9	17	0.18	0.37	1.72	0.85	0.94	0.97	2.22	2.43	-0.17	-0.15
321	5/16/2014	9	27	0.17	0.36	1.76	0.75	1.23	1.25	1.99	2.10	0.28	0.29
322	5/16/2014	9	33	0.20	0.41	1.62	0.61	1.54	1.55	2.23	2.30	0.75	0.76
323	5/16/2014	9	38	0.19	0.39	1.69	0.54	1.56	1.57	2.26	2.31	0.53	0.54

324	5/16/2014	9	44	0.21	0.42	1.60	0.52	1.43	1.44	1.98	2.03	0.81	0.82
325	5/16/2014	9	50	0.23	0.45	1.52	0.49	1.27	1.29	1.89	1.92	0.35	0.36
326	5/16/2014	9	58	0.14	0.31	1.89	0.98	0.79	0.82	1.95	2.46	0.05	0.05
327	5/16/2014	10	9	0.20	0.41	1.61	1.36	1.07	1.10	2.24	2.44	0.09	0.11
328	5/16/2014	10	15	0.20	0.41	1.64	0.79	1.56	1.57	2.15	2.25	1.02	1.02
329	5/16/2014	10	21	0.21	0.42	1.60	0.90	1.69	1.71	2.33	2.37	1.02	1.02
330	5/16/2014	10	28	0.20	0.41	1.62	0.58	1.68	1.70	2.46	2.56	0.79	0.80
331	5/16/2014	10	35	0.17	0.36	1.75	0.58	1.45	1.47	2.01	2.09	0.81	0.82
332	5/16/2014	10	41	0.20	0.40	1.65	0.79	1.33	1.34	2.15	2.26	0.57	0.58
333	5/16/2014	10	47	0.10	0.23	2.11	0.85	0.74	0.75	1.41	1.44	0.04	0.04
334	5/16/2014	10	52	0.21	0.42	1.60	0.67	0.61	0.62	1.32	1.36	-0.23	-0.22
335	5/16/2014	11	3	0.22	0.44	1.53	0.60	1.04	1.07	2.13	2.30	0.15	0.16
336	5/16/2014	11	9	0.22	0.44	1.55	0.59	0.50	0.51	1.36	1.43	-0.33	-0.32
337	5/16/2014	11	14	0.16	0.35	1.80	0.68	0.87	0.89	1.93	2.04	-0.31	-0.29
338	5/16/2014	11	21	0.19	0.40	1.66	0.56	1.25	1.26	1.96	1.98	0.47	0.48
339	5/16/2014	11	40	0.22	0.44	1.54	0.77	1.97	2.00	2.82	2.93	1.19	1.20
340	5/16/2014	11	45	0.21	0.42	1.60	0.47	1.46	1.47	2.08	2.15	0.87	0.87
341	5/16/2014	11	51	0.14	0.30	1.92	3.30	0.95	0.96	1.73	1.78	0.10	0.10
342	5/16/2014	11	57	0.15	0.32	1.86	0.58	0.80	0.81	1.88	2.01	0.00	0.01
343	5/16/2014	12	3	0.58	0.80	0.56	10.75	3.63		3.92		3.17	
344	5/16/2014	12	30	0.35	0.60	1.10	2.40	3.13	3.55	3.84			1.97
345	5/16/2014	12	39	0.11	0.26	2.04	0.90	0.64	0.67	1.46	1.74	-0.23	-0.21
346	5/16/2014	12	44	0.21	0.42	1.59	0.54	1.26	1.27	1.90	1.95	0.63	0.63
347	5/16/2014	12	51	0.21	0.42	1.60	0.95	1.77	1.80	2.58	2.80	0.86	0.88
348	5/16/2014	12	56	0.24	0.47	1.47	0.94	2.32	2.35	2.95	3.00	1.41	1.44
349	5/16/2014	13	6	0.24	0.47	1.46	1.51	2.28	2.30	2.96	3.14	1.56	1.58
350	5/16/2014	13	18	0.11	0.26	2.05	0.40	1.22	1.23	1.84	1.87	0.58	0.58
351	5/16/2014	13	24	0.09	0.21	2.18	0.58	0.91	0.92	1.62	1.70	0.15	0.16
352	5/16/2014	13	37	0.10	0.24	2.08	0.66	0.64	0.67	1.67	1.88	-0.37	-0.35
353	5/16/2014	13	55	0.54	0.77	0.63	6.60			3.69			
354	5/16/2014	14	3	0.14	0.31	1.90	0.53	0.69	0.71	1.39	1.42		
355	5/16/2014	14	11	0.20	0.40	1.64	0.44	1.58	1.59	1.97	1.99	1.06	1.06
356	5/16/2014	14	17	0.21	0.42	1.59	0.48	2.13	2.14	2.46	2.58	1.63	1.63
357	5/16/2014	14	25	0.23	0.45	1.51	0.83	1.91	1.93	2.84	2.95	1.20	1.21
358	5/16/2014	14	32	0.26	0.49	1.39	1.24	1.93	1.98	2.95	3.37	1.19	1.21
359	5/16/2014	14	44	0.14	0.32	1.88	0.52	1.40	1.41	1.96	1.98	0.77	0.78
360	5/16/2014	14	53	0.42	0.67	0.91	5.78			3.39			
361	5/16/2014	15	6	0.10	0.23	2.11	0.64	0.94	0.95	1.47	1.49	0.30	0.31
362	5/16/2014	15	12	0.18	0.37	1.73	0.74	1.25	1.26	1.97	2.02	0.40	0.41
363	5/16/2014	15	19	0.22	0.43	1.55	0.63	1.81	1.82	2.50	2.60	1.07	1.08
364	5/16/2014	15	20	0.22	0.44	1.54	0.92	1.87	1.89	2.48	2.59	1.11	1.12
365	5/16/2014	15	45	0.21	0.43	1.57	0.64	1.84	1.86	2.57	2.68	1.08	1.09
366	5/16/2014	15	56	0.12	0.28	1.99	0.41	1.21	1.22	2.00	2.07	0.53	0.53
367	5/16/2014	16	7	0.23	0.45	1.52	0.61	1.79	1.80	2.53	2.65	1.05	1.06
368	5/16/2014	16	12	0.15	0.32	1.86	0.45	1.42	1.43	2.04	2.10	0.65	0.65
369	5/16/2014	16	18	0.18	0.37	1.73	2.44	0.96	0.98	2.42	2.54	-0.76	-0.73
370	5/16/2014	16	27	0.23	0.45	1.50	1.52	1.80	1.86	2.64	3.57	1.05	1.08
371	5/16/2014	16	39	0.37	0.62	1.03	2.69	2.94		3.81		2.15	2.47
372	5/16/2014	16	46	0.17	0.36	1.75	0.43	1.17	1.18	1.92	1.95	0.37	0.38
373	5/16/2014	16	57	0.16	0.34	1.82	0.38	1.01	1.03	2.38	2.47		
374	5/16/2014	17	4	0.19	0.39	1.68	0.48	1.42	1.42	2.10	2.15	0.72	0.72
375	5/16/2014	17	8	0.15	0.33	1.83	0.44	1.51	1.52	2.26	2.33	0.91	0.92
376	5/16/2014	17	14	0.10	0.24	2.09	0.36	1.21	1.22	1.84	1.86	0.55	0.55
377	5/16/2014	17	23	0.13	0.29	1.94	0.29	1.30	1.31	1.91	1.93	0.59	0.60
378	5/16/2014	17	28	0.19	0.39	1.69	0.43	1.24	1.26	2.15	2.21	0.35	0.36
379	5/16/2014	17	34	0.20	0.40	1.64	0.57	1.11	1.13	2.03	2.17	0.19	0.20
380	5/16/2014	17	40	0.28	0.51	1.34	2.12	2.97	3.54	3.84		0.97	1.08
381	5/17/2014	8	1	0.20	0.41	1.63	0.56	1.34	1.35	2.33	2.53	0.65	0.66
382	5/17/2014	10	33	0.24	0.46	1.47	0.69	1.39	1.42	2.32	2.83	0.70	0.72
383	5/17/2014	14	12	0.27	0.50	1.36	1.51	2.45	2.84	3.75		1.26	1.37

A.4 Critical Shear Stresses

Core ID	Critical shear stress D_{50}	Critical shear stress D_{10}	Critical shear stress D_{90}
1	0.1301	0.0257	0.1347
2	0.1944	0.0325	0.2464
3	0.1975	0.0699	0.2540
4	0.2028	0.1056	0.2672
5	0.2082	0.1226	0.3454
6	0.2109	0.1232	0.3425
7	0.1372	0.0236	0.1392
8	0.2959	0.1958	0.6468
9	0.2230	0.1856	0.2824
10	0.1691	0.0453	0.1895
11	0.1899	0.1572	0.2351
12	0.1720	0.1396	0.2149
13	0.1354	0.0245	0.1427
14	0.2643	0.0675	0.4328

15	0.2467	0.0777	0.3579
16	0.2246	0.1763	0.2983
17	0.2015	0.1207	0.2569
18	0.2071	0.1413	0.2622
19	0.1825	0.0276	0.2177
20	0.2832	0.2066	0.4822
21	0.2495	0.0569	0.4018
22	0.2601	0.2022	0.3835
23	0.2590	0.2014	0.3725
24	0.2168	0.1712	0.3349
25	0.1975	0.1695	0.2326
26	0.1594	0.0389	0.1988
27	0.1504	0.0258	0.1750
28	0.2999	0.1034	0.4730
29	0.2461	0.0566	0.3430
30	0.2341	0.1769	0.3306
31	0.1917	0.1474	0.2930
32	0.2274	0.0223	0.1098
33	0.2405	0.1724	0.3913
34	0.2277	0.1693	0.3804
35	0.2294	0.1812	0.3428
36	0.2190	0.1876	0.2565
37	0.2263	0.1911	0.2789
38	0.2276	0.1127	0.3005
39	0.2304	0.1751	0.3420
40	0.1887	0.0308	0.2174
41	0.1321	0.0311	0.1457
42	0.2024	0.0771	0.2612
43	0.1976	0.0444	0.2638
44	0.2109	0.1716	0.3036
45	0.1299	0.0251	0.1338
46	0.2125	0.1318	0.3191
47	0.1306	0.0249	0.1345
48	0.1945	0.0345	0.2576
49	0.2080	0.1336	0.2900
50	0.1991	0.0543	0.2601
51	0.1846	0.0349	0.2346
52	0.2223	0.1418	0.3374
53	0.2194	0.0286	0.2811
54	0.2566	0.1859	0.4714
55	0.2444	0.1717	0.6393
56	0.2227	0.1602	0.3160
57	0.2524	0.1688	0.4857
58	0.2345	0.1862	0.3272
59	0.2245	0.1910	0.2848
60	0.2710	0.1797	0.4366
61	0.2190	0.1529	0.3047
62	0.2532	0.1996	0.3447
63	0.2547	0.1928	0.6246
64	0.1302	0.0233	0.1291
65	0.1293	0.0230	0.1259
66	0.1303	0.0242	0.1329
67	0.1340	0.0258	0.1548

68	0.1907	0.0524	0.2335
69	0.2105	0.0714	0.4294
70	0.2061	0.1618	0.2738
71	0.1921	0.1360	0.3069
72	0.2323	0.1260	1.2059
73	0.2648	0.1044	0.3818
74	0.2682	0.0537	0.4372
75	0.1418	0.0249	0.1604
76	0.1623	0.0759	0.1871
77	0.2020	0.1382	0.2666
78	0.2860	0.1935	0.4692
79	0.2394	0.0418	0.4212
80	0.1363	0.0260	0.1488
81	0.2110	0.0674	0.3326
82	0.2381	0.1817	0.4147
83	0.1989	0.0490	0.2394
84	0.2083	0.0286	0.2568
85	0.2740	0.1009	0.4367
86	0.2127	0.0236	0.2155
87	0.2451	0.1937	0.4015
88	0.2630	0.1962	0.4156
89	0.2217	0.1140	0.3294
90	0.1457	0.0235	0.1461
91	0.2058	0.1783	0.2482
92	0.4537	0.1917	1.1252
93	0.2509	0.0256	0.3582
94	0.2923	0.1928	0.4960
95	0.1672	0.1233	0.1868
96	0.2422	0.1945	0.3374
97	0.2612	0.1943	0.4294
98	0.2870	0.1979	0.5590
99	0.3361	0.0619	0.6684
100	0.2320	0.1761	0.3087
101	0.1869	0.1510	0.3027
102	0.2002	0.1160	0.2496
103	0.1801	0.0275	0.2057
104	0.2274	0.1855	0.3261
105	0.2500	0.0456	0.4220
106	0.1296	0.0238	0.1309
107	0.1349	0.0237	0.1367
108	0.1317	0.0663	0.1458
109	0.2054	0.0429	0.2968
110	0.1921	0.0746	0.2796
111	0.1844	0.0283	0.2176
112	0.1958	0.0401	0.2814
113	0.1967	0.0325	0.2593
114	0.1363	0.0253	0.1637
115	0.2217	0.1245	0.2582
116	0.2092	0.1207	0.2589
117	0.2721	0.2184	0.3885
118	0.1649	0.0342	0.2100
119	0.2204	0.0680	0.3195
120	0.1293	0.0225	0.1136

121	0.2974	0.1932	0.4993
122	0.2321	0.0845	0.4586
123	0.2099	0.0956	0.2913
124	0.2004	0.1383	0.3076
125	0.2098	0.1796	0.2589
126	0.1419	0.0526	0.1617
127	0.2536	0.1943	0.3697
128	0.2217	0.1647	0.4573
129	0.2224	0.1815	0.3291
130	0.2099	0.1765	0.2613
131	0.2377	0.1263	0.3230
132	0.2399	0.1810	0.3642
133	0.2463	0.1738	0.4174
134	0.2324	0.1920	0.3197
135	0.2235	0.1920	0.2766
136	0.1293	0.0225	0.1133
137	0.2968	0.1238	0.5769
138	0.1743	0.0371	0.2117
139	0.1831	0.0753	0.2124
140	0.1729	0.0994	0.2143
141	0.1884	0.1277	0.2433
142	0.2081	0.1722	0.2755
143	0.1944	0.0306	0.2387
144	0.2797	0.0897	0.4434
145	0.2567	0.2025	0.3424
146	0.3357	0.1586	0.6070
147	0.1306	0.0248	0.1343
148	0.1304	0.0239	0.1321
149	0.2515	0.0439	0.3807
150	0.2499	0.0648	0.3610
151	0.2110	0.1222	0.2797
152	0.2123	0.1632	0.2722
153	0.1678	0.0973	0.1882
154	0.2041	0.0442	0.2643
155	0.2362	0.0713	0.5004
156	0.2671	0.0388	0.4070
157	0.1385	0.0287	0.1686
158	0.1573	0.0285	0.2043
159	0.1323	0.0247	0.1366
160	0.3163	0.0458	1.4479
161	0.2495	0.0535	0.3429
162	0.2197	0.0441	0.2785
163	0.2353	0.1233	1.6532
164	0.2065	0.0738	0.2511
165	0.1376	0.0259	0.1556
166	0.2057	0.0602	0.2632
167	0.2025	0.0965	0.2802
168	0.1980	0.0903	0.5596
169	0.1869	0.0618	0.2789
170	0.2054	0.1081	0.3088
171	0.1956	0.0651	0.2793
172	0.1435	0.0333	0.2101
173	0.1993	0.0500	0.2601

174	0.1409	0.0415	0.1853
175	0.1510	0.0424	0.2002
176	0.1307	0.0235	0.1309
177	0.1457	0.0255	0.2037
178	0.2072	0.1230	0.2676
179	0.1916	0.0894	0.2443
180	0.2034	0.0728	0.3342
181	0.1362	0.0270	0.1910
182	0.2682	0.1338	0.4547
183	0.1891	0.0771	0.2442
184	0.1819	0.0473	0.2263
185	0.2224	0.1693	0.3305
186	0.2199	0.1828	0.3093
187	0.2512	0.0665	0.4005
188	0.2082	0.0605	0.2929
189	0.2504	0.1655	0.6201
190	0.2515	0.1899	0.4320
191	0.1666	0.0376	0.2033
192	0.2261	0.0951	0.3046
193	0.2478	0.1883	0.4376
194	0.2453	0.1692	1.4174
195	0.2315	0.1904	0.3247
196	0.2386	0.1922	0.3164
197	0.1971	0.1024	0.2397
198	0.2099	0.1721	0.2606
199	0.2822	0.2100	0.4745
200	0.2420	0.1857	0.3501
201	0.2558	0.1925	0.3418
202	0.1977	0.1616	0.2429
203	0.2116	0.1732	0.3030
204	0.2354	0.1577	0.3455
205	0.2345	0.1753	0.3282
206	0.1323	0.0257	0.1378
207	0.2110	0.1603	0.2659
208	0.1927	0.0674	0.2441
209	0.2459	0.1838	0.3339
210	0.2542	0.1762	0.4423
211	0.1595	0.0337	0.1965
212	0.2170	0.1847	0.2826
213	0.2198	0.1883	0.2628
214	0.2281	0.0762	0.3542
215	0.1737	0.0634	0.2220
216	0.2065	0.1747	0.2607
217	0.2326	0.1784	0.3394
218	0.2647	0.0881	0.6075
219	0.2955	0.2087	0.5418
220	0.2501	0.1963	0.3283
221	0.2667	0.2141	0.4077
222	0.2462	0.1977	0.3428
223	0.2049	0.1721	0.2577
224	0.1704	0.0307	0.2321
225	0.1439	0.0260	0.1604
226	0.1933	0.0439	0.2166

227	0.2387	0.1820	0.4363
228	0.2775	0.2003	0.4589
229	0.2781	0.1648	0.4429
230	0.2468	0.1999	0.3321
231	0.2460	0.1737	0.4171
232	0.1922	0.1540	0.2216
233	0.2278	0.1925	0.2971
234	0.2641	0.1975	0.5150
235	0.2358	0.1701	0.3371
236	0.1490	0.0309	0.2721
237	0.1837	0.1360	0.2443
238	0.2243	0.1738	0.3587
239	0.1995	0.0413	0.2418
240	0.1908	0.0510	0.2509
241	0.2457	0.1127	0.3373
242	0.1457	0.0383	0.2037
243	0.1836	0.0352	0.2320
244	0.1303	0.0241	0.1327
245	0.1503	0.0261	0.1958
246	0.1343	0.0286	0.1830
247	0.2509	0.1974	0.3339
248	0.1913	0.0540	0.2396
249	0.1996	0.1260	0.2490
250	0.2165	0.1749	0.3225
251	0.2227	0.0254	0.3117
252	0.2875	0.1847	0.5829
253	0.1310	0.0247	0.1349
254	0.1738	0.0562	0.2203
255	0.2242	0.1810	0.3106
256	0.2231	0.1851	0.2978
257	0.1745	0.0275	0.1984
258	0.1784	0.0535	0.2096
259	0.2405	0.0710	0.3540
260	0.1293	0.0225	0.1166
261	0.1293	0.0228	0.1229
262	0.1968	0.0338	0.2440
263	0.1364	0.0293	0.2001
264	0.1945	0.0861	0.2516
265	0.2049	0.0611	0.2811
266	0.1926	0.0379	0.2385
267	0.1978	0.0805	0.2524
268	0.2246	0.0421	0.2932
269	0.2054	0.0729	0.2531
270	0.1293	0.0230	0.1264
271	0.1979	0.0465	0.2441
272	0.2329	0.0561	0.3083
273	0.2218	0.0496	0.2849
274	0.8842	0.1750	1.6955
275	0.1801	0.0370	0.2100
276	0.2013	0.1587	0.2358
277	0.1696	0.0369	0.2001
278	0.2332	0.1631	0.3051
279	0.2316	0.1770	0.3092

280	0.2124	0.1567	0.2600
281	0.2260	0.1928	0.2928
282	0.2189	0.1288	0.3240
283	0.1797	0.0817	0.2179
284	0.1847	0.1412	0.2170
285	0.2532	0.1930	0.7265
286	0.2120	0.1784	0.3009
287	0.2115	0.1740	0.3680
288	0.2325	0.1785	0.3473
289	0.2568	0.1926	0.4423
290	0.2430	0.1927	0.3288
291	0.2438	0.1701	1.2885
292	0.2266	0.1465	0.2992
293	0.2321	0.1788	0.3393
294	0.2135	0.1765	0.2950
295	0.1965	0.1305	0.2393
296	0.2164	0.1738	0.3009
297	0.2056	0.1735	0.2641
298	0.2332	0.1784	0.4916
299	0.2717	0.1956	0.5321
300	0.2156	0.0341	0.2852
301	0.2427	0.1912	0.3614
302	0.2310	0.1860	0.3847
303	0.1795	0.1458	0.2122
304	0.1362	0.0243	0.1431
305	0.2194	0.1722	0.3290
306	0.2309	0.1878	0.4213
307	0.2370	0.1966	0.3128
308	0.2770	0.2152	0.4549
309	0.2920	0.2206	0.4507
310	0.2058	0.1748	0.2619
311	0.2592	0.1931	0.3644
312	0.2610	0.1662	0.7452
313	0.2280	0.1732	1.3726
314	0.2255	0.1732	0.3744
315	0.2244	0.1919	0.3092
316	0.2032	0.1755	0.2517
317	0.2399	0.1841	1.1676
318	0.3020	0.1918	1.5200
319	0.2775	0.2186	0.4056
320	0.2705	0.1727	0.5471
321	0.2393	0.1858	0.3913
322	0.2152	0.1775	0.2960
323	0.2142	0.1773	0.3337
324	0.2230	0.1889	0.2865
325	0.2354	0.1937	0.3741
326	0.2901	0.1717	0.4649
327	0.2555	0.1725	0.4469
328	0.2140	0.1796	0.2606
329	0.2057	0.1750	0.2605
330	0.2067	0.1682	0.2897
331	0.2211	0.1860	0.2869
332	0.2310	0.1793	0.3271

333	0.2985	0.2224	0.4690
334	0.3203	0.2280	0.5792
335	0.2590	0.1778	0.4300
336	0.3428	0.2231	0.6320
337	0.2789	0.1881	0.6157
338	0.2372	0.1908	0.3470
339	0.1913	0.1559	0.2416
340	0.2209	0.1835	0.2790
341	0.2687	0.2012	0.4476
342	0.2896	0.1898	0.4825
343	0.1328	0.0225	0.1144
344	0.1491	0.0387	0.1913
345	0.3150	0.2030	0.5768
346	0.2364	0.1926	0.3168
347	0.2016	0.1601	0.2783
348	0.1768	0.1535	0.2225
349	0.1785	0.1490	0.2129
350	0.2401	0.1961	0.3260
351	0.2745	0.2055	0.4302
352	0.3146	0.1958	0.6498
353	1.2296	0.0251	1.4739
354	0.3061	0.2239	1.3555
355	0.2126	0.1908	0.2564
356	0.1846	0.1676	0.2095
357	0.1946	0.1552	0.2413
358	0.1934	0.1413	0.2412
359	0.2254	0.1909	0.2926
360	1.3701	0.0264	1.6202
361	0.2706	0.2187	0.3867
362	0.2377	0.1891	0.3630
363	0.1996	0.1669	0.2542
364	0.1961	0.1671	0.2500
365	0.1978	0.1642	0.2530
366	0.2409	0.1872	0.3360
367	0.2006	0.1650	0.2563
368	0.2235	0.1856	0.3127
369	0.2684	0.1689	0.9149
370	0.1997	0.1348	0.2544
371	0.1553	0.0272	0.1712
372	0.2452	0.1926	0.3704
373	0.2623	0.1714	1.4983
374	0.2239	0.1836	0.3011
375	0.2174	0.1766	0.2731
376	0.2412	0.1966	0.3319
377	0.2333	0.1932	0.3234
378	0.2381	0.1812	0.3752
379	0.2510	0.1828	0.4181
380	0.1545	0.0416	0.2542
381	0.2302	0.1692	0.3116
382	0.2260	0.1592	0.3017
383	0.1722	0.0556	0.2276

Appendix B: Water Column Data

B.1 Anchor Station Data

Cast	Date	Hour	Minute	Second	Latitude	Longitude	taub_qsl	ustar
1	5/14/13	14	40	nan	41.3374	72.35728333	0.8833	0.02951448
2	5/14/13	15	2	nan	41.3374	72.35728333	0.6787	0.025871401
3	5/14/13	15	21	nan	41.33738333	72.35695	0.7058	0.026382859
4	5/15/13	6	42	nan	41.27975	72.34735	0.0849	0.00915029
5	5/15/13	7	5	nan	41.27943333	72.34665	0.1051	0.010180811
6	5/15/13	7	25	nan	41.2796	72.34661667	0.1404	0.011766968
7	5/15/13	7	41	nan	41.2796	72.34661667	0.0497	0.007000986
8	5/15/13	8	2	nan	41.2796	72.34661667	0.0342	0.005807565
9	5/15/13	8	20	nan	41.27961667	72.34666667	0.0318	0.005600085
10	5/15/13	8	40	nan	41.27953333	72.34665	0.0737	0.0085254
11	5/15/13	11	18	nan	41.29511667	72.34928333	0.7476	0.027152866
12	5/15/13	11	37	nan	41.2951	72.34928333	1.0202	0.031719306
13	5/15/13	12	0	nan	41.28988333	72.35058333	0.1457	0.011987008
14	5/15/13	12	23	nan	41.28985	72.3506	0.1837	0.013459707
15	5/15/13	12	43	nan	41.28985	72.3506	0.2515	0.015748892
16	5/15/13	13	2	nan	41.28988333	72.35055	0.4861	0.021894944
17	5/15/13	13	22	nan	41.28985	72.35056667	0.3575	0.01877669
18	5/16/13	8	9	nan	41.30793333	72.34951667	0.1671	0.012837169
19	5/16/13	8	37	nan	41.30793333	72.34955	0.1717	0.013012663
20	5/16/13	8	52	nan	41.30793333	72.34951667	0.0697	0.008290819
21	5/16/13	9	10	nan	41.30791667	72.3495	0.0334	0.005739238
22	5/16/13	9	33	nan	41.30793333	72.34946667	0.0997	0.009915819
23	5/16/13	9	55	nan	41.30793333	72.34943333	0.0643	0.00796318
24	5/16/13	10	10	nan	41.3079	72.34948333	0.0797	0.008865642
25	5/16/13	10	55	nan	41.27436667	72.34128333	0.0062	0.002472731
26	5/16/13	11	15	nan	41.27443333	72.34125	0.0077	0.002755665
27	5/16/13	11	38	nan	41.27443333	72.34116667	0.1855	0.013525489
28	5/16/13	11	53	nan	41.27448333	72.34111667	0.3493	0.0185601
29	5/16/13	12	19	nan	41.27473333	72.3412	0.5408	0.023094011
30	5/16/13	12	40	nan	41.27471667	72.34123333	0.5625	0.023552786
31	11/5/13	8	53	nan	41.33916667	72.36091667	0.2706	0.01633597
32	11/5/13	9	18	nan	41.33913333	72.361	0.3347	0.018168074
33	11/5/13	9	40	44	41.33905	72.36101667	0.3638	0.018941413
34	11/5/13	10	1	53	41.33918333	72.361	0.3455	0.018458867
35	11/5/13	10	17	17	41.33916667	72.36098333	0.3674	0.0190349
36	11/5/13	10	35	16	41.33916667	72.36101667	0.5313	0.022890271
37	11/5/13	10	51	21	41.33925	72.36101667	0.7018	0.026307992
38	11/5/13	11	7	18	41.33921667	72.36101667	0.9127	0.030001644

39	11/5/13	11	24	54	41.33925	72.36096667	0.9155	0.030047628
40	11/5/13	11	38	41	41.33925	72.3609	0.6166	0.024659416
41	11/5/13	11	55	45	41.33928333	72.3608	0.3896	0.019601554
42	11/5/13	12	9	15	41.33925	72.3608	0.2477	0.015629462
43	11/5/13	12	28	0	41.33923333	72.36081667	0.2558	0.015882955
44	11/5/13	12	47	5	41.33925	72.36085	0.2276	0.014981909
45	11/5/13	13	4	59	41.33916667	72.36055	0.0472	0.006822633
46	11/5/13	13	25	25	41.33881667	72.36036667	0.0051	0.002242674
47	11/5/13	13	41	16	41.33876667	72.36035	0.0060	0.002432521
48	11/5/13	13	57	20	41.33876667	72.36038333	0.0031	0.001748485
49	11/5/13	14	20	50	41.3388	72.36038333	0.0071	0.002646124
50	11/5/13	14	38	19	41.33878333	72.36033333	0.0454	0.006691276
51	11/5/13	14	56	25	41.33871667	72.3602	0.0079	0.002791223
52	11/5/13	15	14	59	41.33866667	72.35998333	0.0352	0.005891859
53	11/5/13	15	33	2	41.33851667	72.3599	0.0260	0.005063697
54	11/5/13	15	50	36	41.33855	72.35983333	0.0150	0.003846154
55	11/5/13	16	7	46	41.33845	72.35965	0.0054	0.002307692
56	11/5/13	16	25	18	41.33846667	72.35963333	0.0003	0.000543928
57	11/6/13	8	6	7	41.2831	72.34835	3.8484	0.061605732
58	11/6/13	8	25	22	41.2832	72.34836667	3.8484	0.061605732
59	11/6/13	8	43	12	41.28356667	72.34838333	3.8484	0.061605732
60	11/6/13	8	59	39	41.2836	72.34841667	3.8484	0.061605732
61	11/6/13	9	17	31	41.28366667	72.3485	3.8484	0.061605732
62	11/6/13	9	34	57	41.2837	72.34845	3.8484	0.061605732
63	11/6/13	9	52	20	41.2837	72.34845	1.2638	0.035303698
64	11/6/13	10	43	23	41.3342	72.3586	3.8484	0.061605732
65	11/6/13	11	1	14	41.3342	72.35853333	3.8484	0.061605732
66	11/6/13	11	18	13	41.3342	72.35345	3.8484	0.061605732
67	11/6/13	11	37	10	41.33415	72.3584	3.8484	0.061605732
68	11/6/13	11	55	21	41.33416667	72.35843333	3.8484	0.061605732
69	11/6/13	12	12	4	41.33413333	72.35838333	3.8484	0.061605732
70	11/6/13	12	30	30	41.33413333	72.3583	3.8484	0.061605732
71	11/6/13	12	48	48	41.33408333	72.35831667	3.8484	0.061605732
72	11/6/13	13	4	53	41.33391667	72.35818333	3.8484	0.061605732
73	11/6/13	13	22	54	41.33383333	72.3582	3.8484	0.061605732
74	11/6/13	13	42	36	41.33398333	72.3582	3.8484	0.061605732
75	11/6/13	13	58	33	41.3337	72.3583	3.8484	0.061605732
76	11/6/13	14	15	48	41.33373333	72.35828333	3.8484	0.061605732
77	11/6/13	14	32	57	41.33365	72.35841667	3.8484	0.061605732
78	11/6/13	14	50	58	41.3337	72.35833333	3.8484	0.061605732
79	11/7/13	7	44	30	41.27438333	72.34103333	0.0360	0.005958436
80	11/7/13	8	3	12	41.2744	72.34103333	0.0675	0.008158924
81	11/7/13	8	21	2	41.27448333	72.34096667	0.0820	0.008992655
82	11/7/13	8	42	11	41.27463333	72.34095	0.2459	0.01557257

83	11/7/13	8	59	50	41.27465	72.34095	0.1389	0.011703942
84	11/7/13	9	16	28	41.27461667	72.34098333	0.3196	0.017753517
85	11/7/13	9	33	51	41.27465	72.34095	0.3444	0.018429459
86	11/7/13	9	51	49	41.27481667	72.34111667	0.4636	0.021382217
87	11/7/13	10	11	11	41.27475	72.34116667	0.5998	0.024321158
88	11/7/13	10	53	34	41.30986667	72.34925	0.9223	0.030159013
89	11/7/13	11	11	28	41.30993333	72.34931667	1.8776	0.043031111
90	11/7/13	11	29	10	41.30986667	72.34915	1.8567	0.042790946
91	11/7/13	11	46	31	41.30981667	72.34915	0.7377	0.026972482
92	11/7/13	12	5	20	41.30983333	72.34916667	0.6809	0.025913298
93	11/7/13	12	43	4	41.33818333	72.35783333	0.8193	0.028425133
94	11/7/13	12	59	44	41.33823333	72.3578	0.6348	0.025020701
95	11/7/13	13	18	12	41.33826667	72.35771667	0.4662	0.021442092
96	11/7/13	13	35	14	41.3383	72.35766667	0.3632	0.018925787
97	11/7/13	14	4	48	41.34271667	72.36998333	0.4328	0.02065973
98	11/7/13	14	23	25	41.34258333	72.36995	0.3723	0.019161413
99	11/7/13	14	41	3	41.34253333	72.36998333	0.1848	0.013499945
100	11/7/13	15	30	9	41.3234	72.34676667	0.2480	0.015638924
101	11/7/13	15	45	46	41.32343333	72.34676667	0.1851	0.013510899
102	11/7/13	16	1	27	41.32336667	72.34681667	0.2950	0.017056583
103	11/8/13	6	52	0	41.33898333	72.36021667	0.0886	0.009347552
104	11/8/13	7	14	19	41.33905	72.36021667	0.0266	0.005121791
105	11/8/13	7	35	44	41.33905	72.36021667	0.0269	0.005150592
106	11/8/13	7	50	59	41.33908333	72.36023333	0.0178	0.004189778
107	11/8/13	8	6	7	41.3391	72.36025	0.0137	0.003675711
108	11/8/13	8	21	33	41.33901667	72.36021667	0.0271	0.005169704
109	11/8/13	8	37	45	41.33905	72.36018333	0.0222	0.004679048
110	11/8/13	8	53	51	41.33908333	72.36018333	0.0589	0.007621469
111	11/8/13	9	10	37	41.33905	72.36021667	0.0828	0.009036415
112	11/8/13	9	56	53	41.3097	72.34938333	0.3330	0.018121875
113	11/8/13	10	13	54	41.30971667	72.34936667	0.2394	0.015365373
114	11/8/13	10	35	51	41.3097	72.34938333	0.2283	0.01500493
115	11/8/13	10	52	59	41.30973333	72.34935	0.2071	0.014291278
116	11/8/13	11	11	25	41.30951667	72.34946667	0.8668	0.029237516
117	11/8/13	11	29	9	41.30948333	72.34953333	1.0848	0.032708141
118	11/8/13	11	46	44	41.3097	72.34935	0.3459	0.01846955
119	11/8/13	12	4	6	41.30953333	72.34946667	0.1369	0.011619374
120	11/8/13	12	24	23	41.3098	72.34936667	0.8019	0.028121671
121	11/8/13	12	41	16	41.30978333	72.3494	0.6539	0.025394326
122	5/14/14	9	53	23	41.31631667	72.34716667	0.0894	0.009389658
123	5/14/14	10	19	14	41.3163	72.34728333	0.0791	0.008832208
124	5/14/14	10	46	18	41.31623333	72.34741667	0.0991	0.009885937
125	5/14/14	11	9	30	41.31626667	72.34745	0.0792	0.008837789
126	5/14/14	11	32	58	41.31615	72.34773333	0.2260	0.014929156

127	5/14/14	11	56	19	41.31543333	72.34756667	0.0762	0.008668791
128	5/14/14	12	22	17	41.31531667	72.3475	0.0035	0.001857869
129	5/14/14	12	45	50	41.31581667	72.3475	0.0285	0.005301557
130	5/14/14	13	8	27	41.31523333	72.34738333	0.0663	0.008086075
131	5/14/14	13	36	34	41.3153	72.34735	0.1172	0.0107509
132	5/14/14	14	0	13	41.31525	72.34728333	0.2655	0.016181295
133	5/14/14	14	17	5	41.31526667	72.34731667	0.5308	0.022879497
134	5/14/14	14	39	26	41.31525	72.34741667	0.6412	0.025146513
135	5/14/14	15	4	35	41.31526667	72.3473	1.5036	0.038507665
136	5/14/14	15	28	5	41.31523333	72.34738333	1.5165	0.038672498
137	5/14/14	15	51	0	41.31521667	72.34733333	1.3481	0.036462134
138	5/14/14	16	13	48	41.31525	72.34736667	1.2436	0.035020422
139	5/14/14	16	37	14	41.31526667	72.34723333	1.1953	0.034333611
140	5/15/14	8	35	13	41.28563333	72.3492	0.0041	0.002010819
141	5/15/14	8	57	30	41.28571667	72.3492	0.6204	0.024735285
142	5/15/14	9	18	55	41.2857	72.34923333	0.8318	0.028641152
143	5/15/14	9	40	31	41.2857	72.34923333	1.2457	0.035049978
144	5/15/14	10	3	22	41.28571667	72.34925	1.0817	0.032661373
145	5/15/14	10	24	57	41.28573333	72.34928333	0.8765	0.029400653
146	5/15/14	10	46	18	41.28573333	72.34923333	0.6509	0.025336006
147	5/15/14	11	7	49	41.28573333	72.34923333	0.4783	0.021718569
148	5/15/14	11	29	40	41.28573333	72.34918333	0.4091	0.020086107
149	5/15/14	11	51	43	41.28571667	72.34923333	0.2340	0.015191091
150	5/15/14	12	14	36	41.28535	72.34921667	0.1152	0.010658774
151	5/15/14	12	37	31	41.28516667	72.34891667	0.0423	0.006458791
152	5/15/14	12	59	49	41.28518333	72.34883333	0.0024	0.001538462
153	5/15/14	13	23	38	41.28515	72.34881667	0.0073	0.002683135
154	5/15/14	13	46	29	41.28513333	72.34883333	0.0353	0.005900222
155	5/15/14	14	9	53	41.28513333	72.34876667	0.0846	0.009134109
156	5/15/14	14	33	47	41.28513333	72.3488	0.0059	0.002412165
157	5/15/14	14	56	6	41.28513333	72.34878333	0.0065	0.002531848
158	5/15/14	15	18	49	41.28513333	72.34878333	0.0027	0.001631785
159	5/15/14	15	41	4	41.28513333	72.3488	0.0145	0.003781508
160	5/15/14	16	3	40	41.28513333	72.34881667	0.0052	0.002264554
161	5/15/14	16	24	22	41.28511667	72.34883333	0.0396	0.00624926
162	5/15/14	16	45	51	41.2851	72.3488	0.0544	0.007324542
163	5/15/14	17	7	47	41.2851	72.34883333	0.0175	0.004154321
164	5/15/14	17	30	20	41.28515	72.3488	0.0339	0.005782037
165	5/17/14	8	27	40	41.29166667	72.34896667	0.7263	0.026763262
166	5/17/14	8	48	27	41.29163333	72.34893333	0.4231	0.020426903
167	5/17/14	9	8	54	41.2916	72.34898333	0.2509	0.015730095
168	5/17/14	9	29	27	41.29158333	72.34903333	0.1448	0.011949928
169	5/17/14	9	49	32	41.29163333	72.3489	0.0262	0.005083135
170	5/17/14	10	11	57	41.29163333	72.34918333	0.0067	0.002570505

171	5/17/14	10	44	40	41.2918	72.3487	0.0576	0.007536892
172	5/17/14	11	6	28	41.2921	72.34863333	0.9296	0.030278132
173	5/17/14	11	28	29	41.29213333	72.34863333	0.5740	0.02379233
174	5/17/14	11	51	29	41.29216667	72.34865	0.5269	0.02279529
175	5/17/14	12	13	52	41.29213333	72.34865	0.4423	0.020885241
176	5/17/14	12	38	25	41.2921	72.34865	0.4182	0.020308275
177	5/17/14	13	4	48	41.29208333	72.34863333	0.2910	0.01694055
178	5/17/14	13	26	16	41.29205	72.34863333	0.2220	0.014796449
179	5/17/14	13	48	17	41.29195	72.34865	0.1403	0.011762777
180	5/17/14	14	26	9	41.29185	72.3486	0.0268	0.00514101
181	5/17/14	15	28	10	41.30971667	72.34978333	0.0413	0.006381989
182	5/17/14	15	52	8	41.3096	72.34971667	0.0048	0.002175713
183	5/17/14	16	13	46	41.3095	72.34973333	0.0387	0.006177838
184	5/17/14	16	34	59	41.30945	72.34966667	0.0198	0.004418894

B.2 Data Quality Tests

Cast	1. Mean velocity >10 cm/s	2. Mean velocity > 5 cm/s	3. % Change in mean velocity <25 %	4. % Change in mean velocity < 10%	5. Visual Pressure Check	6. w = 0	7. Pitch and tilt visual	Comments	Heading (<10 degree change)
1	1	1	1	1	1	1	0	fixed, passes all tests now - shortened time series	1
2	1	1	1	1	1	1	0	fixed, passes all tests now - shortened time series	1
3	1	1	1	1	1	1	0	fixed, passes all tests now - shortened time series	1
4	1	1	1	0	1	1	1		1
5	1	1	0	0	1	1	1		1
6	1	1	1	0	1	1	1		1
7	1	1	1	1	1	1	1		1
8	0	1	1	0	1	1	1		1
9	0	1	1	0	1	1	1		1
10	1	1	1	0	1	1	1		1
11	1	1	1	1	1	1	0	fixed, passes all tests now - shortened time series	1
12	1	1	1	1	1	1	0	fixed, passes all tests now - shortened time series	1
13	1	1	1	0	1	1	1		1
14	1	1	1	0	1	1	1		1
15	1	1	1	0	1	1	1		1
16	1	1	1	0	1	1	1		1
17	1	1	0	0	1	1	1		1

18	1	1	1	1	1	1	1		1
19	1	1	1	1	1	1	1		1
20	1	1	1	1	1	1	1		1
21	0	1	1	1	1	1	1		1
22	1	1	1	0	1	1	1		1
23	1	1	1	0	1	1	1		1
24	1	1	1	0	1	1	1		1
25	0	0	0	0	1	1	1		1
26	0	0	0	0	1	1	1		1
27	1	1	0	0	1	1	0	fixed, passes most tests - shortened time series	1
28	1	1	0	0	1	1	1		1
29	1	1	1	1	1	1	1		1
30	1	1	1	1	1	1	1		1
1	1	1	1	1	1	1	-2	fixed, passes all tests now - shortened time series	1
2	1	1	0	0	1	1	1		1
3	1	1	1	1	1	1	1		1
4	1	1	1	1	1	1	1		1
5	1	1	1	0	1	1	1		1
6	1	1	0	0	1	1	1		1
7	1	1	1	1	1	1	-2	fixed, passes all tests now - shortened time series	1
8	1	1	1	1	1	1	1		1
9	1	1	1	0	0	1	0	not sure if salvagable - 3 min 20 sec of usuable data	0
10	1	1	0	0	1	1	1		1
11	1	1	1	0	1	1	-2	fixed, passes most tests - shortened time series	1
12	1	1	1	1	1	1	1		1
13	1	1	1	1	1	1	1		1
14	1	1	0	0	1	1	1		1
15	1	1	1	0	1	1	1		1
16	0	0	0	0	1	1	-2	fixed pitch.tilt issue	1
17	0	0	0	0	1	1	1		1
18	0	0	1	1	1	1	1		1
19	0	0	0	0	1	1	1		1
20	1	1	0	0	1	1	1		1
2	0	0	0	0	1	1	-2		1

1									
22	0	1	1	0	1	1	-2		1
23	0	1	0	0	1	1	-2		1
24	0	1	1	0	1	1	-2		1
25	0	0	0	0	1	1	-2		1
26	0	0	0	0	1	1	1		1
27	1	1	1	0	1	1	1		1
28	1	1	1	0	1	1	1		1
29	1	1	1	1	1	1	1		1
30	1	1	1	1	1	1	1		1
31	1	1	1	1	1	1	1		1
32	1	1	1	1	1	1	1		1
33	1	1	1	1	1	1	2	fixed, passes all tests now - shortened time series	1
34	1	1	0	0	1	1	1		1
35	1	1	1	0	1	1	1		1
36	1	1	1	1	1	1	1		1
37	1	1	1	1	1	1	1		1
38	1	1	1	0	1	1	1		1
39	1	1	1	0	1	1	1		1
40	1	1	1	1	1	1	1		1
41	1	1	1	0	1	1	1		1
42	1	1	1	0	1	1	1		1
43	0	1	1	0	1	1	1		1
44	1	1	1	1	1	1	1		1
45	1	1	1	1	1	1	1		1
46	0	1	0	0	1	1	1		1
47	0	0	0	0	1	1	1		1
48	0	1	0	0	1	1	1		1
49	0	1	1	1	1	1	1		1
50	1	1	0	0	1	1	1		1
51	1	1	1	1	1	1	1		1
52	1	1	1	0	1	1	1		1
53	1	1	0	0	1	1	1		1
5	1	1	1	1	1	1	1		1

4									
55	1	1	1	1	1	1	1		1
56	1	1	1	0	1	1	1		1
57	1	1	1	1	1	1	1		1
58	1	1	0	0	1	0	0	not sure if salvagable - 3 min of usuable data	0
59	1	1	1	1	1	1	0	fixed, passes all tests now - shortened time series	1
60	1	1	0	1	1	0	0	fixed, passes most tests - shortened time series	1
61	1	1	1	0	1	1	1		1
62	1	1	0	0	1	1	1		1
63	1	1	1	0	1	1	1		1
64	1	1	1	0	1	1	1		1
65	1	1	1	0	1	1	1		1
66	1	1	1	0	1	1	1		1
67	1	1	1	1	1	1	1		1
68	1	1	1	0	1	1	1		1
69	1	1	0	0	1	1	1		1
70	1	1	1	1	1	1	1		1
71	1	1	1	0	1	1	1		1
72	1	1	1	1	1	1	1		1
73	1	1	0	0	1	1	1		1
74	0	1	0	0	1	1	1		1
75	0	1	1	0	1	1	1		1
76	0	1	1	1	1	1	1		1
77	0	1	1	1	1	1	1		1
78	0	1	0	0	1	1	1		1
79	0	1	0	0	1	1	1		1
80	1	1	0	0	1	1	1		1
81	1	1	1	1	1	1	1		1
82	1	1	1	1	1	1	1		1
83	1	1	1	0	1	1	1		1
84	1	1	0	0	1	1	0	fixed, passes most tests - shortened time series	1
85	1	1	1	1	1	1	2	fixed, passes all tests now - shortened time series	1
86	1	1	1	1	1	1	1		1

87	1	1	1	1	1	1	2	rolls off, not sure if fixable	1
88	1	1	1	0	1	1	1		1
89	1	1	0	0	0	1	0	not salvagable	0
90	1	1	1	1	1	1	1		1
91	1	1	0	0	1	1	1		1
1	1	1	1	0	1	1	1		1
2	1	1	0	0	1	1	1		1
3	1	1	0	0	1	1	1		1
4	1	1	1	0	1	1	1		1
5	1	1	1	1	0	1	0	fixed, passes all tests now - shortened time series	1
6	1	1	0	0	1	1	1		1
7	0	0	0	0	1	1	1		0
8	0	1	1	0	1	1	1		1
9	1	1	0	0	1	1	1		1
10	1	1	1	1	1	1	1		1
11	1	1	1	0	1	1	1		1
12	1	1	0	0	1	1	1		1
13	1	1	0	0	1	1	1		1
14	1	1	1	1	1	1	1		1
15	1	1	1	1	1	1	1		1
16	1	1	1	1	1	1	1		1
17	1	1	1	1	1	1	1		1
18	1	1	1	0	1	1	1		1
19	0	0	0	0	1	1	1		1
20	1	1	1	1	1	1	1		1
21	1	1	0	0	1	1	1		1
22	1	1	1	1	1	1	1		1
23	1	1	1	0	1	1	1		1
24	1	1	1	1	1	1	1		1
25	1	1	1	1	1	1	1		1
26	1	1	1	0	1	1	1		1
27	1	1	1	1	1	1	0	fixed, passes all tests now - shortened time series	1
28	1	1	1	1	1	1	1		1
29	1	1	1	0	1	1	0	fixed, passes all tests now - shortened time series	1

30	1	1	0	0	1	1	0	fixed, passes all tests now - shortened time series	1
31	0	0	0	0	1	1	1		1
32	0	0	0	0	1	1	1		0
33	0	1	1	1	1	1	1		1
34	1	1	0	0	1	1	1		1
35	0	0	0	0	1	1	1		1
36	0	0	0	0	1	1	1		1
37	0	0	0	0	1	1	1		1
38	0	1	0	0	1	1	1		1
39	0	0	0	0	1	1	1		1
40	0	1	1	1	1	1	1		1
41	1	1	1	1	1	1	1		1
42	0	1	0	0	1	1	1		1
43	0	1	1	0	1	1	1		1
44	1	1	1	0	1	1	1		0
45	1	1	1	0	1	1	1		1
46	1	1	1	0	1	1	1		0
47	1	1	1	1	1	1	1		1
48	0	1	0	0	0	1	0	probably not salvagable, 3 min of workable data	0
49	0	0	0	0	1	1	1		1
50	0	0	0	0	0	1	0	fixed, passes all tests now - shortened time series (4.5 min time series)	1
51	1	1	0	0	1	1	1		1
52	1	1	0	0	1	1	1		1
53	1	1	1	1	1	1	1		1
54	1	1	1	0	1	1	1		1
55	1	1	1	1	1	1	1		1
56	1	1	1	1	1	1	1		1
57	1	1	1	0	1	1	1		1
58	1	1	1	1	1	1	1		0
59	0	1	0	0	1	1	1		1
60	1	1	1	0	0	1	0	unsalvagable - pitch and tilt	0
61	0	0	0	0	1	1	0		1

62	0	1	0	0	1	1	1		1
63	0	1	0	0	0	1	0	fixed, passes some tests - time series shortened	1